

**DIFFERENTIAL REGULATION OF SYNAPTIC PLASTICITY, MOOD AND REWARD
BEHAVIOR BY CIRCADIAN GENES**

by

Puja K. Parekh

B.S., The College of William and Mary in Virginia, 2008

Submitted to the Graduate Faculty of
The School of Medicine in partial fulfillment
of the requirements for the degree of
Doctor of Philosophy

University of Pittsburgh

2017

UNIVERSITY OF PITTSBURGH
SCHOOL OF MEDICINE

This dissertation was presented

by

Puja K. Parekh

It was defended on

February 20, 2017

and approved by

Committee chair: Bitá Moghaddam, Ph.D., Professor, Dept. of Neuroscience

Yanhua Huang, Ph.D., Assistant Professor, Dept. of Psychiatry

Yan Dong, Ph.D., Professor, Dept. of Neuroscience

Oliver Schlüter, Ph.D., Assistant Professor, Dept. of Neuroscience

Outside Examiner: Ming-Hu Han, Ph.D., Associate Professor, Dept. of Neuroscience, Icahn

School of Medicine at Mt. Sinai

Dissertation Advisor: Colleen McClung, Ph.D., Associate Professor, Dept. of Psychiatry

Copyright © by Puja K. Parekh

2017

**DIFFERENTIAL REGULATION OF SYNAPTIC PLASTICITY, MOOD AND
REWARD BEHAVIOR BY CIRCADIAN GENES**

Puja K. Parekh, Ph.D.

University of Pittsburgh, 2017

Endogenously generated circadian rhythms allow living organisms to entrain to photic and non-photic cues in a changing environment. The master pacemaker region, the suprachiasmatic nucleus (SCN) coordinates the activity of several sub-oscillators throughout the brain and periphery to produce daily variation in physiology and activity patterns. However, SCN-autonomous rhythms also exist in mesocorticolimbic brain regions. The disruption of these rhythms at the molecular level can have dire consequences for physical and mental health. Clinical and preclinical studies provide a strong link between circadian gene perturbations and the development and progression of mood and substance abuse disorders including bipolar disorder (BD) and co-morbid addiction. While much is known about the inner workings of the SCN clock, the specific underlying mechanisms governing the regulation of mood and reward-related behavior by extra-SCN clock proteins are yet to be fully elucidated.

Molecular rhythms are maintained by transcription factors, CLOCK and NPAS2, which are homologous in structure and function but differentially expressed throughout the brain. Genetic variants of both have been found to associate with neuropsychiatric illnesses in human populations. The expression profiles and uniquely regulated gene targets of these proteins however, may contribute to differences in their ability to modulate behavior. The work presented here focuses on how disruptions in CLOCK and NPAS2 alter mesolimbic excitatory neurotransmission and their effects on mood and reward-related behavior. We find that a mutation in CLOCK, which produces a dominant negative protein, and a behavioral phenotype in mice closely resembling human mania,

leads to a reduction in excitatory neurotransmission in the nucleus accumbens (NAc) a region critical for sensorimotor and limbic integration. These mice have also been characterized to be hyperhedonic with increased reward sensitivity. In contrast, a disruption in NPAS2 by viral-mediated knockdown, increases NAc excitatory synaptic transmission and incidentally decreases reward sensitivity in a cell-type specific manner. Electrophysiological, molecular, biochemical and behavioral studies contained within this dissertation aim to uncover the differential regulation of behavior by these core circadian proteins. The understanding of these mechanisms may help to inform targeted therapeutic strategies against BD and other disorders for which there is a strong circadian component.

TABLE OF CONTENTS

PREFACE.....	XIII
1.0 INTRODUCTION: THE MAMMALIAN CIRCADIAN CLOCK.....	1
1.1 CIRCADIAN RHYTHMS IN PSYCHIATRIC ILLNESS	5
1.1.1 Central pathways involved in mood and reward regulation.....	8
1.1.2 Bipolar disorder and the clock	10
1.1.3 Circadian rhythms in addiction	13
1.1.4 Circadian regulation of reward-related regions and dopaminergic transmission	14
1.2 ANIMAL MODELS OF NEUROPSYCHIATRIC ILLNESS.....	18
1.2.1 Genetic models of bipolar mania	20
1.3 DISSERTATION AIMS	24
20 ALTERED GLUA1 FUNCTION AND ACCUMBAL SYNAPTIC PLASTICITY IN THE <i>CLOCKΔ19</i> MODEL OF BIPOLAR MANIA.....	25
21 INTRODUCTION	26
22 MATERIALS AND METHODS.....	28
2.2.1 Animal use.....	28
2.2.2 NAc slice preparation.....	29
2.2.3 Whole-cell patch-clamp recordings	30
2.2.4 Surface GLUA1 detection.....	31
2.2.5 Viral gene transfer and stereotaxic surgery.....	32
2.2.6 Immunohistochemistry	33

2.2.7	Animal behavior	33
2.2.8	Real-time Polymerase Chain Reaction.....	34
2.2.9	Data analysis	35
23	RESULTS	35
2.3.1	<i>Clock</i> Δ 19 mice have reduced AMPAR-mediated synaptic transmission and strength at NAc MSNs throughout the light/dark cycle	35
2.3.2	Presynaptic release of glutamate onto NAc MSNs is unaltered in <i>Clock</i> mutants throughout the light/dark cycle.....	40
2.3.3	Membrane levels and rhythm of GLUA1 protein are reduced in the NAc of <i>Clock</i> Δ 19 mice.....	41
2.3.4	<i>Clock</i> mutant MSNs display subtle alterations in intrinsic membrane properties	46
2.3.5	Overexpression of <i>GluA1</i> in the NAc normalizes “manic-like” behavior in <i>Clock</i> Δ 19 mice.....	48
24	DISCUSSION.....	54
25	FUTURE DIRECTIONS	58
3.0	CELL-TYPE SPECIFIC EFFECTS OF NPAS2 DISRUPTION ON ACCUMBAL SYNAPTIC PLASTICITY AND COCAINE SENSITIVITY	63
3.1	INTRODUCTION	64
3.2	MATERIALS AND METHODS.....	66
3.2.1	Animal use.....	66
3.2.2	Viral gene transfer and stereotaxic surgery.....	67
3.2.3	Quantitative real-time RT-PCR.....	67

3.2.4	NAc slice preparation.....	68
3.2.5	Whole-cell patch clamp recording.....	69
3.2.6	Dendritic spine labeling and imaging.	70
3.2.7	Generation and validation of Cre-inducible viruses.....	71
3.2.8	Cocaine conditioned place preference	71
3.2.9	Data analysis.....	72
3.3	RESULTS.....	72
3.3.1	Knockdown of NPAS2 within the NAc leads to an increase in glutamatergic transmission at MSNs	72
3.3.2	Effects of NPAS2 reduction on NAc glutamatergic gene expression	75
3.3.3	Increased excitatory synaptic transmission following NPAS2 knockdown is specific to D1 MSNs	76
3.3.4	The role of NPAS2 in cocaine-induced MSN dendritic spine alterations.....	79
3.3.5	D1-MSN-specific NPAS2 knockdown in the NAc reduces cocaine reward sensitivity.....	82
3.4	DISCUSSION.....	83
3.5	FUTURE DIRECTIONS	86
4.0	GENERAL DISCUSSION	91
	APPENDIX A	94
	APPENDIX B	124
	BIBLIOGRAPHY.....	150

LIST OF TABLES

Table 1 The <i>Clock</i> Δ 19 mutant mouse as a model of bipolar mania	23
Table 2 Intrinsic membrane properties of <i>Clock</i> mutant and WT MSNs during light and dark phases	48
Table 3 Bioavailability of AUT1 with oral administration	106

LIST OF FIGURES

Figure 1. A series of transcriptional and translational feedback loops comprise the core molecular clock in mammals	3
Figure 2. Variants of core circadian genes strongly associate with mood disorders in humans. ..	7
Figure 3. Hallmarks of bipolar I disorder.....	12
Figure 4. Elements of dopaminergic transmission are directly under circadian control	16
Figure 5. <i>Clock</i> Δ 19 mutation modifies MSN AMPAR-mediated synaptic transmission across the light/dark cycle.....	36
Figure 6. <i>Clock</i> Δ 19 MSNs show reduced glutamatergic transmission in both core and shell subregions of the NAc.....	37
Figure 7. AMPAR-mediated synaptic strength of MSNs is reduced by the <i>Clock</i> Δ 19 mutation.	39
Figure 8. <i>Clock</i> Δ 19 mutation does not alter the presynaptic release of glutamate onto MSNs.	41
Figure 9. The surface/intracellular ratio of GLUA1 expression is significantly reduced in <i>Clock</i> Δ 19 NAc during the light and dark phases	43
Figure 10. A diurnal rhythm in GLUA1 expression in the NAc is abolished in <i>Clock</i> Δ 19 mice.	45
Figure 11. Excitability of MSNs is unaltered by <i>Clock</i> Δ 19 mutation however diurnal variation exists in evoked firing rates.....	47
Figure 12. Functional up-regulation of <i>GluA1</i> in the NAc of <i>Clock</i> Δ 19 mice.....	50
Figure 13. Overexpression of <i>GluA1</i> in the accumbens of <i>Clock</i> Δ 19 mice reverses elevated exploratory drive behavior	52

Figure 14. Cocaine sensitivity is normalized following GluA1 up-regulation in <i>Clock</i> Δ 19.	53
Figure 15. Knockdown of <i>Clock</i> in the NAc of WT mice does not alter excitatory transmission.	57
Figure 16. Proposed model of the effects of the <i>Clock</i> Δ 19 mutation on NAc MSN activity.....	58
Figure 17. Knockdown of NPAS2 in the NAc leads to an increase in excitatory transmission onto MSNs	74
Figure 18. Knockdown of NPAS2 in the NAc does not significantly change AMPAR and NMDAR subunit gene expression	76
Figure 19. Increased excitatory synaptic transmission following NPAS2 knockdown is specific to D1-containing MSNs.	78
Figure 20. NPAS2 may be important for cocaine-induced changes in MSN structural plasticity.	80
Figure 21. Viral-mediated knockdown of NPAS2 specifically in D1 MSNs reduces cocaine place preference.....	82
Figure 22. FACS-RNAseq for the identification of gene targets regulated by NPAS2 in D1 and D2 MSNs	88
Figure 23. Summary of the differential roles of CLOCK and NPAS2 in the regulation of neural activity and behavior	93
Figure 24. A Kv3.1 channel modulator (AUT1) prevents amphetamine-induced hyperactivity.	105
Figure 25. AUT1 does not attenuate amphetamine-induced hyperactivity in Kv3.1 null mice and these mice exhibit manic-related behaviors	108
Figure 26. AUT1 prevents amphetamine-induced hyperactivity in Kv3.2 KO mice	110
Figure 27. AUT1 reverses hyperactivity in the <i>Clock</i> Δ 19 mutant mouse model of mania.....	113

Figure 28. The firing rate of <i>Clock</i> Δ 19 VTA dopamine neurons is attenuated by AUT1.....	115
Figure 29. AUT1 modulates action potential properties of <i>Clock</i> Δ 19 dopamine and GABAergic neurons.....	117
Figure 30. Lithium restores abnormal Kv3.1b protein levels in a mouse model of mania	119
Figure 31. Chronic unpredictable mild stress results in a robust and significant increase in diurnal NAc <i>Npas2</i> expression as compared with control mice	137
Figure 32. <i>Npas2</i> mutant mice exhibit reduced anxiety-like behavior	138
Figure 33. NAc <i>Npas2</i> knockdown results in reduced anxiety-like behavior.....	140
Figure 34. Effect of <i>Npas2</i> knockdown on diurnal expression of GABA _A alpha 1 (<i>Gabra1</i>) subunit in the NAc	142
Figure 35. <i>Npas2</i> knockdown prevents diazepam-induced potentiation of IPSC amplitude in NAc MSNs	144

PREFACE

The past several years have marked a tremendous period of growth for me, intellectually, personally and professionally. With it have come the inevitable growing pains, the challenges faced with any undertaking of significant worth. However, the ultimate satisfaction of growth that can only be appreciated when taking stock is valuable beyond measure. For the opportunity to explore my interests, learn a considerable amount about the natural world and put an inquisitive mind to practice, I would like to express my gratitude to several individuals and organizations. Foremost are my mentors, Dr. Colleen McClung and Dr. Yanhua Huang, who have guided me through the technical aspects of the studies I describe in this dissertation, but who have also both taught me a great deal about how to approach the profession of a scientist, with its unique demands and responsibilities. Colleen has given me the freedom to ask questions and seek answers in my own style, forcing me to define what that style should be as I move forward in my career. Yanhua has given me unrestricted access to resources, undoubtedly the most valuable of which has been her expertise and sharp, analytical mind. I admire, respect, and hope to emulate both of my exemplary mentors. Additionally, I would like to thank both current and former members of my committee and especially my Chair, Dr. Bitu Moghaddam. The valuable input from these individuals has enriched my learning experience and helped to focus my studies. For continued support and unparalleled training, I am proud to belong to the CNUP graduate program, the CNBC joint certificate program and the TNP. These organizations truly embody the spirit of the collaborative, innovative and thriving neuroscience community in Pittsburgh with their emphasis on fostering the potential of trainees. Lastly, I am indebted to countless peers whose camaraderie

and generosity have made a lasting impression on me. Sharing in our frustrations and fears has lessened their burden and likewise celebrating our accomplishments together has enhanced their meaning. As I look forward, I am comforted to know that my scientific colleagues will be the brilliant and unique individuals I have had the privilege to befriend here.

1.0 INTRODUCTION: THE MAMMALIAN CIRCADIAN CLOCK

The rotation of the Earth on its axis creates a periodic shifting of light conditions, which has necessitated the evolution of a biological system to allow organisms to adaptively entrain to daily and seasonal cues. Circadian rhythms serve this purpose and are indispensable for maintaining proper physiological and behavioral responses to ensure survival (Milhiet *et al*, 2014). Biological rhythms are an ancient and highly conserved phenomenon and were first described in plants (Bunning, 1935; Chandrashekar, 1998). Since then, countless species of invertebrate and vertebrate animals have been subjects of chronobiological studies. Mammals possess specialized melanopsin-containing retinal structures termed intrinsically photosensitive retinal ganglion cells (ipRGCs), which transmit light information from the environment via the retinohypothalamic tract to the master pacemaker region in the brain called the suprachiasmatic nucleus (SCN) (Hattar *et al*, 2006; Panda *et al*, 2003; Schmidt *et al*, 2011). The SCN, found in the anterior hypothalamus, is a highly coupled network of oscillators whose output synchronizes and coordinates the rhythmic activity of a number of subsidiary or “slave” oscillators throughout the brain and in peripheral tissues (Li *et al*, 2012; Quintero *et al*, 2003). In this way, daily molecular rhythms and activity patterns are set. While light is the most potent entraining cue or “zeitgeber,” from the German word “time keeper,” non-photic zeitgebers such as the availability of food or drugs of abuse can also act as signals around which animals consolidate their activity (Damiola *et al*, 2000).

At the molecular level, rhythms in gene and protein expression and activity exist in almost all cells in the body. Current estimates suggest that roughly 43% of the genome is rhythmic, the actual value may be higher as we continue to uncover cellular events under circadian or diurnal regulation (Zhang *et al*, 2014). The molecular basis of rhythm generation in mammals is a complex hierarchical series of interlocked transcriptional-translational feedback loops (TTFLs) with added regulatory control via kinase-dependent mechanisms (figure 1). Many homologous components of the molecular clock can be found in species as varied as *Neurospora crassa*, *Drosophila melanogaster*, rodents and humans (Mackey, 2007). Within the primary loop of the mammalian clock are the positive effectors, CLOCK (circadian locomotor output cycles kaput) and BMAL1 (brain and muscle ARNT-like protein 1).

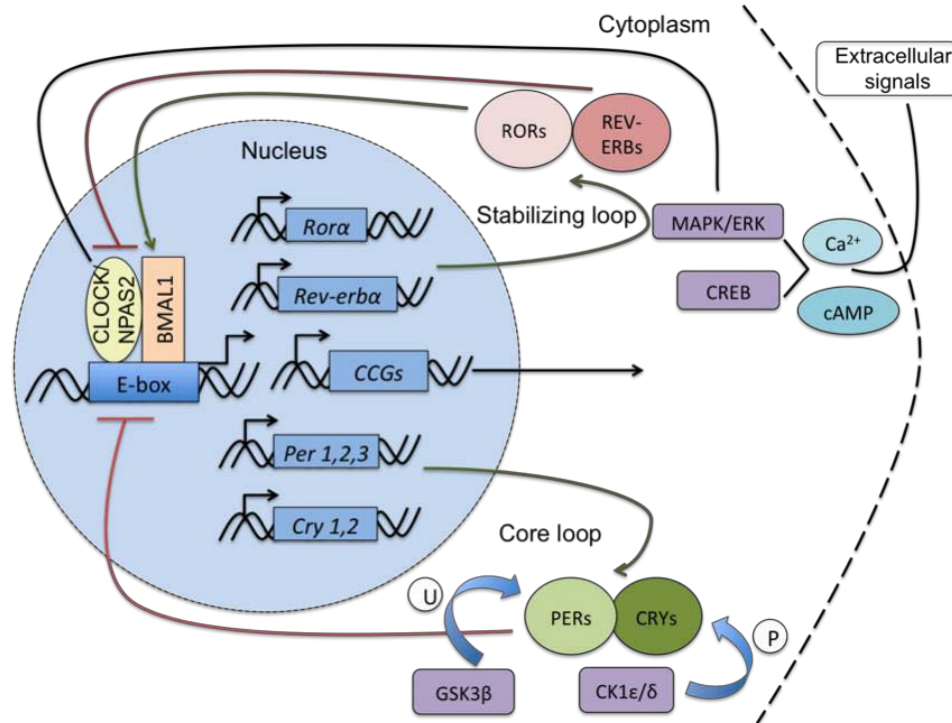


Figure 1. A series of transcriptional and translational feedback loops comprise the core molecular clock in mammals. At the heart of the clock are the transcription factors, CLOCK (or NPAS2) and BMAL1 which heterodimerize in the nucleus and bind to Enhancer Box (E-box) sequences in many genes to regulate their transcription. Targets include the *Per* and *Cry* genes. Over the course of 24 hours, PER and CRY proteins dimerize and shuttle back into the nucleus where CRY directly inhibits the CLOCK/NPAS2-BMAL1 complex, forming a negative feedback mechanism. Additionally, CLOCK/NPAS2 and BMAL1 also regulate the expression of nuclear hormone receptors, *Rev-erba* and *Rora*, which can repress or activate *Bmal1* transcription. Other regulatory proteins act on the clock through phosphorylation, including Casein kinase 1 proteins and ubiquitination by Glycogen synthase kinase beta. Intracellular calcium signaling cascades can also act to regulate the activity of core circadian proteins through kinase-dependent pathways. CCGs – Clock controlled genes; P – phosphorylation; U – ubiquitination. From (Parekh *et al.*, 2015).

These are bHLH-PAS domain-containing transcription factors that heterodimerize within the cytoplasm, enter the nucleus and bind to the canonical E-box sequence (CACGTG) in the promoter regions of Period (*Per1*, *Per2* and *Per3*) and Cryptochrome (*Cry1*, and *Cry2*) genes. Together, these genes make up the negative limb of the core feedback loop. In the cytoplasm, CRY and PER proteins form hetero- and homodimers, translocate to the nucleus and inhibit the activity of CLOCK/NPAS2-BMAL1 (Ko and Takahashi, 2006; Lowrey and Takahashi, 2011; McDearmon *et al*, 2006; Meijer and Schwartz, 2003). *Per* and *Cry* transcript and protein levels decline over time as their degradation is induced by casein kinase 1 δ (CK1 δ) and CK1 ϵ phosphorylation activity. This leads to a disinhibition of the CLOCK/NPAS2-BMAL1 complex, resetting the cycle. Ubiquitination by glycogen synthase kinase beta (GSK3 β), a serine/threonine protein kinase, also plays a role in regulating the inhibition of the complex by PER/CRY. The timing of accumulation and degradation of these circadian proteins is critical to maintaining the period and amplitude of rhythms (Lee and Kim, 2014; Lee *et al*, 2011). *Bmal1* expression is further regulated by a second, stabilizing loop feedback mechanism involving genes that encode the retinoic-acid-related orphan nuclear receptors REV-ERB α and ROR α , which bind the ROR element in the *Bmal1* promoter. ROR and REV-ERB proteins activate and repress expression of *Bmal1*, respectively, maintaining its robust rhythm *in vivo* (Preitner *et al*, 2002; Ripperger and Albrecht, 2012).

The transcriptional activity of the CLOCK/NPAS2-BMAL1 heterodimer is conferred by CLOCK's role as a histone acetyl transferase (HAT) (Doi *et al*, 2006). CLOCK HAT-dependent acetylation of histone H3 promotes transcription allowing for the "opening" of chromatin that is normally tightly condensed. This posttranslational modification of chromatin state provides access to the transcriptional machinery and thus the ability for the heterodimer to activate or repress

downstream genes involved in maintaining rhythms or other “clock-controlled genes” (CCGs) (Hardin and Yu, 2006). Importantly, the many CCGs that are targets of circadian transcriptional activation or repression are found in various regions throughout the central nervous system and periphery. A similar E-box-mediated transcriptional mechanism governs the regulation of these genes as well. Some of these genes have direct relevance in pathways important for normal and abnormal mood and reward-related behaviors in animals (McClung, 2007; Parekh and McClung, 2015).

1.1 CIRCADIAN RHYTHMS IN PSYCHIATRIC ILLNESS

The de-synchronization of circadian rhythms appears to be both a symptom and a precipitating feature of some neuropsychiatric conditions. Normal “phase shifting” of the endogenous clock in response to changing environmental stimuli is an adaptive mechanism that allows organisms to flexibly entrain to new conditions. However, phase shifting processes can be inappropriately activated in a modern industrialized society where light availability is constant (Karatsoreos, 2014). Dim light at night for instance, can offset normal circadian organization and contribute to depressed mood and reduced cognitive performance (Bedrosian and Nelson, 2013; Dunn *et al*, 2010). Furthermore, scheduled activity that is misaligned with internal time such as trans-meridian travel or shift work can exacerbate the negative effects of circadian disruption (Cho *et al*, 2000; Katz *et al*, 2001; Scott *et al*, 1997). The “social jet lag hypothesis” suggests that the weekly disturbances in sleep-wake rhythms imposed by work or school obligations, particularly in adolescence, correlate with affective and substance abuse disorders (Hagenauer and Lee, 2012; Wittmann *et al*, 2006). Consequently, sleep problems can cause individuals to self-

medicate through drug or alcohol abuse or to become depressed (Hasler and Clark, 2013; Hasler *et al*, 2015). Seasonal Affective Disorder (SAD), a condition in which individuals exhibit symptoms of depression during winter months occurs at a higher rate in populations living in temperate climates with seasonal variation in daylight hours (Lam and Levitan, 2000; Magnusson and Boivin, 2003). Compellingly, genome wide association studies (GWAS) link polymorphisms and other mutations in core circadian genes with predisposition towards SAD, major depression (MDD), addiction disorders and bipolar disorder (BD) which is characterized by spontaneous mood cycling through depressive, euthymic and manic phases (Benedetti *et al*, 2008; Kovanen *et al*, 2013; Soria *et al*, 2010; Kovanen *et al*, 2010; Mansour *et al*, 2009). McCarthy and Welsh provide a detailed description of known circadian gene variants in humans associated with mood disorders (figure 3). Almost all core circadian genes are represented (McCarthy and Welsh, 2012; McCarthy *et al*, 2012). A genetic basis for chronotype (preference for morning or evening consolidation of activity) in humans has been suggested by a number of studies (Carpen *et al*, 2005, 2006; Katzenberg *et al*, 1998). Chronotype plays a role in mood and addiction disorders where “eveningness” is characteristic of bipolar patients many of whom display co-morbid substance abuse problems (Broms *et al*, 2014; Etain *et al*, 2014; Kontinen *et al*, 2014; Zhang *et al*, 2015).

Circadian rhythms in the use and sensitivity to several different classes of drugs have been observed as well (Broms *et al*, 2011; Danel *et al*, 2003; Gallerani *et al*, 2001; Kosobud *et al*, 2007). Circadian gene variants and chronotype can also correlate with an abnormal response to reward (Hasler *et al*, 2012). A particular single nucleotide polymorphism (SNP) in the human *Period* gene, for instance, disrupts prefrontal reward responsivity and cortico-striatal activation following a rewarding stimulus (Forbes *et al*, 2012). These and other findings suggest an important role for circadian misalignment in the pathophysiology of mood and substance abuse disorders.

Gene	Strongest Association	Clinical Association	Reference
ARNTL	rs7107287	BD	Mansour, 2006
ARNTL	rs895682	BD	Mansour, 2006
ARNTL	rs2278749	BD	Nievergelt, 2006
ARNTL	rs2290035	Seasonal affective/winter depression	Partonen, 2007
CLOCK	rs1801260	BD—illness recurrence	Benedetti, 2003
CLOCK	rs10462028	BD	Soria, 2010
CLOCK	rs3736544	Fluvoxamine response (MDD)	Kishi, 2009
CLOCK	rs1801260	Chronotype in BD	Lee, 2010
CLOCK	rs2412646	Comorbid BD + alcohol	Sjöholm, 2010a
CRY1	rs2287161	BD + MDD	Soria, 2010
CRY2	rs10838524	Seasonal affective/winter depression	Lavebratt, 2010b
CRY2	rs10838524	Rapid-cycling BD	Sjöholm, 2010b
NPAS2	rs11541353 (S471L)	Seasonal affective/winter depression	Johansson, 2003
NPAS2	rs11123857	BD + MDD	Soria, 2010
NR1D1	rs2314339	BD	Kripke, 2009
NR1D1	rs2314339	Lithium response	Campos-De Souza, 2010
NR1D1	rs2071427	Lithium response	McCarthy, 2011
PER2	rs10462023	Depression	Lavebratt, 2010a
PER2	rs2304674	Seasonal affective/winter depression	Partonen, 2007
PER2	rs56013859 (10870)	Seasonal affective/winter depression	Partonen, 2007
PER3	rs2859387	Schizoaffective disorder	Mansour, 2006
PER3	rs228729	BD	Nievergelt, 2006
PER3	VNTR	BD—postpartum onset	Dallaspezia, 2011
PER3	VNTR	BD—age of onset	Benedetti, 2008
RORA	rs2028122	MDD	Lavebratt, 2010a
RORB	rs7022435	BD (pediatric)	McGrath, 2009
3-gene interaction	Multiple	BD	Shi, 2008

Figure 2. Variants of core circadian genes strongly associate with mood disorders in humans. An enrichment of mood disorder associations among core clock genes indicates that *Arntl* (BMAL1), *Clock*, *Cry1*, *Npas2*, *Nr1d1* (REV-ERB α), *Per3* and *Rorb* in particular are associated with aspects of bipolar disorder, onset of the disease, comorbidity with other psychiatric conditions or responsiveness to the main-line therapeutic agent, lithium. From (McCarthy and Welsh, 2012).

1.1.1 Central pathways involved in mood and reward regulation

Decades of preclinical and clinical investigations into the mechanisms of neuropsychiatric illness highlight the central role of proper signaling in several key brain regions to maintain biochemical and neurophysiological balance within circuits. Reward circuitry is directly impinged upon by drugs of abuse and is also the main site of dysregulation in some mood disorders including BD (van Enkhuizen *et al*, 2015; Russo and Nestler, 2013). In the traditional view of the reward system, projections between certain regions are highlighted as critical to the expression and maintenance of proper reward sensitivity and behavioral response. Among these are dopaminergic (DA) and GABAergic (gamma-aminobutyric acid) projections from the ventral tegmental area (VTA) and substantia nigra (SN) to the nucleus accumbens (NAc) and dorsal striatum (Str) respectively (Koob and Volkow, 2010; Russo and Nestler, 2013). Dopamine, a monoaminergic neurotransmitter, is a highly complex signaling molecule, however, a key feature of the midbrain DA system is to confer incentive salience to environmental stimuli and promote motivational or goal-directed action. Its function in reinforcement learning forms the basis for a model to explain the unique value of drugs of abuse over natural reinforcers (Berridge and Robinson, 1998; Nestler, 2005; Schultz, 2006; Schultz *et al*, 1997). Rapid pharmacokinetic effects of drugs on dopamine release may promote over-learning on drug-related stimuli or cues (Hyman, 2005). The VTA also sends afferent inputs to the prefrontal cortex (PFC), a major site of executive function and cognitive control over behavior, and in humans, abnormal dopaminergic signaling within the PFC has been correlated with a drug-addicted state (Ballard *et al*, 2011; Juarez and Han, 2016).

The NAc is considered to be an integrator of sensorimotor and limbic information to gate emotional responses and drive appetitive and aversive behaviors (Goto and Grace, 2008; Richard *et al*, 2013). Its extensive afferent and efferent connections serve to underscore this function.

Chiefly, the NAc receives glutamatergic inputs from the PFC, amygdala (Amy) and hippocampus (Hipp) and provides GABAergic input to the VTA as well as the ventral pallidum (VP) (Britt *et al*, 2012; Tye, 2012). GABAergic medium spiny projection neurons (MSNs) serve as the output cells and make up approximately 90-95% of the NAc. Smaller populations of cholinergic and parvalbumin interneurons regulate the activity of the MSNs (Kauer and Malenka, 2007). Two major subclasses of MSNs predominantly express either dopamine 1-like (D1) or 2-like (D2) receptors (Le Moine and Bloch, 1995). These G-protein coupled receptors (GPCRs) differ in their intracellular signaling mechanisms in response to dopamine, effects on intrinsic excitability and synaptic transmission of MSNs, peptide expression and projection pathways (Lu *et al*, 1998). Generally, D1-containing MSNs belong to the striatonigral direct pathway while D2 MSNs comprise the striatopallidal indirect pathway. Activation of these distinct pathways has been shown to produce divergent effects on reward related behavior with direct pathway stimulation promoting reward value and seeking and indirect pathway activation attenuating reward-related behavioral responses (Baik, 2013; Gerfen *et al*, 1990; Kravitz *et al*, 2013; Smith *et al*, 2013).

While direct projection targets of the SCN, including the medial pre-optic area (mPOA) and dorsomedial hypothalamic nucleus (DmH) are not central to the reward circuitry, they may modulate it through indirect neural connections (Mendoza and Challet, 2014). Orexinergic neurons in the DmH for instance encode information about arousal, energy balance and reward and project to the VTA (Aston-Jones *et al*, 2001, 2009). The dorsal raphe nuclei of the midbrain receive direct light input from the circadian visual system and also indirect input from the SCN and are the primary regions containing serotonin (5-HT) neurons in the brain (Ciarleglio *et al*, 2011; Morin, 2013). Serotonergic neurotransmission is involved in the regulation of mood and a widely utilized class of antidepressants targets the 5-HT re-uptake mechanism (SSRIs)

(Anguelova *et al*, 2003; Lucas *et al*, 2007). Interestingly, this system is affected by photoperiod, where day length during development can alter firing properties of 5-HT neurons as well as extracellular levels of the neurotransmitter and norepinephrine. These light-induced changes further affect anxiety and depressive-like behavior (Green *et al*, 2015). The lateral habenula (LHb) in the midbrain also receives direct SCN input and has been shown to be an important inhibitor of DAergic activity in the VTA, thus exerting a more robust influence over mood and reward regulation (Bourdy and Barrot, 2012; Lecca *et al*, 2012). Each of these critical extra-SCN brain regions maintains rhythms and expresses circadian genes and proteins with clock and non-clock regulatory functions (Parekh and McClung, 2016). They therefore control mood and reward behavior through both circuit-level and molecular mechanisms.

1.1.2 Bipolar disorder and the clock

Mental illness and affective disorders in particular are a leading cause of disability worldwide according to the World Health Organization. The Diagnostic and Statistical Manual of Mental Disorders, Fifth Edition (DSM-5) defines bipolar I disorder as being characterized by at least one manic episode with ‘...abnormally and persistently elevated, expansive or irritable mood and abnormally and persistently increased activity or energy...’ Manic episodes also present with certain hallmarks including a decreased need for sleep and increased goal-directed activity and high-risk behaviors. Individuals can experience major depressive episodes preceding or following manic episodes with periods of euthymic or normal mood in between (figure 3). The severity of mood disturbance is sufficient to produce marked impairments in individuals’ social or occupational functioning. The prevalence of the disorder among adults in the U.S. is estimated to be approximately 2.5% of the population and co-morbidity with other conditions including anxiety

and substance abuse disorders is common (DSM-V). Sleep disturbances as well as the general cyclic nature of mood states characterizing BD have led researchers to speculate about circadian abnormalities underlying the illness (McClung, 2013; Melo *et al*, 2016; Mendlewicz, 2009). Symptoms can be tied to seasonal variation and shifts in mood state can be precipitated by erratic changes in daily activity schedules (McClung, 2013). The mood-stabilizing effects of tightly regulating sleep/wake schedules further underscore the importance of the clock in BD (Wirz-Justice *et al*, 2005). Social Rhythm Therapy and chronotherapeutics represent novel strategies to combat rhythm misalignment in patients and lessen the severity of symptoms (Coogan and Thome, 2011; Dallspezia *et al*, 2015; Haynes *et al*, 2016; Henriksen *et al*, 2016). Additionally, traditional mood stabilizers such as the antipsychotic compounds, lithium and valproate, have been shown to increase circadian period in rodents and humans and to change expression profiles of circadian genes (Landgraf *et al*, 2016; Milhiet *et al*, 2014). Together, these abnormalities may serve as trait markers of susceptibility for BD.

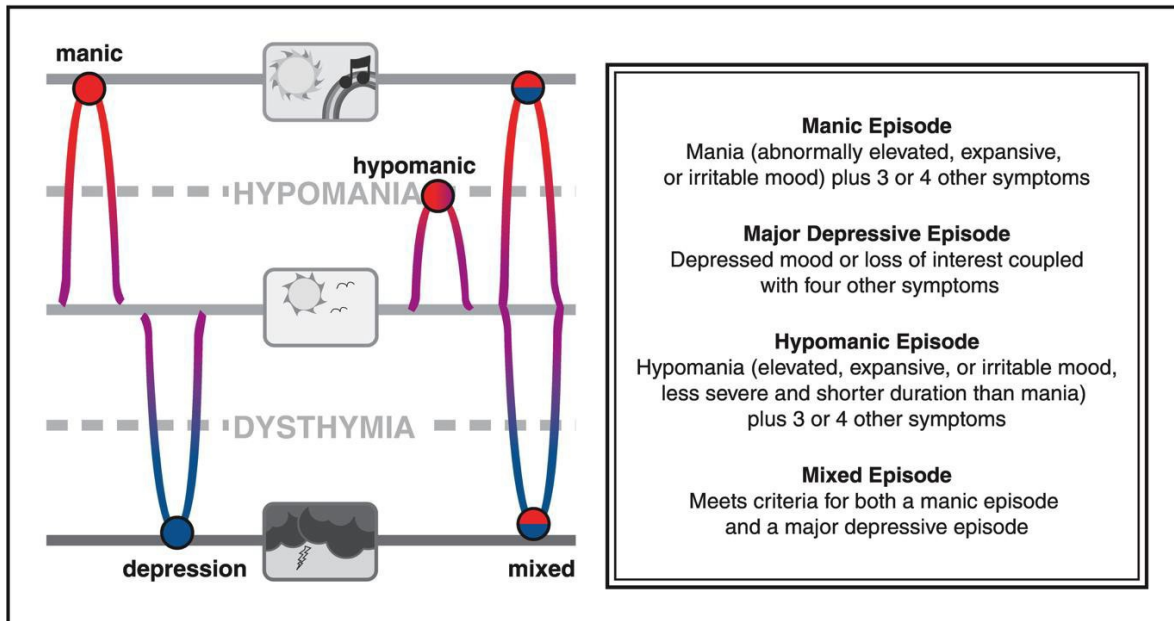


Figure 3. Hallmarks of bipolar I disorder. Distinct phases illness episodes in BD must meet DSM-V criteria and be characterized by a number of symptoms that distinguish the disease from others such as generalized anxiety, unipolar depression, or pharmacological features of drug abuse. A manic episode persisting for at least one week followed by euthymic or dysthymic states, hypomania or mixed states must occur for a BD diagnosis. From Stahl's Essential Psychopharmacology, 4thed.

Numerous human genetic studies have identified positive associations between core circadian genes including *Clock*, *Npas2*, *Bmal1*, and *Per3* with BD (Milhiet *et al*, 2014). A particular single-nucleotide polymorphism (SNP) in the 3'UTR of *Clock* (3111 T to C) is associated with a higher rate of bipolar episodes, as well as sleep disruption in bipolar patients (Benedetti *et al*, 2003, 2007). Recent work from our lab provides further evidence of functional consequences of the 3111T/C SNP. CLOCK-deficient mouse embryonic fibroblasts (MEFs) transfected with the human mutant construct showed altered expression, function and stability of *Clock* transcript (Ozburn *et al*, 2016). Additionally, haplotypes and SNPs in *Bmal1* have been found to significantly associate with BD (Mansour *et al*, 2006). These and other studies suggest a

strong implication of the molecular clock in the underlying mechanisms contributing to the development and progression of BD.

1.1.3 Circadian rhythms in addiction

Addiction is a widespread public health issue with social and economic ramifications. Koob and Volkow (2010) review decades of clinical and pre-clinical studies showing that discrete aspects of mesocorticolimbic circuitry are engaged during binge drug use, withdrawal/negative affect, and relapse, encompassing all stages of the addiction cycle (Koob and Volkow, 2010). Drugs of abuse including alcohol, cocaine, methamphetamine, and opioids act directly on the dopamine system and other signaling pathways to promote seeking behavior. Generally, these substances elicit their effects by increasing dopamine release from the VTA to its target regions (Kauer and Malenka, 2007). Drugs of abuse can alter rhythmicity of core clock genes and the activity of these genes can in turn affect the expression of proteins important for plasticity suggesting a bidirectional relationship between the circadian and reward systems (Falcon *et al*, 2013; Lynch *et al*, 2008; Ozburn *et al*, 2015).

Addictive drugs are able to serve as zeitgebers and can reliably entrain anticipatory activity rhythms in animals when given regularly. This locomotor activity has been likened to the seeking behavior characteristic of drug addiction. For example, daily methamphetamine injections have been shown to entrain animals and induce anticipatory locomotor activity to the time of injection (Kosobud *et al*, 1998). Ethanol, cocaine, and nicotine are all able to induce this anticipatory behavior and alter behavioral rhythms (Gillman *et al*, 2010; Kosobud *et al*, 2007; White *et al*, 2000). Diurnal variations in amphetamine-induced locomotor activity, conditioned place preference for amphetamine, and the expression of *TH* mRNA in the VTA and NAc have also

been observed (Webb *et al*, 2010). In rodents with SCN lesions methamphetamine in the drinking water restores activity rhythms in a robust manner (Masubuchi *et al*, 2000). Rewarding stimuli such as food or chocolate can entrain both behavioral and *Per1* expression rhythms, which persist for several days in several brain regions (including dorsal medial hypothalamus, NAc, PFC, and the central amygdala) (Angeles-Castellanos *et al*, 2008). Therefore, both behavioral and molecular rhythms appear to be affected by rewarding stimuli, and especially potently by drugs of abuse.

1.1.4 Circadian regulation of reward-related regions and dopaminergic transmission

The role of circadian genes in the direct regulation of dopaminergic reward circuitry has been well established. Within mesolimbic nuclei, virtually all aspects of dopaminergic activity including neuronal firing patterns, neurotransmitter synthesis, release, degradation and postsynaptic actions are subject to circadian transcriptional influence and display diurnal variation (McClung, 2007). This regulation of signaling is important for reward-related behavior as all drugs of abuse exert their actions by impinging on dopaminergic circuitry and any disruption of this system may increase vulnerability to the rewarding properties of drugs (Kauer and Malenka, 2007). Additionally, diurnal variation in dopaminergic neuronal activity may underlie the diurnal variation in behavioral responses to drugs as previously described. While it has long been thought that VTA DA neurons do not have a diurnal rhythm in firing rate, a recent study suggests that this may not be the case as an intradiurnal rhythmic pattern of VTA DA neuronal activity has been measured in anesthetized rats (Domínguez-López *et al*, 2014). Furthermore, the rhythm in extracellular levels of DA appears to be governed by a rhythm in the expression and activity of the dopamine transporter (DAT) (Ferris *et al*, 2014). It is still unclear whether a strong link exists

between firing and extracellular release of DA however in behaving animals. More work is needed to concretely establish these mechanisms.

Within the VTA, rhythms have been observed in the expression of DA receptors as well as tyrosine hydroxylase (TH) and monoamine oxidase (MAOA), the enzymes responsible for the synthesis and degradation of DA respectively (McClung *et al*, 2005; Hampp *et al*, 2008; McClung, 2007; *et al*, 2007; Sleipness *et al*, 2008; Weber *et al*, 2004). There is also evidence to support the idea that these regulatory genes may be clock-controlled genes (CCGs), as they contain canonical E-box sites in their promoter regions and are bound by CLOCK and BMAL1 (Sleipness *et al*, 2007; Hampp *et al*, 2008). Moreover, diurnal variations in extracellular levels of the neurotransmitters, DA, glutamate and GABA have been described in the NAc (Castañeda *et al*, 2004). Our lab has demonstrated that cholecystokinin (CCK), a peptide negatively associated with DA activity *in vivo* and implicated in anxiety and drug response, is also a direct gene target of CLOCK (Arey *et al*, 2014). In a recent study from our group, chromatin immunoprecipitation followed by deep sequencing (ChIP-seq) revealed a role for NPAS2 in directly regulating the expression of the dopamine D3 receptor subtype in the striatum of mice (Ozburn *et al*, 2015). This receptor is often found co-localized with D1Rs on striatal MSNs and is involved in mediating rewarding effects of cocaine (Sokoloff *et al*, 2001).

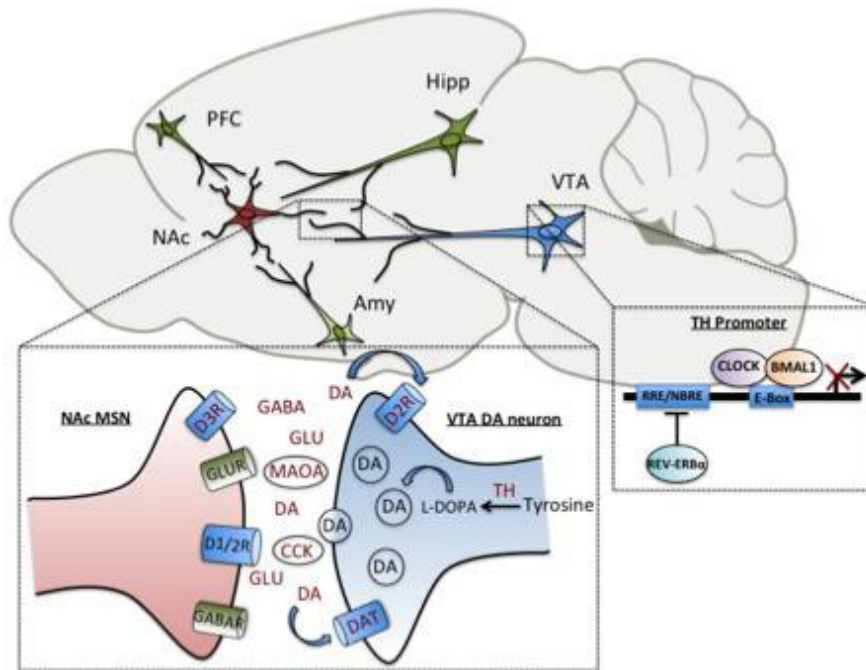


Figure 4. Elements of dopaminergic transmission are directly under circadian control. Within the VTA-NAc circuitry, clock genes regulate the transcription of several genes involved in the synthesis, uptake, transmission and degradation of dopamine, including tyrosine hydroxylase (TH), dopamine transporter (DAT), pre-synaptic dopamine type-2 receptor (D2R), dopamine type-3 receptor (D3R), monoamine oxidase A (MAOA), and cholecystokinin (CCK). Within the NAc, diurnal rhythms in levels of the neurotransmitters, dopamine, glutamate and GABA have been measured as well. The transcription of TH is repressed by the circadian transcription factor, CLOCK as well as the nuclear receptor, REV-ERBa, which bind to enhancer box (E-Box) and ROR response element (RRE) sites in the promoter region, respectively. From (Parekh and McClung, 2016).

The lateral habenula (LHb) in the midbrain also receives direct SCN input and has been shown to be an important inhibitor of DAergic activity in the VTA, thus exerting a more robust influence over mood and reward regulation (Bourdy and Barrot, 2012; Guilding *et al*, 2010; Lecca *et al*, 2012). The neuronal activity of the LHb and medial habenula (MHb) shows rhythmic oscillation both *in vitro* and *in vivo* and firing rates of neurons in both of these regions are altered in response to retinal illumination *in vivo*. The LHb maintains endogenous molecular rhythms as

well with oscillations in *Per2* gene and protein levels across the light/dark cycle. Temporal variation in electrophysiological properties in each of these neuronal populations is absent in mice lacking a functional intracellular molecular clock. These findings support the idea that intrinsic circadian signals can shape the contribution of habenular nuclei to affective and reward behavior (McCarthy and Welsh, 2012; Sakhi *et al*, 2014; Zhao and Rusak, 2005). Another reward-related region in the thalamus, the paraventricular nucleus (PVT), which sits at the midline and projects to many limbic structures including the NAc, also displays rhythms in activity. The PVT receives input from the SCN and the DmH and has been shown to play role in the anticipatory locomotor response to food. The firing rate of PVT neurons varies throughout the day with greatest activity seen during the animal's active phase (Alamilla *et al*, 2015; Colavito *et al*, 2015; Kirouac, 2015; Kolaj *et al*, 2012). The influence of this small nucleus on reward sensitivity and drug seeking is beginning to be further elucidated (Dayas *et al*, 2008; Matzeu *et al*, 2014). Work from the Aston-Jones lab has provided insights into the circadian regulation of activity of noradrenergic neurons in the locus coeruleus (LC), a key mediator of wakefulness and behavioral arousal. Using single-unit recordings of LC neurons in anesthetized rats, they have demonstrated that the neurons fire significantly faster during the active phase compared with rest phases. Additionally, the diurnal rhythm of noradrenergic neuronal activity correlates with the rhythm of activation of DmH orexin neurons, which project preferentially to the LC (Gompf and Aston-Jones, 2008; González and Aston-Jones, 2006). These findings suggest that important aspects of neuronal activity throughout the brain are under circadian influence and that the rhythmic activity of mood and reward-related regions may be relevant for behavioral outcomes.

1.2 ANIMAL MODELS OF NEUROPSYCHIATRIC ILLNESS

The value of animal models to understand mechanisms underlying disorders of the central nervous system cannot be overstated. From early plant and invertebrate models we have pieced together the mechanisms of the interlocked feedback loops behind circadian rhythm generation and maintenance (Mackey, 2007). Additionally, self-report measures in humans have been reliable in understanding how natural zeitgebers influence individual phase of entrainment or chronotype, a factor that has been linked to mood states and reward response (Horne and Ostberg, 1976). Technological advances can extend the functionality of questionnaire-based self-report measurements. The use of a smartphone app to monitor daily eating patterns in humans, for instance, has revealed a largely erratic rhythm, deviating from the commonly reported “3 meals a day” structure (Gill and Panda, 2015). This information has relevance for individual metabolic health and epidemiological issues regarding obesity. Furthermore, cells derived from human psychiatric patients have been a fruitful model of molecular changes in SCN and SCN-independent clocks. Reporters of rhythmic clock gene expression in patients’ cells show correlations with severity of alcohol use disorders and predict lithium sensitivity in BD (McCarthy *et al*, 2013a, 2013b). Blood biomarkers, inducible pluripotent stem cells (iPSCs) and skin fibroblasts have all yielded a wealth of information about cellular abnormalities in disease state suggesting diagnostic potential (McCarthy and Welsh, 2012).

Rodent models, however, are particularly useful in providing clues about how the biological clock system interacts with neurobiological systems relevant for psychiatric illness. Basic evidence for a role of the SCN clock in mood comes from lesion studies demonstrating an anti-depressant effect of bilateral SCN lesions in rats (Tataroglu *et al*, 2004). In an attempt to

model zeitgeber effects on behavior in rodents, a number of studies have utilized circadian misalignment paradigms. Long and short photoperiods, or light phases produce desynchrony of internal clocks to various degrees of severity (Craig and McDonald, 2008; Johnson *et al*, 2003). Chronic constant light or darkness can both lead to depression and anxiety-like behavior with constant light also dramatically dampening circadian patterns in the hormones, melatonin and corticosterone (Tapia-Osorio *et al*, 2013). Recently, a depressive-like phenotype including anhedonia, a loss of interest in once pleasurable activity, and sexual dysfunction has been described in rats undergoing exposure to a 22-hr light/dark cycle (LD22). This forced desynchrony of the central clock also altered levels and turnover of monoamines in the PFC (Ben-Hamo *et al*, 2016). These findings expand upon earlier results indicating monoamine content and metabolism in the hippocampus and amygdala of mice are disrupted by constantly shifting light-dark cycles (Moriya *et al*, 2015). Other theories have been put forth suggesting that internal desynchronization or bifurcation of SCN rhythms in mammals might underlie rapid cycling manic-depressive disorders or mania (Kripke *et al*, 2015). Together, these and other important findings point to the variety of valuable techniques to probe the influence of the circadian system on affective and reward-related behavior.

Building upon information gained from more crude lesion studies, Landgraf and colleagues have more recently shown that direct disruption of SCN circadian rhythms by viral-mediated knockdown of the core circadian gene, *Bmal1*, produces a behavioral phenotype including helplessness, behavioral despair and anxiety-like behavior (Landgraf *et al*, 2016). Rapid progress in forward genetic approaches has revolutionized the study of gene and environment contributions and interactions in disease susceptibility and progression. Sophisticated and precise mutations in clock genes allow for the systematic characterization of their roles in regulating behavior.

1.2.1 Genetic models of bipolar mania

Several models of mania have been described to elucidate the pathophysiology of bipolar mania; Logan and McClung (2016) thoroughly review and evaluate these. Many of these models utilize genetically modified mice to target particular genes, proteins or pathways known to be important for mood and reward regulation. As with all animal models, it is not possible to capture the full spectrum of a complex human disorder in any one manipulation. However, aspects of these models represent face, construct or predictive validity (Logan and McClung, 2016). While the DSM-V distinguishes a manic episode from the behavioral effects of psychostimulant drug exposure, amphetamine-induced hyperactivity has long been considered a model of mania because of its responsiveness to acute anti-psychotic treatment (Gould *et al*, 2001; Young *et al*, 2011). Additionally, amphetamine produces reliable alterations in mesolimbic dopamine circuitry that resemble those seen in BD patients, particularly an elevation of extracellular dopamine (Cousins *et al*, 2009).

One widely used mutant model of mania is the dopamine transporter knockdown mouse (DAT-KD). Neuroimaging evidence suggests altered DA neurotransmission in un-medicated BD patients may be a result of lowered DAT expression in the SN (Pinsonneault *et al*, 2011) and reduced DAT availability in striatal regions (Anand *et al*, 2011). The human Behavioral Pattern Monitor (BPM) is used to characterize hyperactivity and increased exploration in BD patients and has been modified by Young and colleagues to assess manic-like behavior in mice. They have found that DAT-KD mice show a similar BPM profile as well as high-reward risk-preference consistent with BD (Gould *et al*, 2001; Young *et al*, 2011b). Impulsivity as measured by the Iowa Gambling Task (IGT) is another hallmark of BD sufferers and a feature shared by DAT-KD mice performing a rodent version of the assay (van Enkhuizen *et al*, 2013). Therefore, findings using

this model suggest that impaired function of the dopamine transporter may lead to a hyperdopaminergic state that negatively impacts decision making and promotes risky, goal-directed and impulsive actions.

Polymorphisms in the circadian gene, *Clock*, have been associated with manic features in BD (Benedetti *et al*, 2003; Serretti *et al*, 2003) and perhaps the most well characterized genetic mouse model of mania is the *Clock* Δ 19 mutant mouse. A single nucleotide transversion leads to an excision of exon 19 in the *Clock* gene of these mice, producing a dominant negative protein that is capable of dimerization with BMAL1 and E-box binding but dysfunctional in transcriptional activity (King *et al*, 1997). Aspects of circadian rhythm disruption in mutants are similar to those seen in BD patients including reduced circadian amplitude and delayed phase (Rock *et al*, 2014; Vitaterna *et al*, 2006) as well as sleep disturbances (Naylor *et al*, 2000). In measures of affective behavior, *Clock* mutants exhibit increased locomotor activity in response to novelty, reduced anxiety-like and depression-like behavior, and increased intracranial self-stimulation (ICSS) at a lower threshold (Easton *et al*, 2003; McClung *et al*, 2005; Roybal *et al*, 2007).

Clock can act as a negative regulator of drug reward. Our group has identified a key role for the *Clock* gene in mediating the effects of drugs of abuse. *Clock* Δ 19 mice exhibit increased cocaine conditioned place preference (CPP), a measure of reward sensitivity, compared with wildtype (WT) littermates (McClung *et al*, 2005). Ozburn and colleagues further examined whether results from the conditioned reward study were relevant to cocaine intake using a clinically relevant operant intravenous cocaine self-administration paradigm (IVSA). They found that WT mice exhibit a diurnal variation in acquisition and maintenance of drug intake that is absent in *Clock* Δ 19 mice. A greater percentage of *Clock* mutant mice acquired cocaine self-administration, regardless of time of day tested. Furthermore, mutant mice self-administered more cocaine than WT mice (Ozburn *et al*, 2012). Using fixed ratio (to assess sensitivity to reinforcing

properties of cocaine) and progressive ratio (to assess motivation for cocaine) schedules of reinforcement dose-response paradigms, they also found that cocaine is a more efficacious reinforcer in *Clock* Δ 19 mice compared with WT littermates. Importantly, *Clock* Δ 19 mice exhibited similar learning and readily acquired food self-administration (Ozburn *et al*, 2012). *Clock* Δ 19 mutants also show enhanced preference for the rewarding aspects of ethanol and sucrose and have an increase in dopaminergic activity in the VTA, which is normalized by chronic lithium treatment (McClung *et al*, 2005; Coque *et al*, 2011; Ozburn *et al*, 2013). Many of the mutant behavioral and physiological phenotypes are rescued by expressing functional CLOCK in the VTA or are recapitulated by reducing *Clock* expression in the VTA of WT mice via RNA interference, however this leads to a mixed-manic state (Mukherjee *et al*, 2010; Roybal *et al*, 2007). The key manic-like characteristics of *Clock* Δ 19 mutants are compared with symptoms of human bipolar mania in Table 1.

Table 1. The *Clock* Δ 19 mutant mouse as a model of bipolar mania. The behavioral phenotype of *Clock* Δ 19 mice closely resembles characteristics of human mania.

Human Bipolar Mania	<i>Clock</i>Δ19 mutation
Increased activity and psychomotor agitation	Locomotor hyperactivity in response to novelty (Roybal et al., 2007)
Decreased need for sleep	Reduced and fragmented sleep; altered REM patterns (Naylor et al., 2000)
Excessive involvement in potentially painful activities	Increased exploratory drive and risk-taking behavior (Roybal et al., 2007; Easton et al., 2003; Young et al., 2011)
Persistently elevated or expansive mood; Euphoric feelings	Decreased depressive-like behavior (Roybal et al., 2007)
Increased goal-directed activity	Greater sensitivity to rewarding substances including cocaine, ethanol and sucrose (McClung et al., 2005; Ozburn et al., 2012, Ozburn et al., 2013)
Spontaneous cycling into alternative mood states	Diurnal mood cycling between manic-like and euthymic states (Sidor et al., 2015)
Treatment of mood symptoms by lithium chloride	Reversal of mood phenotype by chronic lithium treatment (Roybal et al., 2007)

Subcortical, striato-thalamic and prefrontal circuit dysfunction has also been described in BD (Strakowski *et al.*, 2005). Imaging studies of BD patients have revealed a functional imbalance between hyperactive limbic areas and hypoactive cognitive areas, circuitry that is also important for the processing of rewarding stimuli (Lois *et al.*, 2014; Edwards and Koob, 2010). The synchronization and coherence of neural activity across brain regions is thought to be important for normal anxiety-like behavior and cognitive functions (Dzirasa *et al.*, 2010). In addition to abnormalities in dopaminergic signaling, *Clock* Δ 19 mice also exhibit alterations in cortico-striatal signaling that are indicative of aberrant behavior. When exploring a novel environment, *Clock* Δ 19 mice, have been shown to have profound deficits in cross-frequency phase coupling of NAc delta (1-4Hz) and low gamma (30-55Hz) oscillations, which correlate with enhanced exploratory drive (Dzirasa *et al.*, 2010). The entrainment of NAc neurons to afferent input has been theorized to

depend upon the balance of synaptic weights. Shifting of these weights can influence behavior (Wolf *et al*, 2005). Dopamine is known to modulate glutamatergic signaling within the NAc, providing a possible mechanistic avenue through which cortical-striatal circuitry could be impaired in *Clock* mutants and manic patients. The specific mechanisms contributing to circadian regulation of synaptic dysfunction in mesocorticolimbic areas remain poorly understood. Therefore, it will be important to systematically interrogate these systems, making use of appropriate models.

1.3 DISSERTATION AIMS

Studies contained within this dissertation focus on NAc excitatory signaling as potentially critical for *Clock* Δ 19 manic-like behavior, and additionally seek to uncover the role of NPAS2 in glutamatergic transmission in the NAc as it relates to reward behavior. The central hypothesis of this study is that disrupted AMPAR-mediated synaptic transmission at NAc MSNs underlies reward-related behavioral abnormalities in *Clock* Δ 19 mice. Additionally, we hypothesize that NPAS2 regulates excitatory synaptic strength and reward sensitivity through cell-type specific mechanisms in the NAc. We test these hypotheses through the following experimental aims:

Aim 1: Identify baseline changes in glutamatergic synaptic strength and intrinsic excitability of MSNs in *Clock* Δ 19 mice and the diurnal profile of GluA1 expression in the NAc.

Aim 2: Manipulate AMPAR-mediated signaling in the NAc of *Clock* Δ 19 mice and assess the impact on mood and reward-related behavior.

Aim 3: Determine the cell-type specific effects of NPAS2 knockdown on glutamatergic synaptic strength in WT MSNs as well as the conditioned reward response.

2.0 ALTERED GLUA1 FUNCTION AND ACCUMBAL SYNAPTIC PLASTICITY IN THE *CLOCK* Δ 19 MODEL OF BIPOLAR MANIA

Parekh PK, Becker-Krail D, Sundaravelu P, Ishigaki S, Okado H, Sobue G, Huang YH, and McClung CA. (Under revision for *Biological Psychiatry*)

Disruptions in circadian rhythms are associated with an increased risk for bipolar disorder (BD). Moreover, studies show that the circadian protein CLOCK is involved in regulating monoaminergic systems and mood-related behavior. However the molecular and synaptic mechanisms underlying this relationship remain poorly understood. Using *ex vivo* whole cell patch clamp electrophysiology in *Clock* Δ 19 mutant and wildtype (WT) mice we characterized alterations in excitatory synaptic transmission, strength and intrinsic excitability of nucleus accumbens (NAc) neurons. We performed protein crosslinking and Western blot analysis to examine surface and intracellular levels and rhythm of the glutamate receptor subunit, GLUA1, in the NAc. Viral-mediated overexpression of *GluA1* in the NAc and behavioral assays were also used. Compared with WT mice, *Clock* Δ 19 mice display reduced AMPAR-mediated excitatory synaptic responses at NAc medium spiny neurons (MSNs) across the light/dark cycle. These alterations are likely postsynaptic as presynaptic release of glutamate onto MSNs is unaltered in mutants. Additionally, NAc surface protein levels and the rhythm of GLUA1 are decreased in *Clock* Δ 19 mice diurnally, consistent with reduced functional synaptic response. Furthermore, we observed a significantly

hyperpolarized resting membrane potential of *Clock* Δ 19 MSNs suggesting lowered intrinsic excitability. Lastly, overexpression of functional *GluA1* in the NAc of mutants was able to normalize increased exploratory drive and reward sensitivity behavior. Together, our findings demonstrate that NAc excitatory signaling via GLUA1 expression is integral to the effects of *Clock* gene disruption on “manic-like” behaviors.

2.1 INTRODUCTION

Recently, BD has been re-conceptualized by some as a synaptic disorder where the functions of various postsynaptic proteins are altered in prefrontal and striatal regions, potentially producing circuit-level consequences affecting normal mood and reward response (Meador-Woodruff *et al*, 2001; De Bartolomeis *et al*, 2014). Additionally, mood-stabilizing agents exert some of their effects by acting directly on elements of synaptic activity including glutamatergic transmission (De Bartolomeis *et al*, 2014; Du *et al*, 2004). *Clock* Δ 19 mice are hyperdopaminergic, displaying elevated ventral tegmental area (VTA) dopamine neuron activity and dopamine synthesis in the nucleus accumbens (NAc) (McClung *et al*, 2005; Spencer *et al*, 2012; Coque *et al*, 2011). Dopamine reliably modulates the activity of glutamate at MSN synapses via G-protein coupled receptor signaling, having implications for substance abuse and mood disorders (Nicola *et al*, 2000; Beurrier and Malenka, 2002; Russo and Nestler, 2013). Moreover, PET studies of unmedicated BD patients indicate significantly lower striatal dopamine transporter (DAT) availability suggesting abnormal DA transmission and reward processing in this region (Anand *et al*, 2011). Along with decreased DAT transcript and protein levels in BD post-mortem cortical tissue and the correlation between DAT gene polymorphisms with predisposition to BD, there is

strong evidence to support the role of dopamine homeostatic dysregulation in the disorder (Greenwood *et al*, 2006; Rao *et al*, 2012). Dopamine receptor density changes are somewhat inconsistent however glutamatergic abnormalities are more clearly seen in BD patients. Findings have reported reduced levels of ionotropic glutamate receptor α -amino-3-hydroxy-5-methyl-4-isoxazolepropionic acid (AMPA) subunits in cortical areas of mood disorder subjects and reduced gene expression of the GluA1 subunit in striatal regions of BD patients (Beneyto and Meador-Woodruff, 2006). Additional proteins associated with the structural integrity of the postsynaptic density and proper trafficking of glutamate receptors to the membrane, including the scaffolding protein, PSD-95, and synapse-associated protein 102 (SAP102), have been found to be altered in post-mortem brains of BD patients (Sans *et al*, 2003; Kristiansen and Meador-Woodruff, 2005). These alterations may potentially lead to disruptions in excitatory signaling in mesocorticolimbic brain regions affecting mood and reward behavior. Additionally, polymorphisms in N-methyl-D-aspartate (NMDA) glutamate receptor genes correlate with susceptibility to BD (Mundo *et al*, 2003; Martucci *et al*, 2006). Given the importance of dopamine-glutamate interaction at postsynaptic sites for normal synaptic plasticity processes, it will be critical to follow up these findings with functional studies in disease models.

The consequences of *Clock* disruption on network activity in mesocorticolimbic circuitry have been investigated in greater depth. In a previous study we reported reduced total NAc protein levels of the α -amino-3-hydroxy-5-methyl-4-isoxazolepropionic acid (AMPA) type glutamate receptor subunit, GLUA1, and phosphorylated GLUA1 (P-GLUA1 Ser⁸⁴⁵) as well as changes in MSN dendritic morphology in *Clock* Δ 19 mice. Furthermore, diminished cross-frequency phase coupling of neural oscillations within the NAc and coherence with cortico-limbic regions during exploration of a novel environment have also been described in mutants (Dzirasa *et al*, 2010). NAc phase coupling is dependent upon glutamatergic signaling and computational models suggest that

altered AMPAR and NMDAR function can shift synaptic weights, disrupting the ability of MSNs to entrain to afferent input (Wolf *et al*, 2005). It has been proposed that this imbalance within accumbal circuitry can alter functioning of downstream target regions within the networks that regulate goal-directed behavior (Dzirasa *et al*, 2010). Given the increased dopaminergic tone of *Clock* Δ 19 mice, we hypothesized that there would be adaptations in NAc microcircuitry indicative of plasticity.

Here we sought to investigate the effects of *Clock* gene disruption on excitatory drive onto NAc MSNs as well as the expression and rhythm of accumbal GLUA1 protein and intrinsic excitability of MSNs. While rhythms in DA, glutamate and GABA neurotransmission have been demonstrated in the NAc (Castañeda *et al*, 2004), *ex vivo* electrophysiological studies of diurnal activity in excitatory synaptic function have largely been limited. We therefore conducted our physiological and biochemical measures across the light/dark cycle. Additionally, we examined whether manipulation of *GluA1* in the NAc could normalize aspects of the “manic-like” behavioral profile in *Clock* Δ 19 mice.

2.2 MATERIALS AND METHODS

2.2.1 Animal use

Clock Δ 19 mice were created by *N*-ethyl-*N*-nitrosurea (ENU) mutagenesis, resulting in a dominant-negative CLOCK protein deficient in transcriptional activity (King *et al*, 1997). *Clock* mutant (*Clock*/*Clock*) and wildtype (+/+) littermates on a BALB/cJ and C57BL/6J mixed background were bred from heterozygote (*Clock* Δ 19 /+) pairs and group housed. Animals used in this study

were maintained on a BALB/cJ background. Male and female mutant and WT mice (6-9wks) were used for electrophysiological experiments and male mice (8-12wks) were used for biochemical and behavioral experiments. The use of younger mice for ease of electrophysiological studies was justified, as hyperactivity in response to novelty, a key manic-like feature of *Clock* Δ 19 mice was apparent within this age range (data not shown). Mice were maintained on a 12:12h light/dark cycle (ZT 0 = lights on 7:00AM; ZT 12 = lights off 7:00PM) or a reverse 12h light cycle for dark phase experiments. For 24hr time-series experiments, mice were group housed in temperature-controlled, soundproof cabinets with light cycles precisely regulated. Food and water were available *ad libitum*. All animal use was conducted in accordance with the National Institute of Health guidelines for the care and use of laboratory animals and approved by the Institutional Animal Care and Use Committee of the University of Pittsburgh.

2.2.2 NAc slice preparation

Clock mutant and wildtype mice were anesthetized rapidly with isoflurane and decapitated. Brains were removed into ice-cold oxygenated (95% O₂/5% CO₂) modified aCSF containing (in mM): 135 *N*-methyl-D-glucamine, 1 KCl, 1.2 KH₂PO₄, 1.5 MgCl₂, 0.5 CaCl₂, 70 choline bicarbonate, and 10 D-glucose; pH 7.4 adjusted with HCL. NAc-containing coronal slices (250 μ m) were sectioned with a vibratome (VT1200S; Leica, Wetzlar, Germany) and incubated for 30 minutes at 37°C in oxygenated aCSF containing (in mM): 119 NaCl, 26 NaHCO₃, 2.5 KCl, 1 NaH₂PO₄, 2.5 CaCl₂, 1.3 MgCl₂, 11 D-glucose. Slices were kept at room temperature until recording then perfused with aCSF (30-32°C).

2.2.3 Whole-cell patch-clamp recordings

Slices were viewed by differential interference contrast (DIC) optics (Leica) and accumbal regions were localized under low magnification. Recordings were made under visual guidance with 40x objective. Borosilicate glass pipettes (3-5M Ω) were filled with (in mM): 117 Cs-MeSO₃, 20 HEPES, 0.4 EGTA, 2.8 NaCl, 5 TEA-Cl, 2.5 Mg-ATP, 0.25 Na-GTP, 5 QX-314; pH 7.3 adjusted with CsOH. Cells were voltage clamped at -70mV. For miniature EPSC (mEPSC) and current clamp recordings, a solution containing (in mM): 119 K-MeSO₄, 2 KCl, 1 MgCl₂, 1 EGTA, 0.1 CaCl₂, 10 HEPES, 2 Mg-ATP, 0.4 Na-GTP; pH 7.3 adjusted with KOH, was used interchangeably with no measured differences. A constant-current isolated stimulator (DS3; Digitimer) was used to stimulate excitatory afferents with a monopolar electrode to record evoked currents (eEPSCs). Single or paired pulses were generated using Clampex software (Molecular Devices, Sunnyvale, CA). Stimulus intensity was adjusted to generate currents with amplitude between 50 and 500pA. Cells with run-up or run-down of more than 15% were excluded from analysis, as were electrophysiologically identified interneurons. Picrotoxin (50 μ M, Sigma Aldrich) was included in the external perfusion aCSF to block GABA_A receptors. TTX (1 μ M, Tocris, Bristol, UK) was used for mEPSC recordings. For EPSC experiments, D-APV (50 μ M, R&D Systems, Minneapolis, MN) was bath applied to block NMDARs at +40mV. In some experiments, D-APV was not applied and the peak amplitude of AMPAR current was measured at -70mV and the NMDAR peak amplitude taken at 40mV, 35ms from the AMPAR peak. Series resistance for all recordings was monitored continuously.

Cells with a change in series resistance beyond 20% were excluded from data analysis.

Synaptic currents were recorded with a MultiClamp 700B amplifier (Molecular Devices). Signals

were filtered at 2.6-3 kHz and amplified 10 times, then digitized at 20 kHz with a Digidata 1322A analog-to-digital converter (Molecular Devices). Miniature current recordings were analyzed using pClamp10 software (Molecular Devices) over a period of approximately 2.5 min during which 250-2500 events were collected. AMPAR/NMDAR ratios were determined by taking the average peak amplitude of EPSCs at 40mV in the absence or presence of D-APV (30 sweeps each) or at -70mV. For paired pulse experiments, a set of two pulses were delivered with an inter-pulse interval of 50-200ms and a minimum of 30 sweeps were recorded with the pulses delivered every 10 seconds. For current clamp recordings, the resting membrane potential was adjusted after stabilization to -70mV with minimal current injection. A current step protocol from -200pA to +400pA (50pA increment) was applied for at least 5 runs to record evoked action potentials.

2.2.4 Surface GLUA1 detection

Experiments were performed using a modified version of a published protocol (Boudreau *et al*, 2012). Single NAc tissue punches were rapidly micro-dissected using a stainless-steel stylet (1mm diameter) from 1 mm-thick coronal sections obtained from a mouse brain matrix. Punched tissue was consistently chopped with a surgical scalpel. NAc tissue was not pooled between mice. One hemisphere of tissue was immersed in ice-cold artificial CSF (aCSF) containing 2 mM Bis(sulfosuccinimidyl) suberate (BS³) (Pierce, Waltham, MA) and incubated for 30 min at 4°C on a rotator. Tissue from the other hemisphere was incubated in aCSF alone. The cross-linking reaction was quenched with 100 mM glycine in aCSF for 10 min at 4°C on a rotator. Samples were centrifuged for 2 min at 4°C. Supernatants were discarded and pellets washed once with aCSF. Samples were re-centrifuged, supernatants were discarded, and pellets were sonicated in ice-cold lysis buffer [0.1% NP-40 buffer in Tris-EDTA, pH 7.4, containing 1× protease inhibitor mixture

(Sigma-Aldrich, St. Louis, MO), 5 mM NaF, and 1× phosphatase inhibitor mixture (Sigma-Aldrich)]. Protein concentration was determined by DC assay (Bio-Rad, Hercules, CA) and 20 µg of protein was loaded on a 4–15% gradient Tris-HCl gel (Bio-Rad) and run at 100 V in 1X TGS buffer (Bio-Rad). Proteins were transferred onto PVDF membranes for 1.5 hrs at 500mA constant current in cold 1X TG buffer (Bio-Rad). Membranes were re-wet and blocked for 4hrs in Odyssey Blocking Buffer (LI-COR Biosciences, Lincoln, NE). They were further processed for GLUA1 immunoblot analysis and probed with anti-mouse GAPDH (37kDa; 1:10000, Santa Cruz Biotechnology, Dallas, TX) and anti-rabbit GluA1 (106kDa; 1:500, Pierce). Following overnight primary incubation at 4°C, blots were incubated in fluorescent secondary antibodies including goat anti-rabbit 800 and goat anti-mouse 680 (1:400, LI-COR Biosciences). Blots were imaged using the LI-COR Odyssey system. Intensity of protein bands was normalized to GAPDH and surface protein levels were determined as the subtraction of the intracellular band intensity from the total band intensity (in arbitrary units). The surface-intracellular ratio was calculated from the obtained values. Rhythms and acrophase measures of GLUA1 expression were determined by multiple harmonic regression using CircWave v1.4 software available from circwave.org. Curves were fit to 2 sine waves and the center of gravity of each fitted waveform was used to determine acrophase.

2.2.5 Viral gene transfer and stereotaxicsurgery

Stereotaxic surgery was performed as previously described (Ozburn & Falcon et al., 2015). Bilateral stereotaxic injections of 0.5µL of purified high titer AAV9 encoding GFP driven by the human synapsin promoter (control virus) or AAV9-hsyn-*GluA1* were delivered into the NAc (from Bregma; angle 10°: AP +1.5mm, Lat. +1.5mm, DV -4.4mm). The efficiency of *GluA1* overexpression was confirmed by real-time RT-PCR from infected NAc tissue. Mice recovered

for 3 weeks allowing for full expression of the virus before behavioral testing. Following behavioral testing, the placement of viral injections was verified using immunohistochemical methods as described in the supplement. Use of AAV-*Clock*-shRNA virus has been previously described (Mukherjee *et al*, 2010).

2.2.6 Immunohistochemistry

Mice were perfused with 1x phosphate-buffered saline (PBS) followed by 4% paraformaldehyde in PBS (pH 7.4). Brains were post-fixed then transferred to 30% sucrose solution. Sections (30 μ m) were taken and processed for GFP and DAPI. Briefly, floating sections were rinsed 3 x with PBS to remove fixative then blocked for one hour in PBS containing 0.2% Triton-X and 5% Normal Donkey Serum (Jackson ImmunoResearch, West Grove, PA). Sections were incubated overnight at room temperature with a rabbit anti-GFP primary antibody (1:20,000; Abcam, Cambridge, UK) on a rotary shaker. The following day, sections were rinsed 3 x with in PBS and incubated with donkey anti-rabbit conjugated to a 488nm fluorophore (1:400; Invitrogen, Carlsbad, CA) for two hours at room temperature on a rotary shaker. Following a final wash in PBS, sections were mounted and coverslipped with DAPI mounting medium (Vector Labs, Burlingame, CA) and imaged at 4x magnification on a fluorescent microscope (Olympus, Center Valley,PA).

2.2.7 Animal behavior

Animals habituated to testing rooms for at least 30 minutes prior to behavioral testing. Animals were tested early in the light phase between ZT0-ZT4. To test locomotor response to novelty, mice were placed inside automated locomotor activity chambers equipped with infrared photobeams

(San Diego Instruments, San Diego, CA) to measure activity. Data were collected continuously for 90 minutes and analyzed in 5-minute time bins. Elevated Plus Maze (EPM) was performed in a dimly lit room (~15 Lux at each open arm). Mice were placed in the center of the maze and both the number of entries into the open and closed arms and the total time spent in the open arms (in seconds) were manually recorded over a 10-minute period. A biased protocol was used to assess cocaine conditioned place preference (CPP). On the pre-test day, mice were allowed to explore all chambers of the place-conditioning apparatus for 20 minutes to determine inherent bias. On conditioning days 1 and 3, mice were given a saline injection (i.p.) paired with the preferred chamber of the apparatus, and on days 2 and 4, they received a cocaine injection (5mg/kg; i.p.) paired with the non-preferred chamber. Conditioning sessions lasted 20 minutes. Following conditioning, on day 6, mice were tested again for time spent on either side of the apparatus and the CPP score was calculated by subtracting the pre-conditioning time spent in the cocaine-paired side from the time spent in the cocaine-paired side on the test day. Data from mice that spent a majority of time in the center of the apparatus were eliminated from analysis.

2.2.8 Real-time Polymerase Chain Reaction

Primers used for qPCR: *GluA1* Fwd: 5' – ACCCTCCATGTGATCGAAATG-3'; *GluA1* Rev: 5'-GGTTCTATTCTGGACGCTTGAG-3'; *Gapdh* Fwd: 5'-CTTTGTCAAGCTCATTTCCTGG-3'; *Gapdh* Rev: 5'-TCTTGCTCAGTGTCCCTTGC-3'. Micro-dissected NAc tissue punches were homogenized both mechanically and by QIAshredder homogenization spin-column (Qiagen, Hilden, Germany). Total RNA was isolated using the RNeasy Plus Micro Kit (Qiagen) as per manufacturer guidelines. gDNA was eliminated with the provided gDNA Eliminator column. RNA concentration and quality was determined using NanoDrop 2000 UV-Vis spectrophotometer

(Thermo Fisher Scientific, Waltham, MA). cDNA was synthesized from 100ng total RNA using SuperScript VILO Master Mix (Invitrogen). Relative gene expression was measured by qPCR with 1ng of cDNA mixed with Power SYBR Green PCR Master Mix (Thermo Fisher Scientific) and primers listed above. Reactions were run in duplicate in an Applied Biosystems 7900HT Fast Real-time PCR System (Applied Biosystems, Foster City, CA). Relative gene expression was calculated using the comparative Ct ($2^{-\Delta\Delta Ct}$) method (Landgraf *et al*, 2014) and normalized to each sample's corresponding *Gapdh* mRNA levels.

2.2.9 Data analysis

Electrophysiological, biochemical and behavioral experiments were conducted blind to genotype. Significant differences were determined by Student's *t*-Test, one-way ANOVA or two-way ANOVA followed by Bonferroni *post hoc* tests. $P < 0.05$ is considered significant for all analyses. All data are presented as mean \pm SEM.

2.3 RESULTS

2.3.1 *Clock* Δ 19 mice have reduced AMPAR-mediated synaptic transmission and strength at NAc MSNs throughout the light/dark cycle

Our results indicate that there is a significant reduction in glutamatergic synaptic transmission in *Clock* mutant MSNs compared with WT across the L/D cycle as indicated by reduced amplitude of AMPAR-mediated miniature excitatory postsynaptic currents (mEPSCs) ($F_{(1,76)} = 16.43$,

$P=0.0001$ genotype effect). We found a significant main effect of phase in mEPSC amplitude as well indicating that perhaps this particular measure has diurnal variability ($F_{(1,76)} = 6.615$, $P=0.0121$ phase effect) (figure 5c).

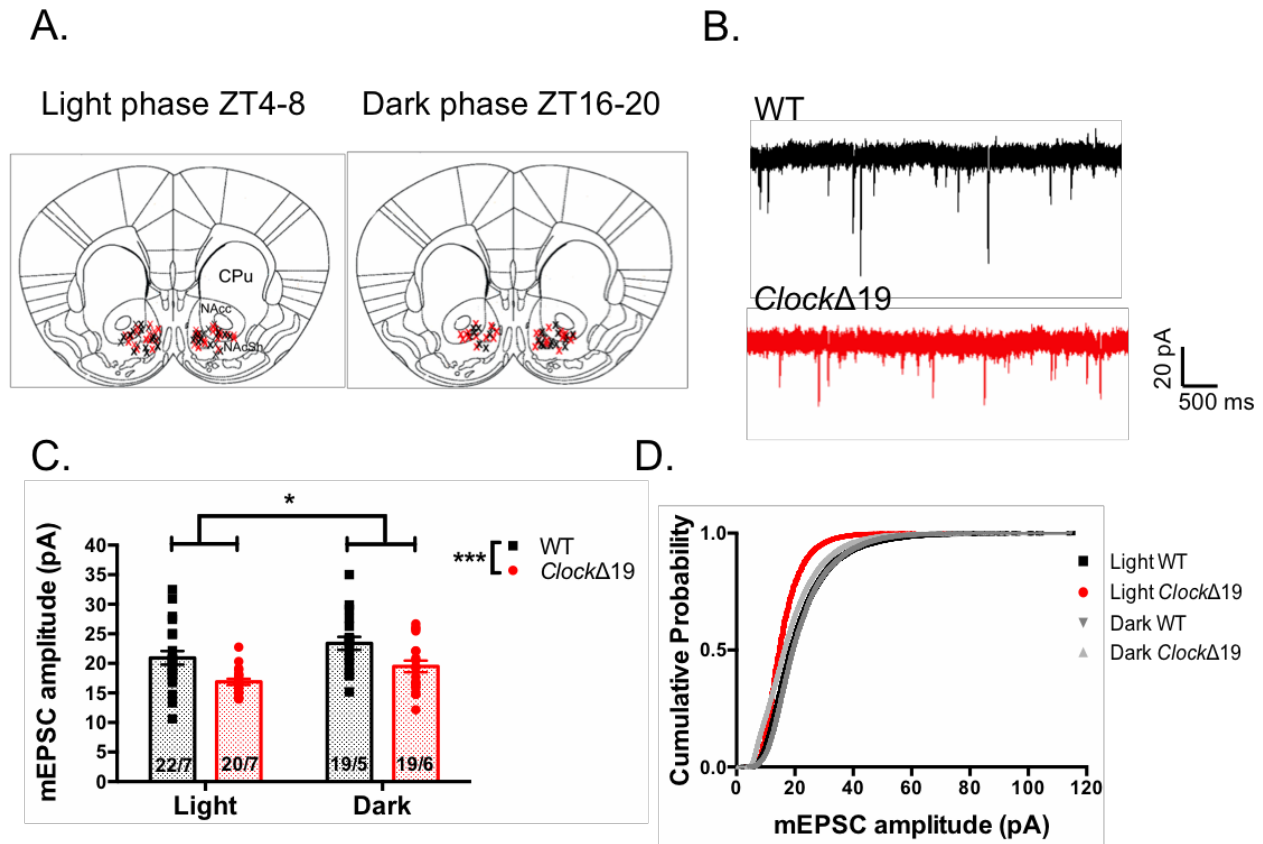


Figure 5. *ClockΔ19* mutation modifies MSN AMPAR-mediated synaptic transmission across the light/dark cycle. (A) Recording sites within the NAc from slices collected during light and dark phases (WT – black; *ClockΔ19* – red; ZT = Zeitgeber time; CPU = caudate putamen; NAcc = NAc core; NAcSh = NAc shell). (B) Representative traces of mEPSCs recorded at -70mV in the presence of 1μM TTX. (C) Summary of mEPSC amplitude of mutant and WT MSNs at both phases (n = cells/animals; all data in bar graphs are presented as mean ± SEM). (D) Plot of cumulative probability of all mEPSC amplitudes across phases. * $P < 0.05$; ** $P < 0.01$; *** $P < 0.001$ in this and all subsequent figures.

Many studies have shown that signaling in core and shell sub-regions of the NAc can mediate affective valence and motivational behavior in a distinct manner (Faure *et al*, 2010; Meredith *et al*, 2008). However, when we further analyzed our mEPSC amplitude data by regional location no significant difference in NAc core versus shell neurons was observed during the light ($F_{(1,37)} = 9.205$, $P=0.0044$ genotype effect; $F_{(1,37)} = 0.0001$, $P=0.9910$ region effect) or the dark ($F_{(1,34)} = 6.715$ $P=0.0140$ genotype effect; $F_{(1,34)} = 0.0491$, $P=0.8259$ subregion effect) (figure 6a-b).

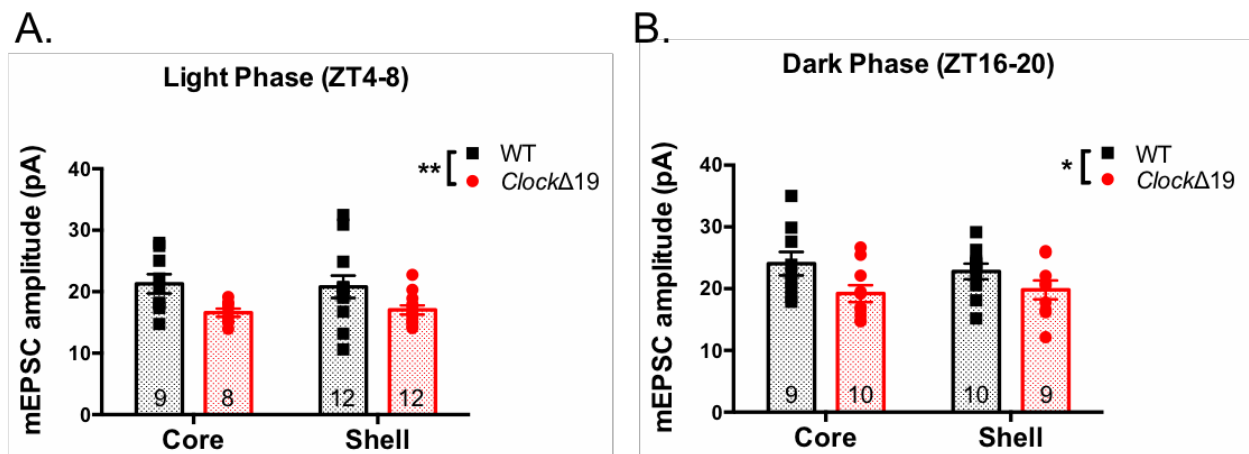


Figure 6. *ClockΔ19* MSNs show reduced glutamatergic transmission in both core and shell subregions of the NAc. (A) Summary of mEPSC amplitude of WT and mutant NAc core and shell MSNs during the light phase. (B) Amplitude of mEPSCs in core and shell subregions during the dark phase.

When calculating AMPAR/NMDAR ratio of evoked EPSCs, a measure of excitatory synaptic strength, there was a significant reduction in A/N of MSNs in *ClockΔ19* mutants consistent across the L/D cycle ($F_{(1,44)} = 11.53$, $P=0.0015$ genotype effect; $F_{(1,44)} = 0.1237$, $P=0.7267$ phase effect) (figure 7b) and no change in the decay kinetics of the evoked NMDA current indicating that subunit stoichiometry of these receptors was not altered in mutants ($F_{(1,39)}$

= 0.1936, $P=0.6624$ genotype effect; $F_{(1,39)} = 2.013$, $P=0.1639$ phase effect). Additionally, we failed to observe an effect of genotype or phase on the CV analysis of NMDAR EPSCs relative to AMPAR EPSCs, a measure directly correlated with the proportion of silent synapses, which lack functional AMPARs ($F_{(1,29)} = 0.0944$, $P=0.7609$ genotype effect; $F_{(1,29)} = 0.4760$, $P=0.4957$ phase effect) (figure 7c-f). This result indicates that the reduced functionality of AMPAR-mediated activity at mutant MSNs likely does not occur through a complete silencing of synapses.

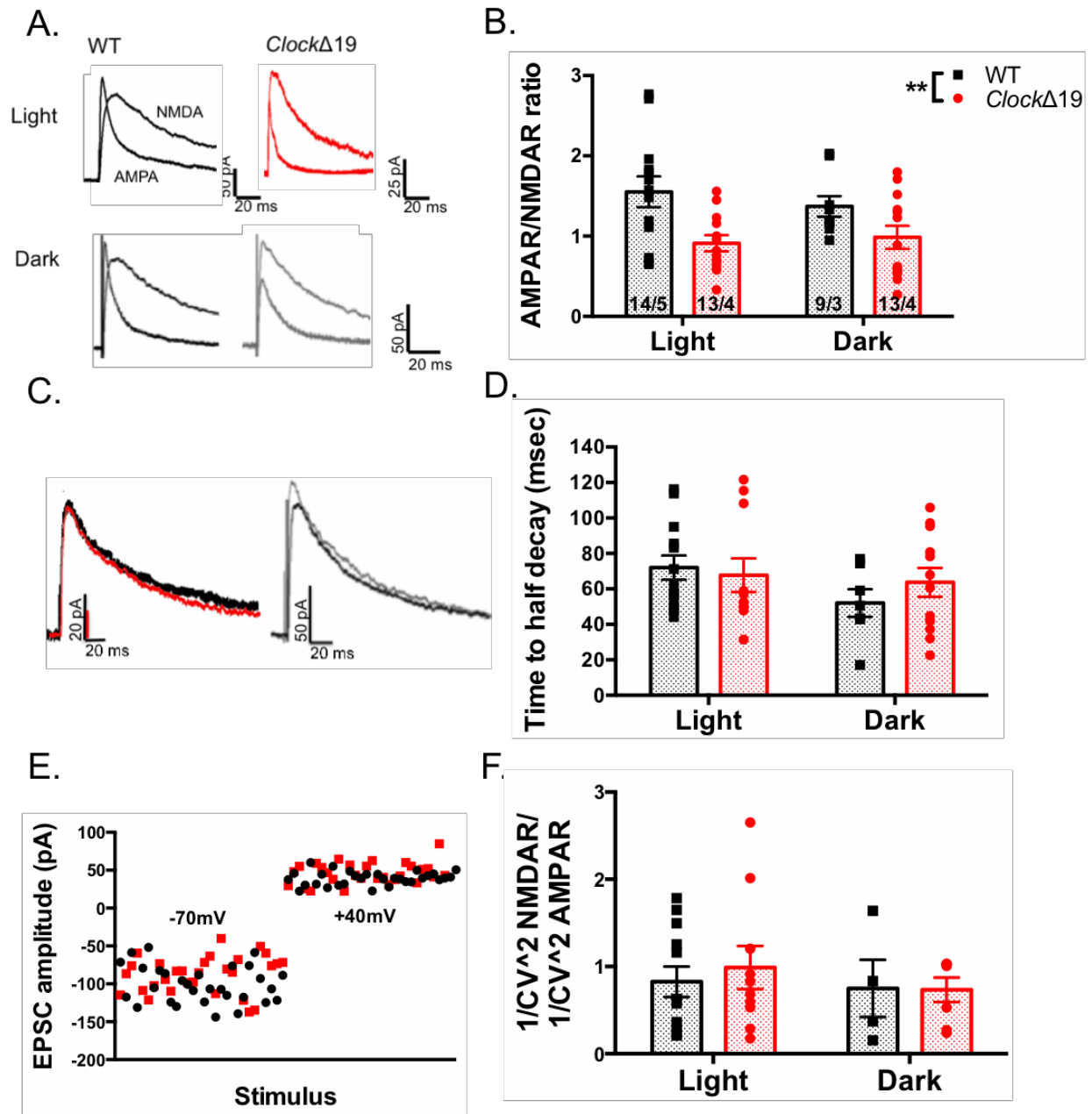


Figure 7. AMPAR-mediated synaptic strength of MSNs is reduced by the *ClockΔ19* mutation. (A) Representative traces of evoked AMPAR and NMDAR-mediated EPSCs at 40mV. (B) Ratio of the peak amplitude of the AMPAR EPSC to the NMDAR EPSC for each group of MSNs. (C) Representative traces of NMDAR-mediated EPSCs in the light phase (WT- black, *ClockΔ19* – red) and dark phase (WT- dark grey, *ClockΔ19* – light grey) MSNs. (D) Summary of NMDAR EPSC decay kinetics. (E) Sample plot of AMPAR EPSC amplitudes at -70mV and

NMDAR EPSCs at 40mV from light phase WT and mutant MSNs. (F) Summary of ratio of $1/CV^2$ NMDAR EPSCs to $1/CV^2$ AMPAR EPSCs from mutant and WT MSNs during both phases.

2.3.2 Presynaptic release of glutamate onto NAc MSNs is unaltered in *Clock* mutants throughout the light/dark cycle

We further analyzed the frequency of mEPSCs as a measure of quantal release probability of glutamate at NAc MSNs in mutant and WT slices. Here, we found no significant difference between groups or by diurnal phase ($F_{(1,72)}= 0.06752$, $P=0.7957$ genotype effect; $F_{(1,72)}= 0.04288$, $P=0.8365$ phase effect) (fig 8a-b). Another standard measure of transmitter release probability at excitatory synapses is the paired pulse ratio (PPR), which is comprised of the peak amplitude of the 2nd of a series of evoked EPSCs to the 1st. The PPR is inversely related to release probability. We determined the PPR at three different inter-pulse intervals and observed no significant difference between mutant and WT groups during either diurnal phase ($F_{(3,25)}= 0.1803$, $P=0.9088$ genotype effect; $F_{(3,25)}= 9.531$, $P=0.0003$ interval effect) (figure 8c-d). These results indicate that synapse number or presynaptic release of glutamate onto MSNs remain unchanged with *Clock* gene disruption and wildtype animals do not show diurnal variability in these measures.

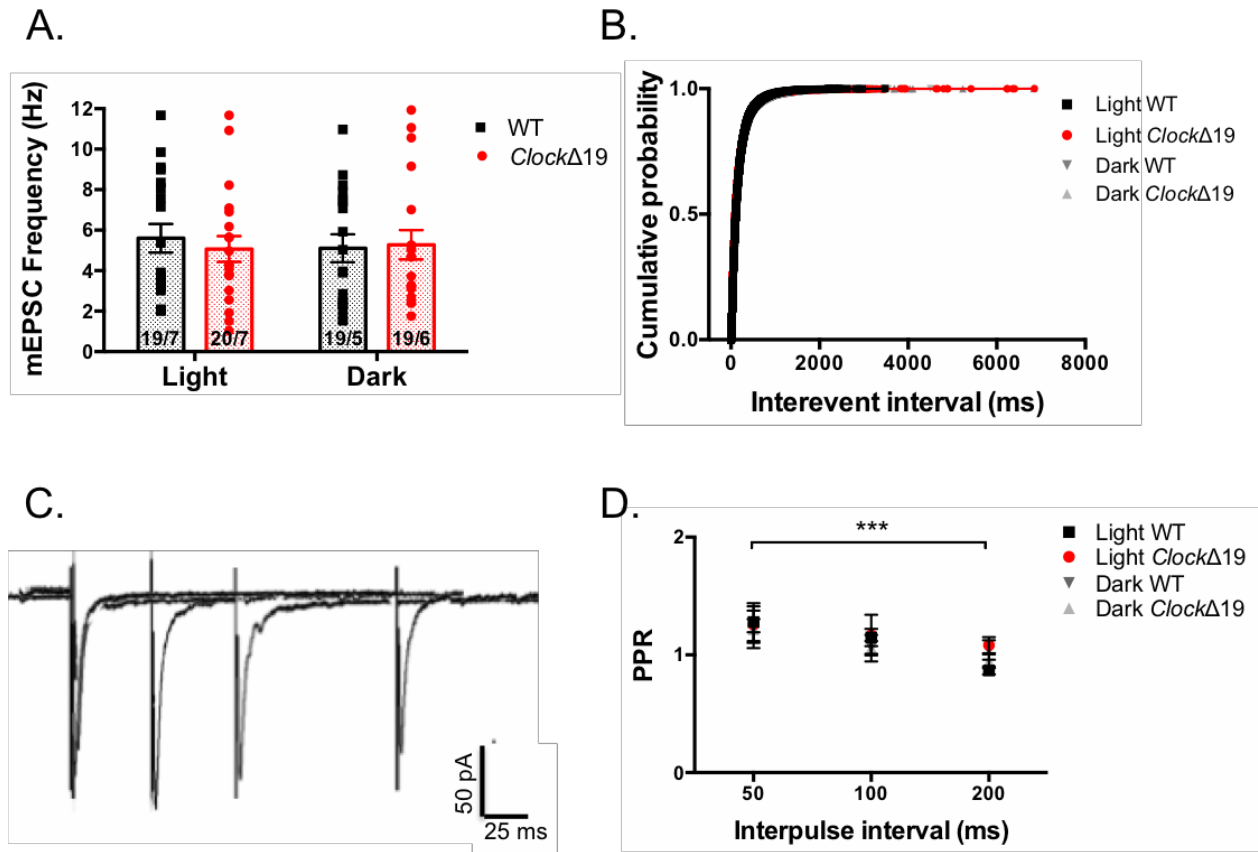


Figure 8. *Clock* Δ 19 mutation does not alter the presynaptic release of glutamate onto NAc MSNs. (A) Frequency of AMPAR mEPSCs recorded from mutant and WT MSNs at light and dark phases. (B) Cumulative probability of inter-event intervals (IEI) of all recorded mEPSCs. (C) Sample traces of pairs of evoked AMPAR EPSCs at -70mV at varying inter-stimulus intervals. (D) Paired-pulse ratio (PPR) calculated as peak amplitude of the second EPSC to the first plotted across inter-stimulus interval.

2.3.3 Membrane levels and rhythm of GLUA1 protein are reduced in the NAc of

Clock Δ 19 mice

In order to investigate the molecular basis for the deficiency in excitatory drive onto MSNs seen in *Clock* mutant accumbens, we measured the protein expression of the AMPAR subunit, GLUA1,

across the light/dark cycle. Previously, we have shown reduced total and phosphorylated protein levels of this particular subunit in mutant NAc during the day (Dzirasa *et al*, 2010). These results indicate a potential deficiency in the translation or trafficking of AMPARs that may underlie microcircuit-level and physiological dysfunction. Here we used BS³ crosslinking to isolate membrane-bound and intracellular fractions of GLUA1. The inherent smearing of crosslinking to detect multi-protein complexes made it difficult to resolve a clear multimer band and we therefore quantified the reduction of the monomer instead to calculate the amount of surface expressed GLUA1-containing AMPA receptors. We found a significant reduction in the surface/intracellular (S/I) ratio of GLUA1 normalized to GAPDH at ZT6 and ZT18 in mutant NAc which corresponded closely with our recording times ($F_{(1, 20)} = 17.67$, $P=0.0004$ genotype effect; $F_{(1, 20)} = 0.8999$, $P=0.3541$ phase effect) (figure 9). These results suggest that reduction in CLOCK protein function may affect the ability of GLUA1-containing AMPARs to be inserted into the membrane for proper excitatory signaling and this deficit appears during both the light and dark phases.

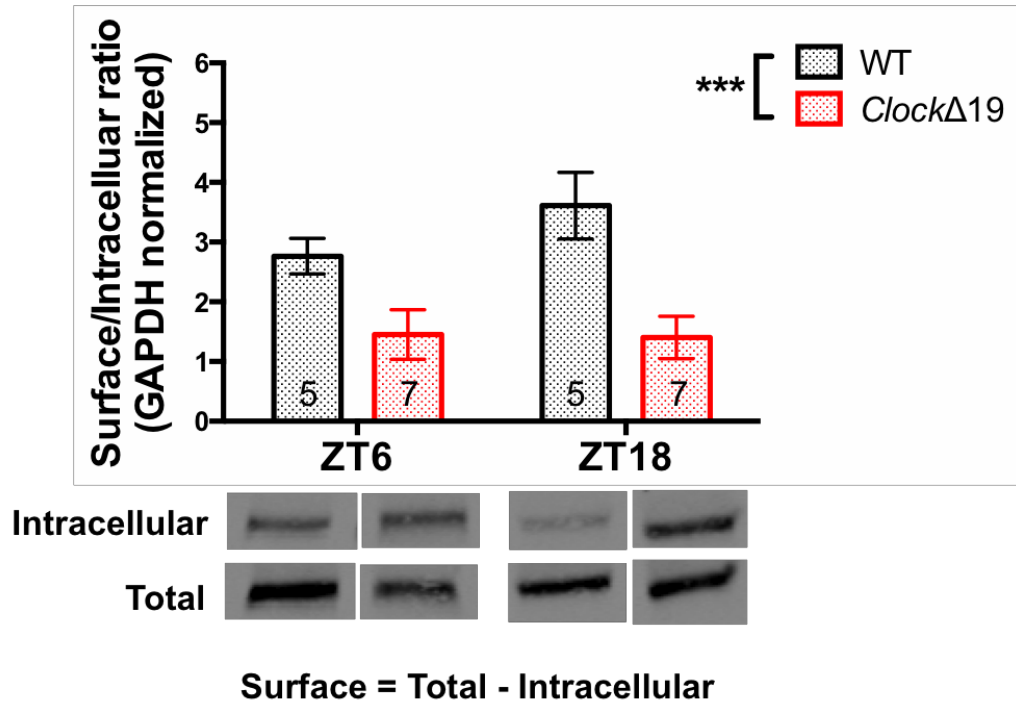


Figure 9. The surface/intracellular ratio of GLUA1 expression is significantly reduced in *Clock* Δ 19 NAc during the light and dark phases. Crosslinked and non-crosslinked NAc tissue from mutant and WT animals allowed for the quantification of total and intracellular protein levels of GLUA1. Surface protein levels were inferred by the subtraction of intracellular protein from total protein. *Clock* Δ 19 mice have significantly reduced S/I ratio of GLUA1 compared with WT littermates at ZT6 and ZT18. Representative bands are shown below. Band intensity was normalized to GAPDH and presented as arbitrary units.

Furthermore, we tested for a rhythm in GLUA1 total protein and S/I ratio in WT and mutant NAc. Our measurements at 6 time points across 24 hours allowed us to apply multiple harmonic regression to detect a significant diurnal rhythm in WT GLUA1, with a bimodal pattern peaking at the midpoint of the light and dark cycles ($P < 0.0001$). A rhythm with similar pattern was also detected in the S/I ratio in WT NAc ($P < 0.001$). In mutant accumbens however, we were unable to curve fit the total and surface GLUA1 data indicating a lack of significant rhythm (figure 10a-b). Additionally, when we analyzed whether *Clock* mutants have a shift in the expression pattern of GLUA1, we found that indeed the acrophase, or estimation of circadian phase corresponding to the peak of the rhythm, was significantly advanced in mutants for both the total protein and S/I ratio ($P < 0.05$) (figure 10c). These results suggest that a biochemical basis contributing to excitatory drive onto MSNs is profoundly affected by a lack of proper CLOCK protein function.

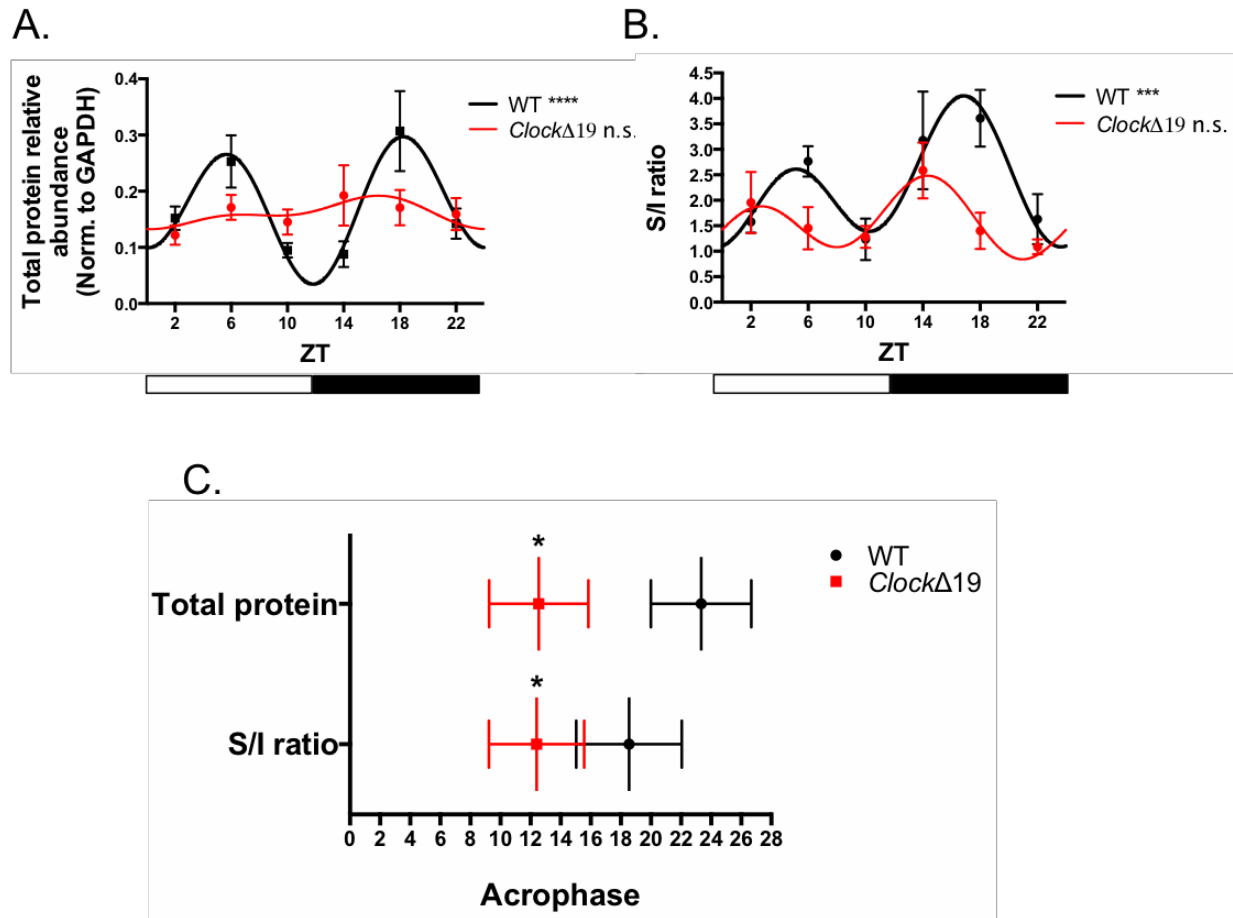


Figure 10. A diurnal rhythm in GLUA1 expression in the NAc is abolished in *Clock*Δ19 mice. (A) The diurnal rhythm of total protein levels of GLUA1 across 6 time points, normalized to GAPDH expression in mutant and WT NAc tissue. A significant curve fit was found in WT but not in mutant data (bars below represent light and dark phases). (B) Rhythmic profile of the GLUA1 S/I ratio in WT and mutant across the light/dark cycle showing a loss of significant rhythm in mutant NAc. (C) Acrophase of diurnal expression rhythms of total GLUA1 and S/I ratio in mutant and WT accumbens. Acrophase measures were derived from the center of gravity of the fitted harmonic curves (+SEM). $n = 5-9$ mice for all groups.

2.3.4 *Clock* mutant MSNs display subtle alterations in intrinsic membrane properties

The functional output of MSNs is dependent upon the integration of synaptic inputs and the membrane excitability inherent to the cells. In order to assess the effects of the *Clock* Δ 19 mutation on MSN functional output, we examined various parameters related to the intrinsic membrane excitability of these cells. We first measured the evoked firing rate of MSNs in response to current injection steps ranging from 100-400pA. While we did not observe a significant difference in spike number between genotypes, interestingly, we saw a robust difference in excitability at the different phases with a highly increased firing rate during the dark cycle (figure 11a-b). When collapsing across genotype we detected significant differences by phase and current injection ($F_{(3, 39)} = 48.87$, $P < 0.0001$ phase effect; $F_{(6, 234)} = 699.8$, $P < 0.0001$ current effect). Relatively few studies have conducted diurnal *ex vivo* measurements of neuronal activity in extra-SCN regions; therefore, the presence of a variable intrinsic excitability profile of NAc MSNs is noteworthy. A number of potential mechanisms could underlie this variability, including *Clock*-regulated fluctuations in the activity of potassium conductances responsible for MSN bi-stable excitability (Shen *et al*, 2004; Vilchis *et al*, 2000; Wickens and Wilson, 1998).

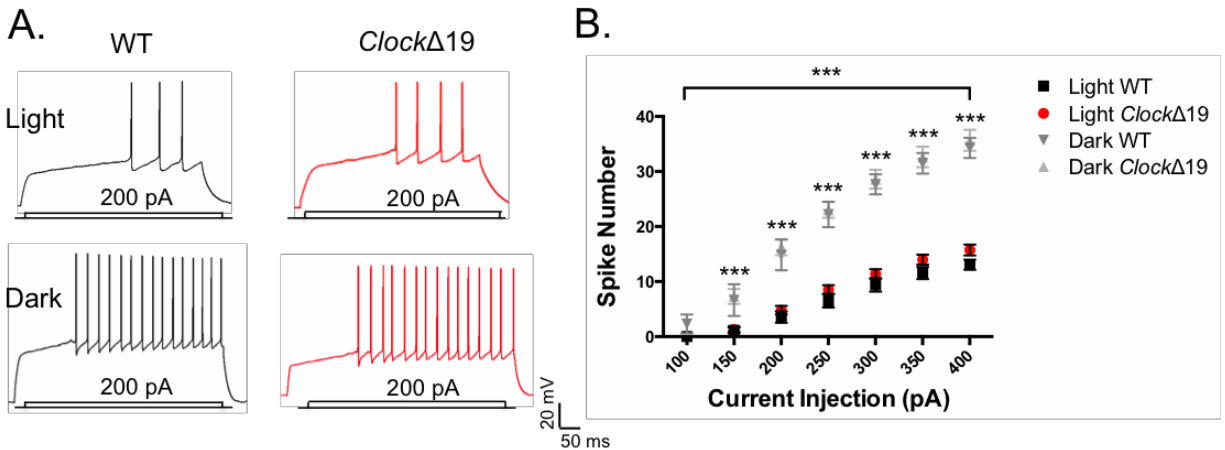


Figure 11. **Excitability of MSNs is unaltered by *ClockΔ19* mutation however diurnal variation exists in evoked firing rates.** (A) Representative traces of action potential firing in response to current injection from mutant and WT MSNs during the light phase. (B) Input-output curve of spikes with varying current steps during both phases in both groups.

We further analyzed several intrinsic membrane properties of MSNs in mutant and WT slices across the light/dark cycle, including the resting membrane potential (RMP) at break-in, the rheobase or minimum current needed to elicit action potential (AP) generation, and the AP threshold (Table 2). In these measures, we saw a significantly lower RMP of *Clock* mutant MSNs compared with WT during the light phase ($t_{(27)} = 2.218$, $P = 0.0352$) and the dark phase ($t_{(14)} = 2.756$, $P = 0.0155$). This suggests that mutant MSNs may rest at a more hyperpolarized membrane potential at baseline and require greater stimulation to enter the “up-state”. We did not find a significant difference in the rheobase during the light phase ($t_{(27)} = 0.4907$, $P = 0.6267$) or dark phase ($t_{(15)} = 0.4971$, $P = 0.6264$). AP threshold was similar during the light phase ($t_{(17)} = 0.9113$, $P = 0.3794$) however was lower in mutant MSNs during the dark phase ($t_{(14)} = 2.322$, $P = 0.0358$). Together, these results suggest that a reduction in CLOCK protein function

does not affect the intrinsic membrane excitability of MSNs, however a lowered resting membrane potential may indicate a more subtle effect on excitability.

Table 2. Intrinsic membrane properties of *Clock* mutant and WT MSNs during light and dark phases.

Additional properties of membrane excitability of MSNs were examined in *Clock* Δ 19 and WT cells including resting membrane potential at break-in, (RMP), rheobase and action potential (AP) threshold.

Light phase MSN membrane properties

Genotype	Wildtype	<i>Clock</i> mutant	<i>p</i> -value
Number of cells	<i>n</i> = 14/6	<i>n</i> = 15/4	
Break-in RMP (mV)	-80.50 \pm 1.929	-85.33 \pm 1.094	0.0352*
Rheobase (pA)	185.7 \pm 15.22	176.7 \pm 10.76	0.62760
AP threshold (mV)	-32.83 \pm 2.530	-35.35 \pm 1.298	0.37940

Dark phase MSN membrane properties

Genotype	Wildtype	<i>Clock</i> mutant	<i>p</i> -value
Number of cells	<i>n</i> = 7/5	<i>n</i> = 9/4	
Break-in RMP (mV)	-83.71 \pm 1.554	-88.11 \pm 0.735	0.0155*
Rheobase (pA)	137.5 \pm 18.30	127.8 \pm 8.784	0.62640
AP threshold (mV)	-34.80 \pm 3.240	-42.29 \pm 1.362	0.0358*

2.3.5 Overexpression of *GluA1* in the NAc normalizes “manic-like” behavior in *Clock* Δ 19 mice

Finally, we sought to determine whether up-regulation of functional *GluA1* expression in *Clock* Δ 19 NAc could rescue their abnormal exploratory drive and reward sensitivity. We injected AAV9-hsyn-*GluA1* or AAV9-hsyn-GFP bilaterally into the accumbens of adult male mutant and

WT mice and allowed 3 weeks for recovery and full expression. Our manipulation resulted in a roughly 3-fold increase in *GluA1* transcript levels as determined by qPCR (figure 12a-c) and a potentiation of MSN excitatory synapses as measured by AMPAR/NMDAR ratio ($P = 0.0036$) (figure 12d-e).

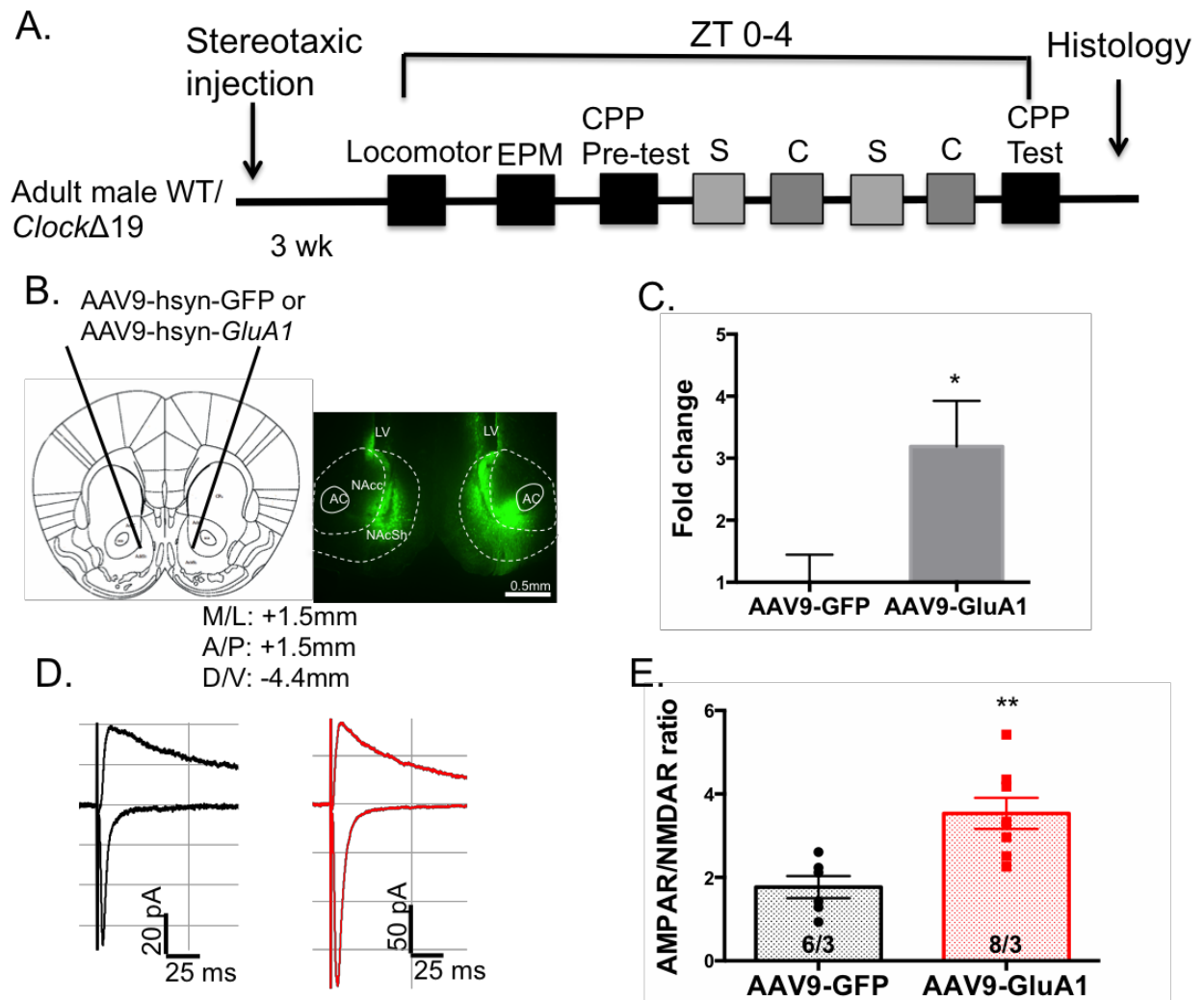


Figure 12. Functional up-regulation of *GluA1* in the NAc of *Clock* Δ 19 mice. (A) Timeline of experimental procedures testing the effect of AAV9-hsyn-*GluA1* or AAV9-hsyn-GFP expression on exploratory drive and conditioned reward behavior. (B) Bilateral localization of viral injections to the NAc (left) and GFP expression (right). (C) Accumbal *GluA1* transcript levels following viral overexpression compared with GFP expression in *Clock* mutants. (D) Representative traces of AMPAR EPSCs (at -70mV) and NMDAR EPSCs (at 40mV) in GFP-expressing (black) and *GluA1*-overexpressing cells (red). (E) AMPAR/NMDAR ratio of evoked EPSCs from virally-infected cells. LV- lateral ventricle; AC – anterior commissure; NAcc – nucleus accumbens core; NAcSh – nucleus accumbens shell.

Similar to lithium treatment (Roybal *et al*, 2007) overexpression of *GluA1* in *Clock* mutant mice did not alter the failure to habituate to a novel environment that was seen in GFP-expressing mutant mice. As expected, WT control groups showed faster locomotor habituation in this assay ($F_{(17, 816)} = 83.17$, $P < 0.0001$ time effect; $F_{(3, 48)} = 3.522$, $P = 0.0218$ treatment effect) (figure 13a). However, comparable to previous studies, we saw that mutant mice expressing GFP had a significantly higher proportion of open arm entries compared with WT GFP-expressing mice in the elevated plus maze ($F_{(1, 54)} = 6.427$, $P = 0.0142$ genotype effect) and similar to lithium treatment, several weeks of NAc-specific *GluA1* overexpression in mutants resulted in a significant reduction in open arm entries compared with GFP expression ($F_{(1, 54)} = 0.9928$, $P = 0.3235$ treatment effect; $F_{(1, 54)} = 6.009$, $P = 0.0175$ interaction; Bonferroni's multiple comparison's test: $*P < 0.05$, $***P < 0.001$). Open arm entries were normalized to total crosses in the apparatus (figure 13c). Additionally, total time spent in the open arms of the EPM was decreased to near WT levels with *GluA1* up-regulation in mutant NAc ($F_{(1, 54)} = 1.498$, $P = 0.2262$ treatment effect; $F_{(1, 54)} = 7.989$, $P = 0.0066$ interaction; Bonferroni's multiple comparison's test: $**P < 0.01$, $***P < 0.001$). As expected, GFP expressing mutant mice displayed increased time in the open arms compared with WT controls ($F_{(1, 54)} = 8.057$, $P = 0.0064$ genotype effect) (figure 13b).

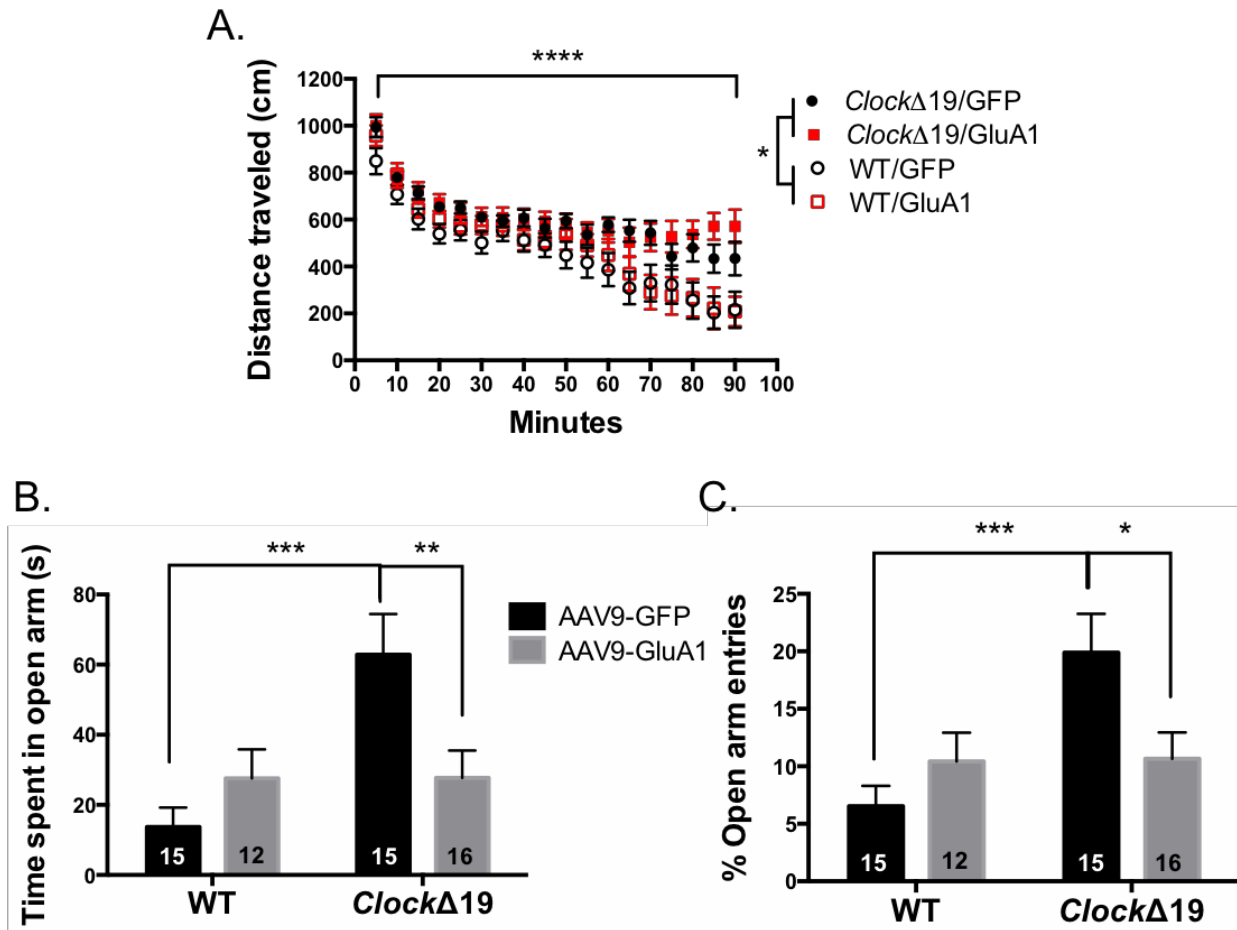


Figure 13. Overexpression of GluA1 in the accumbens of *ClockΔ19* mice reverses elevated exploratory drive behavior. (A) Locomotor activity in a novel environment of mutant and WT animals. (B) Total time spent in the open arms of the EPM during 10 min of testing. (C) Percent open arm entries in the EPM normalized to total crosses.

To determine whether GLUA1-mediated signaling is important for the effects of *Clock* gene disruption on behavioral measures associated with cocaine reward sensitivity, we performed cocaine conditioned place preference (CPP) (figure 14a). Using a dose of 5mg/kg cocaine, which has been shown to increase preference in *Clock* mutant mice compared with WT littermates (McClung *et al*, 2005), we demonstrated a reliably elevated CPP score in GFP-expressing mutants

compared with WT controls ($F_{(1, 53)} = 2.514$, $P = 0.1188$ genotype effect; $F_{(1, 53)} = 1.817$, $P = 0.1834$ treatment effect; $F_{(1, 53)} = 22.78$, $P < 0.0001$ interaction; Bonferroni's multiple comparison's test: $*P < 0.05$, $***P < 0.001$). *GluA1* overexpression in *Clock* mutants was able to normalize conditioned place preference to WT levels. Interestingly, we also observed a marked increase in place preference in WT mice with *GluA1* up-regulation (figure 14b).

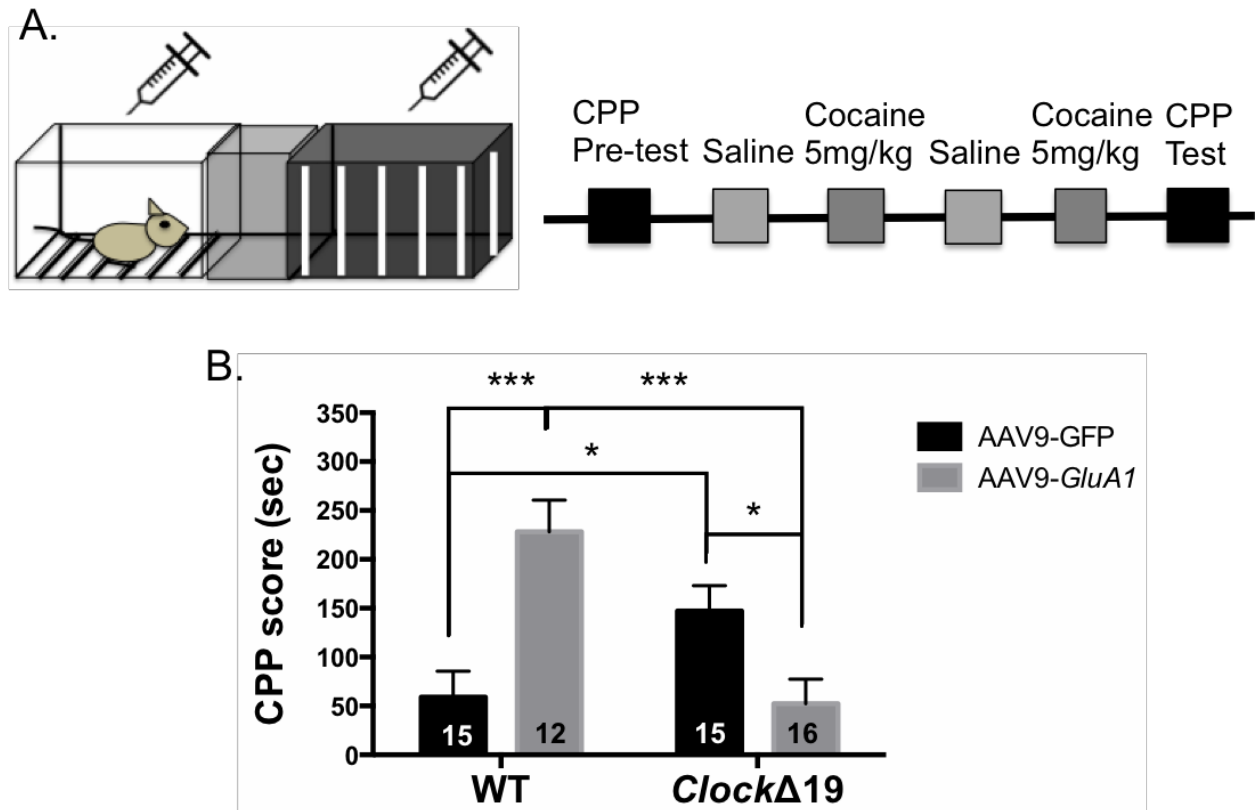


Figure 14. Cocaine sensitivity is normalized following *GluA1* up-regulation in *Clock* Δ 19. (A) Schematic of 3-chambered CPP testing apparatus and timeline of conditioning experiment. (B) Cocaine CPP scores of all experimental groups following a biased conditioning paradigm.

2.4 DISCUSSION

The current study demonstrates that a disruption in CLOCK protein function produces significantly reduced excitatory drive onto medium spiny neurons of the nucleus accumbens. We found that both the amplitude of AMPAR-mediated spontaneous currents as well as the ratio of AMPAR/NMDAR evoked currents was decreased across the day. This deficit in glutamatergic transmission does not appear to occur through silent synapse generation. Adaptations at mutant MSN excitatory synapses are likely postsynaptic as we found no alterations in presynaptic release properties. Additionally, the *Clock* mutation abolished a normal bimodal rhythm in GLUA1 protein expression and advanced the acrophase of the rhythm. In a previous study we reported a significant decrease in both total and phosphorylated GLUA1 protein levels in mutant NAc during the day with no changes in the expression of GLUA2, GLUN1, GLUN2A or GLUN2B subunits (Dzirasa *et al*, 2010). These results were suggestive of a potential deficit in the translation or trafficking of GLUA1-containing AMPARs to NAc synapses. Here we demonstrate that indeed, membrane-bound GLUA1 levels are lowered by *Clock* mutation and this adaptation persists across light and dark phases. Therefore, this suggests that functional impairments in glutamatergic transmission and strength of mutant MSNs are a result of reduced synaptic GLUA1-containing AMPARs. Increased activity of VTA dopamine neurons and elevated extracellular dopamine levels are likely an indirect cause for these abnormalities in *Clock* Δ 19 accumbens neurons. The modulatory function of dopamine on NAc glutamatergic activity is characterized in studies in which drugs of abuse act to elevate dopamine levels. Chronic cocaine administration, for instance, leads to an up-regulation of surface expressed GLUA1 (Boudreau and Wolf, 2005; Conrad *et al*, 2008; Lüscher and Malenka, 2011). Importantly, the plastic changes induced by chronic cocaine are not recapitulated in our model of hyperdopaminergia, implying that the effects we observe are

likely a compensatory response to a state in which dopaminergic activity is continually elevated. Additionally, the manner in which cocaine and dopamine influence both synaptic and intrinsic properties of MSN activity through differential signaling mechanisms has been empirically and theoretically examined (Moyer *et al*, 2007; Mu *et al*, 2010). Modulatory effects of dopamine are thought to differ based upon the specific dopamine receptor expression of MSNs. One limitation of our study is that we were unable to determine the cellular identity of MSNs in *Clock* mutant slices. We have previously reported an imbalance in D1R and D2R-mediated signaling in the striatum of mutants whereby there is a shift towards increased expression and binding activity of D2Rs (Spencer *et al*, 2012). Therefore, it is possible that these changes are occurring more frequently in particular neuronal pathways (i.e. direct versus indirect). When we investigated the intrinsic excitability of mutant and WT MSNs we found that they had similar firing however MSN excitability was significantly elevated during the dark phase. Rhythmicity in a number of ionic mechanisms could underlie this interesting effect. Diurnal variations in resting membrane potential, calcium currents, potassium conductances and *in vitro* firing patterns have been reported in midline thalamic neurons. Activity of these neurons is also elevated during the night phase (Kolaj *et al*, 2012).

As a critical site of integration of limbic and sensorimotor information for gating of salient stimuli, the accumbens is important for maintaining proper mood and reward responses. *Clock* Δ 19 mice display abnormal anxiety and depressive-like behaviors and robustly elevated sensitivity to a variety of rewarding substances. Restoration of functional CLOCK in the VTA and treatment with dopamine depleting pharmacological agents are able to normalize many aspects of the mutant manic-like phenotype (Roybal *et al*, 2007; Sidor *et al*, 2015). Disruption of glutamate receptor expression in the striatum however, has also been linked with neuropsychiatric illness and

increased dopaminergic transmission. Wiedholz and colleagues have characterized a number of impairments in *GluA1* knockout mice relevant to symptoms of schizophrenia including hyperactivity and reduced striatal clearance of extracellular dopamine (Wiedholz *et al*, 2008). A number of other preclinical models describing perturbations in glutamatergic transmission have also been likened to features of clinical BD including *GluN2A* deletion and *GluR6* subunit knockout (Boyce-Rustay and Holmes, 2006; Shaltiel *et al*, 2008). Here, we have demonstrated that restoring functional expression of GLUA1-containing AMPARs to the accumbens is sufficient to normalize the increased exploratory behavior in *Clock* mutants. It will be interesting in future studies to determine whether GLUA1 overexpression can normalize accumbal phase signaling deficits in mutants as well. Up-regulation of GLUA1 in the NAc also reduced cocaine reward sensitivity in mutants. Interestingly, we observed robust increase in preference in WT animals in which GLUA1 was overexpressed. This was a surprising result given that Bachtell and colleagues have demonstrated diminished sensitization and decreased cocaine seeking in extinction and reinstatement following overexpression of *GluA1* in the accumbens of wildtype rats (Bachtell *et al*, 2008). However, the specific mode of up-regulation in these studies varied from our own, in which long-term overexpression may have altered accumbal network activity in a more pronounced manner.

Interestingly, the physiological, behavioral and biochemical changes that we find in the nucleus accumbens of the *Clock* mutant mice do not seem to be due to direct transcriptional mechanisms in these neurons but rather are tied to dysfunctional circuit dynamics. We have previously reported that a viral-mediated knockdown of CLOCK in the NAc does not affect locomotor activity, anxiety-like behavior or cocaine CPP (Ozburn *et al*, 2015) and we find here that it does not alter the amplitude ($F_{(2, 53)} = 4.545$, $P = 0.0151$ treatment effect, Bonferroni's

multiple comparison's test: $*P < 0.05$) and frequency of AMPAR-mediated mEPSCs in MSNs ($F_{(2, 50)} = 0.7478$, $P = 0.4786$ treatment effect) (figure 15a-b).

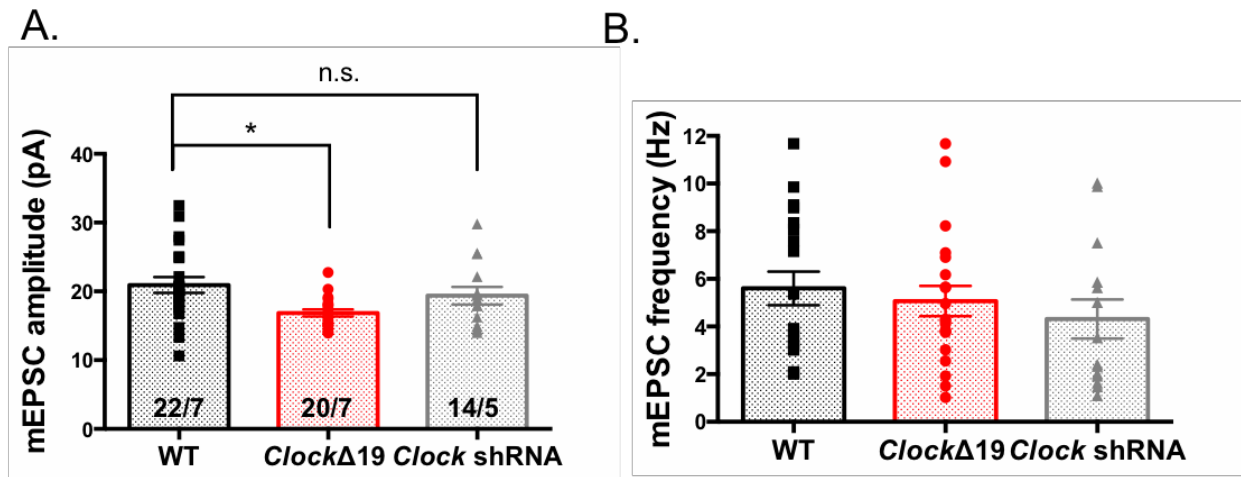


Figure 15. Knockdown of *Clock* in the NAc of WT mice does not alter excitatory transmission. (A) Summary of mEPSC amplitude in MSNs expressing AAV-*Clock*-shRNA. Compared with WT and mutant MSNs (B) Frequency of mEPSCs from all groups.

Together, these results support a model whereby diminished CLOCK function increases dopaminergic activity and tone, altering excitatory drive onto MSNs, most likely as a compensatory mechanism. This may reduce the functional output of the accumbens in feedback dynamics onto the VTA or disinhibit other target regions leading to the elevation of mood, exploratory drive and reward-seeking behavior.

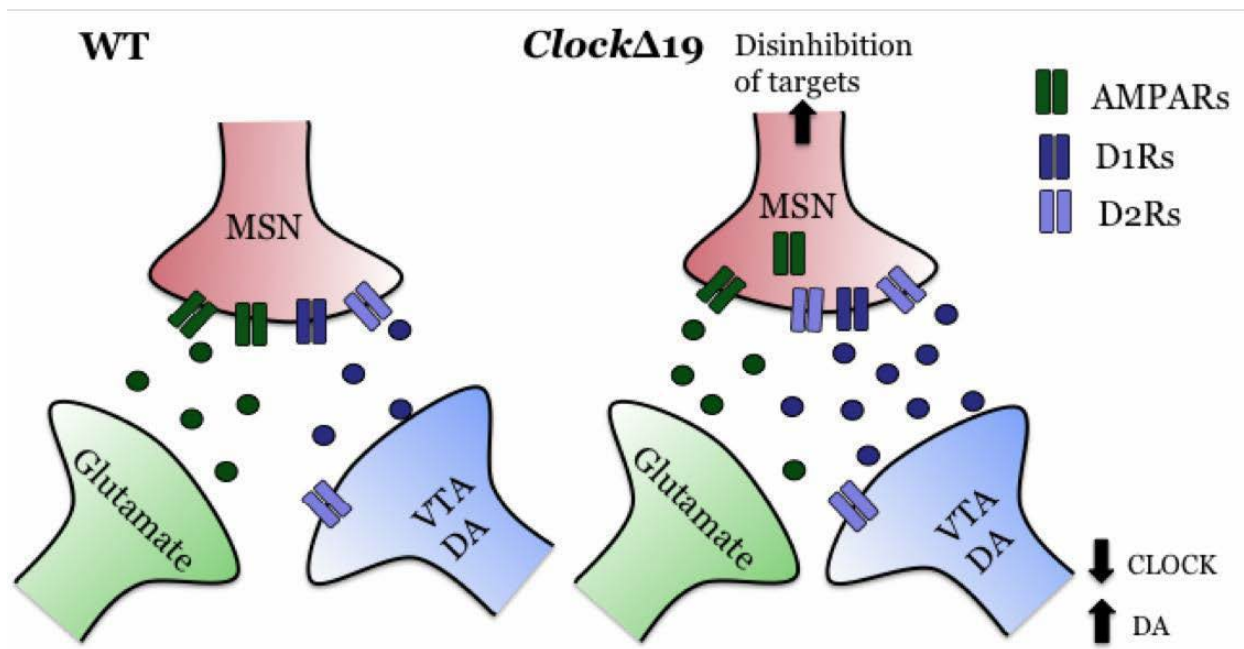


Figure 16. Proposed model of the effects of the *Clock* Δ 19 mutation on NAc MSN activity. CLOCK disruption leads to an elevation of dopamine synthesis and extracellular dopamine (DA) in the accumbens. Previous studies from our lab have revealed that *Clock* Δ 19 mice have altered striatal DA receptor expression and activity with a shift in the D1:D2 ratio favoring D2 signaling. We have now also demonstrated that GluA1-mediated AMPAR expression is reduced at MSN synapses, potentially affecting the output of these GABAergic neurons, which project back to the VTA as well as the ventral pallidum. Disinhibition of these targets may produce mood elevation and reward seeking.

2.5 FUTURE DIRECTIONS

While we have uncovered valuable information regarding specific deficits in nucleus accumbens excitatory signaling that may have important consequences for the functioning of this critical brain region in mania-like behavior, a few outstanding questions remain to be investigated further. *Clock* Δ 19 mutant mice represent a model of bipolar mania with face, construct and predictive validity and their circadian rhythm dysfunction resembles rhythm disturbances seen in bipolar

patients. This is further underscored by a recent discovery from our group that these mice undergo rapid diurnal mood cycling from a daytime manic-like state to a nighttime euthymic condition characterized by normal mood behavior (Sidor *et al*, 2015). Rhythms in the neural activity of VTA dopamine cells as well as the expression and promoter binding of tyrosine hydroxylase by CLOCK point to a strong basis for diurnal variability in reward-related mechanisms in the mesolimbic system, which are disrupted by a dysfunctional CLOCK. Importantly, reduction of dopamine synthesis by the TH inhibitor, AMPT, reversed manic-like behavior specifically in the daytime when DA activity was high in mutants (Sidor *et al*, 2015). Here we have found additional diurnal differences in glutamatergic receptor expression and function in the NAc of mutant animals and have shown that we can rescue behavior with a viral-mediated approach to restore glutamatergic function. However, we only conducted measurements of exploratory drive and reward sensitivity behavior during the light phase. Our results show that excitatory synaptic transmission at MSNs was similarly reduced during both diurnal phases in mutants, as was GluA1 surface protein expression and the resting membrane potential of MSNs. Therefore, it will be important to follow up our findings with behavioral measurements in the dark phase to try to better link these mechanistic changes. We are in the process of conducting these experiments and hope to provide a more comprehensive profile of the role of GluA1 in *Clock* Δ 19 manic-like behavior.

To understand the effects of CLOCK disruption on intrinsic excitability of MSNs, we measured a number of membrane properties and found that while the firing rate of MSNs was increased in the dark phase to a similar extent in both WT and mutants compared to the light phase, AP threshold was also slightly increased in mutant cells during the dark phase. In order to reconcile these results, it will be important to try to characterize the passive membrane properties of the neurons as well. An increase in input resistance or a change in the membrane capacitance could

explain the differential excitability of the neurons across the light/dark cycle. A decreased rheobase during the dark phase could be a result of increased input resistance. Because hyperpolarizing current steps were included in our current clamp protocol, input resistance can be calculated by measuring the amplitude of the membrane potential change from baseline divided by the absolute value of the current injection. Additionally, more subtle properties of the individual action potentials in the evoked spike trains could provide information about potential differences in ionic mechanisms underlying MSN excitability. Cocaine is known to decrease membrane excitability of NAc shell MSNs in part through the up-regulation of SK-type calcium-activated potassium channels (Mu *et al*, 2010). Measuring the medium and fast components of the after-hyperpolarization of spikes would enable us to determine whether these ion channels are differentially regulated in the hyperdopaminergic *Clock* mutants.

Another important question that has arisen from our results is the extent to which GluA1 overexpression affects synaptic transmission and strength in WT MSNs. We confirmed that the overexpression was able to potentiate excitatory synapses in *Clock* mutant MSNs suggesting that this is the mechanism by which it may restore normal behavior, however we did not perform the requisite measure in WTs. This would be especially important because an up-regulation of GluA1 in WT NAc led to a pronounced increase in cocaine CPP compared with GFP expression. This was a surprising result as another study of GluA1 overexpression in the NAc of WT rats demonstrated a decrease in cocaine seeking, particularly during extinction and cocaine-induced reinstatement with no effect on acquisition of self-administration. The passive administration of cocaine in the CPP paradigm differs from the active motivation to self-administer, which is influenced by emotional factors as well as the pharmacological properties of the drug itself in promoting a behavioral reward response (Prus *et al*, 2009). A single manipulation is capable of

driving behavior in these two reward-related measures in opposing directions. NAc overexpression of the cAMP responsive element binding protein (CREB), for instance, reduces cocaine CPP but increases self-administration (Larson *et al*, 2011). It may be possible that while in mutant animals, GluA1 overexpression restores balance to MSN circuitry, an up-regulation of the protein in WT animals could further unbalance the circuit by elevating receptor expression to a non-physiological range. Furthermore, the specific complement of GluA1-containing AMPARs that are inserted into the membrane of MSN synapses following viral overexpression is unknown. AMPARs can exist as homomers of GluA1 subunits or heteromers with GluA1 and most commonly, GluA2 subunits. GluA2-lacking AMPARs have the unique property of being calcium-permeable (CP-AMPARs) and these particular receptors are dynamically altered during drug-induced synaptic plasticity in the accumbens (Conrad *et al*, 2008). We can test for the presence of GluA2-containing AMPARs by measuring evoked currents with local application of the CP-AMPAR selective antagonist, NASPM. If these receptors are present, a percentage of the synaptic response would be blocked by NASPM. Moreover, it is possible that the cocaine conditioning protocol, while acute (2 days of 5mg/kg i.p. injections), is able to alter CP-AMPAR expression in the accumbens of WT mice overexpressing GluA1. To test this, we could also record from infected MSNs after mice have been exposed to a similar cocaine regimen.

Lastly, we hypothesize that the effects of the *Clock* Δ 19 mutation on glutamatergic function in the NAc are a compensatory mechanism indicative of homeostatic plasticity in response to a state of constitutively elevated dopaminergic tone. Given the increased levels of DA and DA metabolites measured in the NAc of *Clock* mutants and the fact that CLOCK knockdown in the NAc does not alter excitatory synaptic transmission or anxiety and reward-related behavior, we believe it is likely that the VTA-NAc projection is necessary for the physiological and behavioral

abnormalities seen in mutants. Because VTA DA projections also target the prefrontal cortex which sends a dense glutamatergic input to the NAc, there is a possibility that activation of this circuit is preferentially contributing to manic-like behavior and plasticity at NAc MSNs. Optogenetic tools allow for the dissection of neural circuits thought to be involved in mood and reward processing in order to assess the exact contribution of each to behavior and physiology (Lenz *et al*, 2013). In order to definitively address the question of whether local transcriptional activity of CLOCK or indirect circuit-level alterations are more important for NAc plasticity, VTA terminals within the NAc could be selectively inhibited with opsins. Sidor and colleagues have demonstrated that chronic optic stimulation of VTA DA neurons produced a manic-like phenotype in TH::Cre mice that persisted for up to 2 weeks following the end of stimulation, we anticipate that chronic inhibition of the VTA-NAc pathway would reverse abnormal mood and reward behavior seen in mutants (Sidor *et al*, 2015). Optical inhibition has been shown to be capable of suppressing dopamine transients that result from actions at both DA cell bodies and terminals and which play a key role in the behavioral response to rewarding substances (McCutcheon *et al*, 2014).

The results of our study are significant because they contribute to a growing body of new studies indicating the involvement of disrupted clock gene function in neuropsychiatric disorders including bipolar disorder. Our understanding of the consequences of defective clock genes on the synapse and circuit level within mesolimbic brain regions is quite limited. Continued research in this direction is therefore very important in order to establish causal mechanisms and inform therapeutic strategies.

3.0 CELL-TYPE SPECIFIC EFFECTS OF NPAS2 DISRUPTION ON ACCUMBAL SYNAPTIC PLASTICITY AND COCAINE SENSITIVITY

The core circadian gene, *Npas2*, has been associated with neuropsychiatric illnesses including bipolar disorder (BP) and is known to regulate the reward value of drugs of abuse. NPAS2 expression is especially enriched in the forebrain including the nucleus accumbens (NAc), a region critical for reward processing and the generation of motivated behavior. Furthermore, its expression appears to be restricted primarily to D1R-containing “direct pathway” medium spiny neurons (MSNs). We have previously demonstrated that a down-regulation of NPAS2 in the NAc decreases the conditioned response to cocaine in mice. Here we sought to further investigate the underlying mechanisms of NPAS2 disruption on accumbal synaptic activity, structural plasticity and reward sensitivity in a cell-type specific manner. Viral-mediated knockdown of NPAS2 in the NAc resulted in an increase in excitatory drive onto MSNs. Preliminary results also suggest that NPAS2 reduction prevents the cocaine-induced up-regulation of spines on secondary dendrites of MSNs. Using *Drd1a*-tdTomato transgenic mice, we found that the synaptic adaptation was specific to D1 MSNs compared with D2 MSNs. Lastly, we validated and utilized a novel Cre-inducible shRNA virus for knockdown of NPAS2 specifically in D1 MSNs of *Drd1a::Cre* mice to demonstrate that direct pathway mechanisms are important for the effects of NPAS2 reduction on cocaine place preference. Together, our results suggest that NPAS2 plays a role in regulating D1 MSN excitatory synapses and cocaine-reward related behavior.

3.1 INTRODUCTION

Circadian rhythm disturbances have been linked to the development and progression of mood-related neuropsychiatric illnesses including bipolar disorder (BD) and major depressive disorder (MDD) (Edgar and McClung, 2013; Karatsoreos, 2014; McClung, 2013). Substance abuse is often co-morbid with these diseases and presents a substantial societal and economic burden. Human genome-wide studies point to a strong association of circadian gene variants and single nucleotide polymorphisms (SNPs) with mood and addiction disorders (Logan *et al*, 2014; McCarthy and Welsh, 2012). Circadian gene perturbations can predispose individuals to substance abuse and addiction vulnerability can be further exacerbated by circadian rhythm disruption producing a negative bidirectional relationship (Parekh *et al*, 2015). At the molecular level, rhythms are maintained by a complex series of transcriptional-translational feedback loops with core and accessory elements (Ko and Takahashi, 2006; Mackey, 2007). The circadian bHLH-PAS domain transcription factor, NPAS2 (neuronal PAS domain protein 2), heterodimerizes with BMAL1 to regulate transcription of genes functioning both within and outside of the molecular clock (Zhou *et al*, 1997). Our group and others have identified direct clock-controlled genes involved in various aspects of dopaminergic transmission within the ventral tegmental area (VTA) to nucleus accumbens (NAc) circuitry, which is critical for reward processing (Arey *et al*, 2014; Hampp *et al*, 2008; Koob and Volkow, 2016; McClung *et al*, 2005; Ozburn *et al*, 2015).

NPAS2 is structurally homologous to CLOCK with only a slight difference in the transactivational domain region (Reick *et al*, 2001). Within the suprachiasmatic nucleus (SCN), or master pacemaker region of the brain, NPAS2 is able to functionally compensate for CLOCK to maintain behavioral and physiological circadian rhythms (DeBruyne *et al*, 2007). Recent

evidence also demonstrates a role of NPAS2 in maintaining peripheral circadian oscillations in the absence of CLOCK (Landgraf *et al*, 2016). However, the expression profile of the two transcription factors within the brain varies, with CLOCK found more ubiquitously throughout and NPAS2 enriched in forebrain structures, particularly the NAc (Garcia *et al*, 2000). These varying patterns of expression may account for differences in the roles of the two proteins in behavioral regulation. NPAS2 has been shown to be critical for allowing mice to adaptively entrain to restricted feeding schedules and for maintaining feeding conditions (Dudley *et al*, 2003; Wu *et al*, 2010). NPAS2-deficient mice also exhibit deficits in the acquisition of cued and contextual fear memory (Garcia *et al*, 2000). Previous studies from our lab have uncovered opposing roles of CLOCK and NPAS2 in mediating drug reward sensitivity. Mice with a specific mutation in the *Clock* gene, *Clock* Δ 19 mice, display a robustly elevated behavioral response to cocaine measured by increased conditioned place preference (CPP), while *Npas2* mutant mice show decreased preference at the same dose (McClung *et al*, 2005; Ozburn *et al*, 2015). Furthermore, viral-mediated shRNA knockdown of NPAS2 exclusively within the accumbens is able to reduce cocaine CPP highlighting its importance in this limbic region (Ozburn *et al*, 2015). Interestingly, knock down of CLOCK in the NAc had no effect on locomotor activity, exploratory drive or cocaine CPP (Ozburn *et al*, 2015). These studies serve to underscore the relevance of region-specific differences in the function of circadian proteins. They also highlight a unique role of accumbal NPAS2 in mediating reward.

NAc medium spiny neurons (MSNs) receive glutamatergic input from a number of regions including the prefrontal cortex and amygdala as well as dopaminergic input from the VTA (Groenewegen *et al*, 1999). Addictive drugs, including cocaine, act to increase mesolimbic dopaminergic signaling, which can remodel NAc excitatory synapses (Lüscher and Malenka,

2011). The NAc consists predominantly of two main types of dopamine receptor subtype-containing MSNs D1+ and D2+ (Lu *et al*, 1998). Their projection pathways, further define these subpopulations with D1 MSNs comprising the “direct” pathway circuitry, promoting goal-directed behavior, and D2 MSNs the “indirect” pathway, generally inhibiting such behavior (Gerfen *et al*, 1990; Lobo *et al*, 2010; Kravitz *et al*, 2013; Lee *et al*, 2016). Using fluorescence-activated cell sorting (FACS) and gene expression profiling, Ozburn and colleagues demonstrated that *Npas2* is enriched in D1 MSNs of the striatum (Ozburn *et al*, 2015). Here we further determined how NPAS2 affects the expression of glutamatergic genes and excitatory synaptic transmission in the NAc. Additionally, using reporter mice, we investigated the effect of *Npas2* disruption on excitatory drive onto D1 and D2 MSNs. Lastly, we’ve begun to explore the role of NPAS2 in structural plasticity of NAc MSNs in response to cocaine as well as reward sensitivity of mice with *Npas2* knocked down specifically in D1 MSNs.

3.2 MATERIALS AND METHODS

3.2.1 Animal use.

C57BL/6J (Jackson Laboratories) and heterozygous and homozygous *Drd1a*-tdTomato (Jackson Laboratories) mice were used for *Npas2* knockdown and electrophysiological experiments. Recordings were made on mice aged 7-9wks. Adult *Npas2* knockout mice were maintained on a C57BL/6J background backcrossed to N10. Homozygous animals and wildtype littermates were used for imaging experiments. Adult male *Drd1a::Cre* mice were used in cre-dependent knock-down and cocaine conditioned place preference experiments. Mice were maintained on a 12:12h

light/dark cycle (ZT 0 = lights on 7:00AM; ZT 12 = lights off 7:00PM). Food and water were available *ad libitum*. All animal use was conducted in accordance with the National Institute of Health guidelines for the care and use of laboratory animals and approved by the Institutional Animal Care and Use Committee of the University of Pittsburgh.

3.2.2 Viral gene transfer and stereotaxic surgery.

Stereotaxic surgery was performed as previously described (Ozburn *et al*, 2015). Bilateral stereotaxic injections of 1 μ L of purified high titer adeno-associated virus (AAV2) encoding *Npas2* shRNA or a scrambled sequence (control) tagged with GFP were delivered into the NAc (from Bregma; angle 10°: AP +1.5mm, Lat. +1.5mm, DV -4.4mm). Mice recovered for 3-4 weeks allowing for full expression of the virus prior to electrophysiological recording. A similar procedure was used to inject AAV2/2.H1lox.mCherry-ShRNA-*Npas2* or AAV2-scramble virus for cocaine place preference testing. Following behavioral testing, the placement of viral injections was verified. Mice were perfused with ice-cold 1x phosphate-buffered saline (PBS) followed by 4% paraformaldehyde in PBS (pH 7.4). Brains were post-fixed for at least 24 hours then transferred to a 30% sucrose solution. 30 μ m-thick tissue sections were mounted onto slides and coverslipped. mCherry signal was not enhanced with immunolabeling. Sections were imaged at 4x magnification using an Olympus fluorescence microscope.

3.2.3 Quantitative real-time RT-PCR

To measure the relative expression of glutamatergic genes from *Npas2* shRNA and scrambled shRNA expressing mice, NAc tissue collection, RNA extraction and cDNA synthesis were

performed as described in (Ozburn *et al*, 2015). Following cDNA synthesis, quantitative real-time polymerase chain reaction (qPCR) was carried out. Primer sets used included: *Gria1* Fwd: 5'-GTGAGCGTCGTCCTCTTC-3', *Gria1* Rev: 5'-GGTTGTCTGATCTCGTCCTT-3';

Gria2 Fwd: 5'-AGTGGGAGAAGTTTGTGTACC-3', *Gria2* Rev: 5'-TGATGCGTCTGAATTCCTGG-3'; *Grin2a* Fwd: 5'-GATTGACCTCGCTCTGCT-3', *Grin2a* Rev: 5'-TCACCTCATTCTTCTCGTTG-3'; *Grin2b* Fwd: 5'-ACATGGCTGGAAGAGACG-3', *Grin2b* Rev: 5'-CATAGCCCGTAGAAGCAAA-3'; *Gapdh* Fwd: 5'-CTTTGTCAAGCTCATTTCCTGG-3'; *Gapdh* Rev: 5'-TCTTGCTCAGTGTCCTTGC-3'.

cDNA (1ng) was mixed with Power SYBR Green PCR Master Mix (Thermo Fisher Scientific) and primers listed above. Reactions were run in duplicate in an Applied Biosystems 7900HT Fast Real-time PCR System (Applied Biosystems, Foster City, CA). Relative gene expression was calculated using the comparative Ct ($2^{-\Delta\Delta Ct}$) method (Landgraf *et al*, 2014) and normalized to each sample's corresponding *Gapdh* mRNA levels.

3.2.4 NAc slice preparation.

C57BL/6J and *Drd1a*-tdTomato mice were anesthetized rapidly with isoflurane and decapitated. Brains were removed into ice-cold oxygenated (95% O₂/5% CO₂) modified aCSF containing (in mM): 135 *N*-methyl-D-glucamine, 1 KCl, 1.2 KH₂PO₄, 1.5 MgCl₂, 0.5 CaCl₂, 70 choline bicarbonate, and 10 D-glucose; pH 7.4 adjusted with HCL. NAc-containing coronal slices (200µm) were sectioned with a vibratome (VT1200S; Leica, Wetzlar, Germany) and incubated for 30 minutes at 37°C in oxygenated aCSF containing (in mM): 119 NaCl, 26 NaHCO₃, 2.5 KCl, 1 NaH₂PO₄, 2.5 CaCl₂, 1.3 MgCl₂, 11 D-glucose. Slices were kept at room temperature until recording then perfused with aCSF (30-32°C).

3.2.5 Whole-cell patch clamp recording.

Slices were viewed by differential interference contrast (DIC) optics (Leica) and accumbal regions were localized under low magnification. Recordings were made under visual guidance with 40x objective. GFP and tdTomato expressing cells were visualized using filters for 488nm and 546nm light respectively. Borosilicate glass pipettes (3-5M Ω) were filled with (in mM): 117 Cs-MeSO₃, 20 HEPES, 0.4 EGTA, 2.8 NaCl, 5 TEA-Cl, 2.5 Mg-ATP, 0.25 Na-GTP, 5 QX-314; pH 7.3 adjusted with CsOH. For miniature EPSC (mEPSC) intracellular solution contained (in mM): 119 K-MeSO₄, 2 KCl, 1 MgCl₂, 1 EGTA, 0.1 CaCl₂, 10 HEPES, 2 Mg-ATP, 0.4 Na-GTP; pH 7.3 adjusted with KOH. Cells were voltage clamped at -70mV. A constant-current isolated stimulator (DS3; Digitimer) was used to stimulate excitatory afferents with a monopolar electrode to record evoked currents (EPSCs). Picrotoxin (50 μ M, Sigma Aldrich) was included in the external perfusion aCSF to block GABA_A receptors. TTX (1 μ M, Tocris, Bristol, UK) was used for mEPSC recordings to block action potential generation. For EPSC experiments, D-APV (50 μ M, R&D Systems, Minneapolis, MN) was bath applied to block NMDARs at 40mV. In some experiments, D-APV was not applied and the peak amplitude of AMPAR current was measured at -70mV and the NMDAR EPSC peak amplitude taken at 40mV, 35ms from the AMPAR EPSC peak.

Series resistance for all recordings was monitored continuously. Cells with a change in series resistance beyond 20% were excluded from data analysis, as were electrophysiologically identified interneurons. Synaptic currents were recorded with a MultiClamp 700B amplifier (Molecular Devices, Sunnyvale, CA). Signals were filtered at 2.6-3 kHz and amplified 10 times, then digitized at 20 kHz with a Digidata 1322A analog-to-digital converter (Molecular Devices).

Miniature current recordings were analyzed using pClamp10 software (Molecular Devices) over a period of approximately 2.5 min during which 250-2500 events were collected.

3.2.6 Dendritic spine labeling and imaging.

NAc MSN dendritic spines were labeled, imaged and analyzed as previously described (Graziane *et al*, 2016). Mice having undergone chronic (7 days) cocaine (20mg/kg; i.p.) injections were sacrificed for dendritic labeling 24 hr following the last injection. Animals were transcardially perfused (15ml/min) with 0.1M sodium phosphate buffer (PB) followed by 1.5% paraformaldehyde (PFA) in 0.1M PB. Brains were removed in to 1.5% PFA and allowed to post-fix for 1hr at room temperature. 100um-thick coronal slices containing the NAc were prepared in room temperature 1x phosphate buffered saline (PBS) using a vibratome. Slices were mounted onto slides and kept wet with PBS. DiI crystals (Invitrogen, Carlsbad, CA) were applied to the accumbens area of slices with a fine brush controlled by a micromanipulator. Slides were kept at 4°C for 36-48hrs to allow crystals to diffuse into tissue and stain cells. Labeled sections were further fixed with 4% PFA for 1hr at room temperature, washed 2-3x with 1x PBS and cover-slipped with aqueous medium prolong (Invitrogen).

DiI was excited with a Helium/Neon 559nm laser and spines were imaged using an Olympus confocal microscope. MSNs were scanned with a 60x oil-immersion objective and individual secondary or tertiary dendrites were zoomed into and scanned at 0.44um steps along the z-axis to capture the full profile. A two-dimensional projection image used for analysis was obtained for each dendrite by stacking all of the planes. Spine density analysis was performed with ImageJ software (NIH). Dendritic segments of 20um length were analyzed at least 5um from a branch point and 8-10 dendrites were sampled from each animal with 4-5 animals/group.

3.2.7 Generation and validation of Cre-inducibleviruses

Cre-inducible shRNA expression for cell-type specific knockdown of NPAS2 was achieved using a modified construct with an H1 polIII promoter driving a loxP flanked STOP cassette and stuffer DNA preventing transcription of *Npas2* shRNA or a scrambled, non-functional sequence. The AAV backbone has been described previously (Arango-Lievano *et al*, 2014). Recombination of the loxP elements in transgenic animals expressing Cre-recombinase under the *Drd1a* receptor promoter (*Drd1a::Cre* mice), allows for the removal of the stuffer DNA and the transcription of the shRNA to achieve knockdown.

3.2.8 Cocaine conditioned placepreference.

Cocaine place preference was assessed using a biased conditioning protocol. On the pre-test day, mice were allowed to explore all chambers of the apparatus for 20 minutes to determine inherent bias. On conditioning days 1 and 3, mice were injected with saline (i.p.) and paired with the preferred chamber of the apparatus, and on days 2 and 4, they received a cocaine injection (5mg/kg; i.p.) paired with the non-preferred chamber. Conditioning sessions lasted 20 minutes. Following conditioning, on day 6, mice were tested again for time spent on either side of the apparatus and the CPP score was calculated by subtracting the pre-conditioning time spent in the cocaine-paired side from the time spent in the cocaine-paired side on the test day. Data from mice that spent a majority of time in the center of the apparatus were eliminated from analysis. Locomotor activity was detected by infrared beam breaks and recorded using Med-PC software (Med Associates, Inc., Fairfax, VT).

3.2.9 Data analysis.

Electrophysiological, imaging, gene expression and behavioral experiments were conducted blind to genotype and/or treatment. Significant differences were determined by Student's *t*-Test, or two-way ANOVA followed by Bonferroni *post hoc* tests. $P < 0.05$ is considered significant for all analyses. All data are presented as mean \pm SEM.

3.3 RESULTS

3.3.1 Knockdown of NPAS2 within the NAc leads to an increase in glutamatergic transmission at MSNs.

Our lab has previously shown that a knockdown of NPAS2 in the accumbens produces a decrease in reward sensitivity as measured by conditioned place preference for cocaine (CPP) (Ozburn *et al*, 2015). Changes in cocaine CPP have been correlated with alterations in excitatory transmission at NAc MSNs including the amplitude of miniature excitatory post-synaptic currents (mEPSCs) and the ratio of evoked AMPAR- and NMDAR-mediated EPSCs (Grueter *et al*, 2013). Here we found that compared with a scrambled control virus, NPAS2 shRNA-infected MSNs showed an increase in the amplitude of mEPSCs ($t_{(20)} = 2.713$, $P = 0.0134$) and a trend-level increase in frequency of events ($t_{(20)} = 2.016$, $P = 0.0574$) (figure 17c,d). Additionally, when analyzing the ratio of the average peak amplitude of AMPAR-mediated evoked currents to that of NMDAR EPSCs (AMPA/NMDAR), a measure of synaptic strength independent of stimulus intensity or synapse number, we found a trend towards an increase with NPAS2 knockdown ($t_{(13)} = 1.795$, $P =$

0.0960) (figure 17f). These results suggest that NPAS2 positively regulates accumbal MSN excitatory postsynaptic transmission and potentially presynaptic release, mechanisms by which it may modulate reward sensitivity.

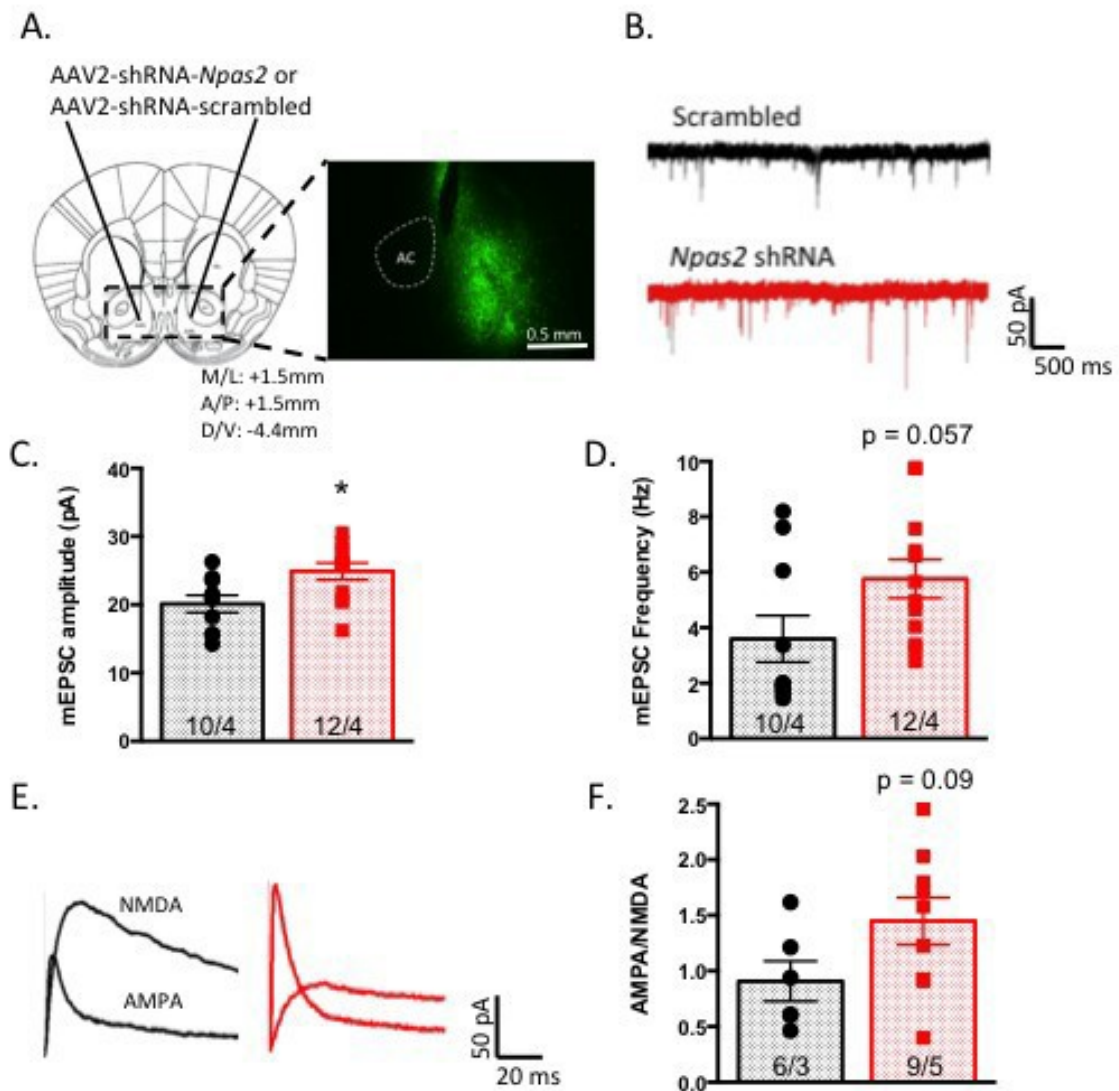


Figure 17. Knockdown of NPAS2 in the NAC leads to an increase in excitatory transmission onto MSNs. (A) Bilateral targeting of AAV2-shRNA-*Npas2* or AAV2-shRNA-scrambled to the NAC (left) and localization of GFP-tagged shRNA (right). (B) Representative traces of mEPSCs sampled from scramble and shRNA infected MSNs. (C) Summary of mEPSC amplitude in cells from both treatment groups. (D) Summary of mEPSC frequency. (E) Representative traces of AMPAR and NMDAR EPSCs from scramble treated (black) and NPAS2 knockdown (red) MSNs. (F) AMPA/NMDA ratio of evoked responses from both groups. n = cells/animals and * $P < 0.05$ for this and all subsequent figures.

3.3.2 Effects of NPAS2 reduction on NAc glutamatergic geneexpression.

Circadian transcription factors including CLOCK and NPAS2 directly regulate the activity of genes with non-clock functions in distinct brain regions. Chromatin immunoprecipitation followed by deep sequencing (ChIP-Seq) performed in a previous study from our lab (Ozburn *et al*, 2015) revealed the binding targets of CLOCK and NPAS2 in the striatum. Several genes related to glutamatergic transmission were among them. We tested the effect of *Npas2* shRNA treatment, compared with scrambled control, on NAc glutamatergic gene expression. We found that knockdown produced an increase in expression of the main AMPAR subunit gene, *Gria1* (GluA1) ($t_{(10)} = 2.23$, $P = 0.050$) with strong trend-level significance (figure 18a). Knockdown of NPAS2 did not significantly alter the expression of the AMPAR subunit gene, *Gria2* (GluA2) ($t_{(10)} = 1.22$, $P = 0.2502$) or the NMDAR subunit genes *Grin2a* (GluN2a) ($t_{(10)} = 0.574$, $P = 0.5785$) and *Grin2b* (GluN2b) ($t_{(4.38)} = 0.940$, $P = 0.3960$; Welch's correction) (figure 18b-d). These findings suggest that while NPAS2 reduction does not appear to significantly affect the expression of several key glutamatergic genes in the NAc, perhaps its role as a negative regulator of excitatory transmission in the NAc may be mediated in part through a subtle alteration in transcription of the major AMPAR subunit, GluA1.

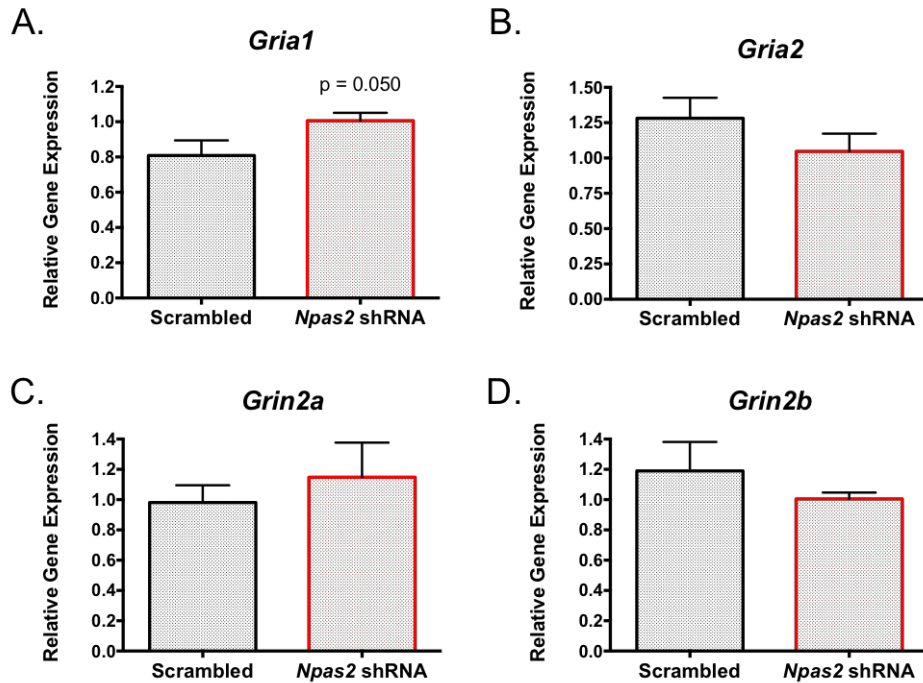


Figure 18. Knockdown of NPAS2 in the NAc does not significantly change AMPAR and NMDAR subunit gene expression. A) A strong trend towards an increase in levels of the GluA1 subunit gene, *Gria1*, was seen following NPAS2 reduction in the NAc. B-D) Relative gene expression of other glutamate receptor subunits, *Gria2*, *Grin2a* and *Grin2b* were not significantly altered by NPAS2 knockdown in NAc tissue. n = 3-4 mice/group.

3.3.3 Increased excitatory synaptic transmission following NPAS2 knockdown is specific to D1 MSNs

Given the restricted expression of NPAS2 to D1-containing MSNs of the striatum (Ozburn *et al*, 2015), we utilized *Drd1a*-tdTomato BAC transgenic mice to identify D1 and non-D1, putatively D2, neurons (Shuen *et al*, 2008) for targeted recordings following *Npas2* shRNA or scramble treatment. Cells co-expressing tdTomato and GFP signals were considered virally infected D1 neurons while those that only expressed GFP signal were considered infected D2 neurons (figure

19a). We again measured glutamatergic transmission by analyzing the amplitude and frequency of AMPAR-mediated mEPSCs. Two-way ANOVA revealed a significant main effect of cell type on mEPSC amplitude ($F_{(1,43)} = 5.394$, $P = 0.0250$ cell type effect; $F_{(1,43)} = 1.705$, $P = 0.1986$ treatment effect; $F_{(1,43)} = 3.657$, $P = 0.0625$ interaction). Bonferroni's *post-hoc* analyses confirmed that mEPSC amplitude was significantly increased in D1 MSNs following NPAS2 knockdown compared with scramble treatment ($P < 0.05$) (figure 19b). We also found that NPAS2 reduction had a significant cell-type specific effect on the frequency of mEPSCs ($F_{(1,43)} = 4.234$, $P = 0.0457$ cell type effect; $F_{(1,43)} = 0.1265$, $P = 0.7239$ treatment effect; $F_{(1,43)} = 4.265$, $P = 0.0450$ interaction) (figure 19c).

Consistent with the increase in AMPAR-mediated synaptic transmission, excitatory synaptic strength was exclusively increased in NPAS2-deficient D1 MSNs as measured by AMPAR/NMDAR ratio ($F_{(1,18)} = 4.275$, $P = 0.0534$ cell type effect; $F_{(1,18)} = 10.34$, $P = 0.0048$ treatment effect; $F_{(1,18)} = 10.76$, $P = 0.0042$ interaction) (figure 19d,e). Together, our findings indicate a specific and robust regulation of glutamatergic signaling in the population of D1-containing MSNs where NPAS2 expression is especially enriched.

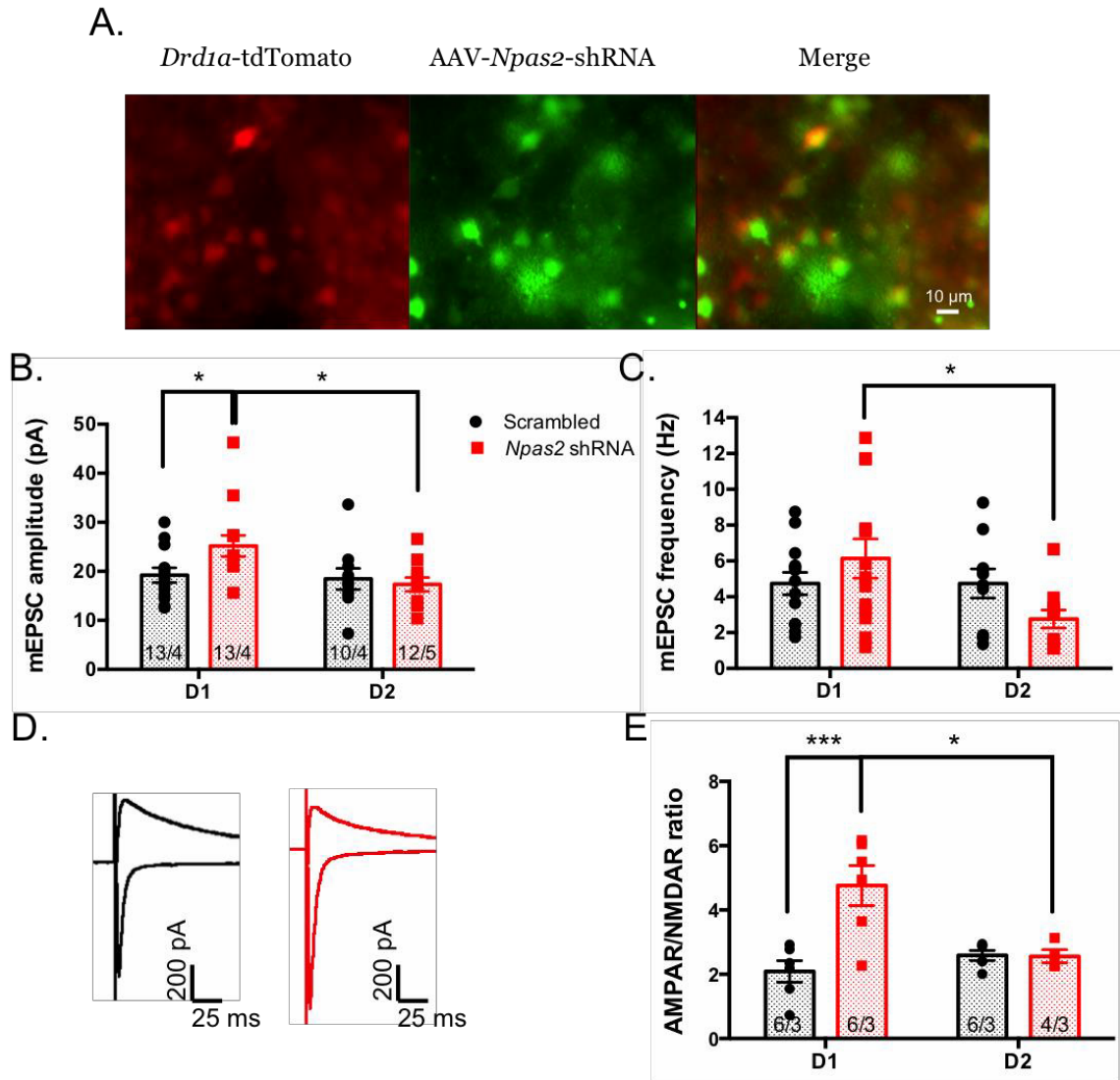
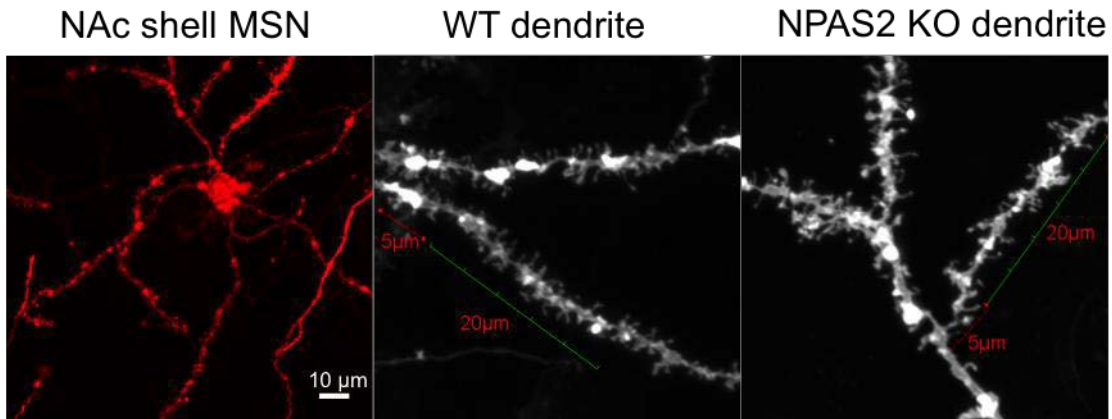


Figure 19. Increased excitatory synaptic transmission following NPAS2 knockdown is specific to D1-containing MSNs. A) *Drd1a*-tdTomato reporter mice were used to visualize D1 and D2 MSNs in NAc slices treated with either AAV-*Npas2*-shRNA or AAV-Scrambled-shRNA virus. B) Summary of mEPSC amplitude in D1 and D2 neurons infected with shRNA or control virus. C) Frequency of miniature events in both groups and cell types. D) Representative traces of AMPAR (-70mV) and NMDAR (40mV) EPSCs from control (black) and *Npas2* shRNA (red) infected D1 cells. E) Summary of AMPAR/NMDAR ratio of evoked currents from all groups. *** $P < 0.001$.

3.3.4 The role of NPAS2 in cocaine-induced MSN dendritic spinealterations

Cocaine's addictive potential lies in its ability to be a powerful mediator of structural and functional plasticity within the brain's reward circuitry. Several studies have demonstrated a dynamic increase in the density of spines on dendrites in the NAc shell following cocaine exposure (Gipson *et al*, 2014; Robinson and Kolb, 2004; Russo *et al*, 2010). Chronic cocaine administration (7d, 15mg/kg, i.p.) also results in a significant up-regulation of *Npas2* expression in the NAc as well as increased promoter binding of the *Per* genes, with no effect on *Clock* or *Bmal1* levels or activity (Falcon *et al*, 2013). Therefore, we sought to determine whether NPAS2 is important for the alterations in MSN spine density mediated by cocaine. NPAS2 knockout (KO) mice and WT littermates (n = 4-5 animals/group) were given 7 days of cocaine (20mg/kg, i.p.). 24 hours after their last injection, animals were sacrificed for DiI labeling of MSN dendrites (figure 20a). Our preliminary results indicate that cocaine-treated NPAS2 KO mice showed a reduction in spine density on secondary dendrites of NAc shell MSNs compared with WT animals, however the data did not reach statistical significance ($t_{(7)}= 2.221$, $P = 0.0618$) (figure 20b). The results of this pilot study are encouraging however in suggesting that NPAS2 may play a role in structural plasticity in the NAc and help explain the robust effect of the transcription factor in regulating the conditioned response to cocaine (Ozburn *et al*, 2015). We are following up with saline controls and increased sample size for all groups.

A.



B.

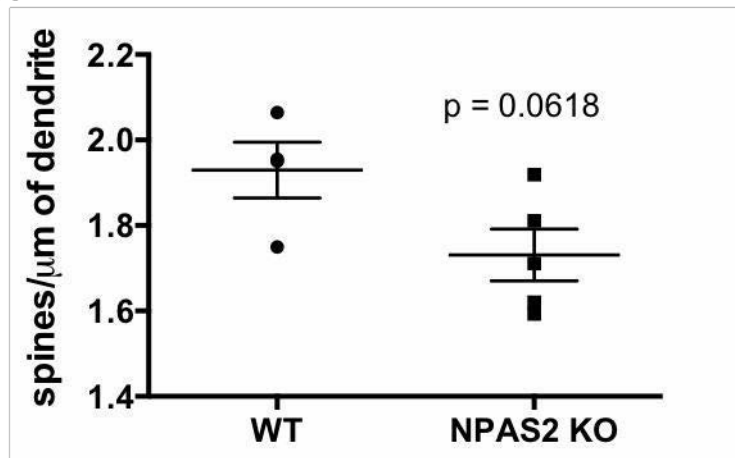


Figure 20. NPAS2 may be important for cocaine-induced changes in MSN structural plasticity. A) DiI dye labeling of MSNs allowed for the visualization of individual spines along secondary dendrites. Spine density was measured on 20 μ m segments at least 5 μ m from branch points off of primary dendrites. B) Spines per micrometer of dendrite were calculated for WT and NPAS2 KO MSNs following chronic cocaine administration. $n = 8-10$ dendrites/animal; 4-5 animals/group.

3.3.5 D1-MSN-specific NPAS2 knockdown in the NAc reduces cocaine reward sensitivity

Cell-type specific molecular mechanisms regulating cocaine reward have not been extensively studied, however, there is evidence for differential actions of another transcription factor, Δ fosB, in accumbal reward-related behaviors. Over-expression of Δ fosB specifically in D1 but not D2 MSNs promotes behavioral responses to cocaine as measured by cocaine conditioned place preference (CPP) and locomotor sensitization (Grueter *et al*, 2013). In the CPP paradigm the conditioned stimulus is experimenter administered and preference is driven by sensitivity to the rewarding value of the drug (Prus *et al*, 2009). Using a novel Cre-inducible shRNA virus modified to selectively knockdown NPAS2 in D1 MSNs of *Drd1a::Cre* mice (or scrambled control) (figure 21a), we used a biased CPP protocol to assess reward sensitivity (figure 21b). We found that cocaine preference was significantly reduced in mice following NPAS2 KD compared with control treated animals ($t_{(20)} = 2.451$, $P = 0.0236$). These results suggest that the decrease in preference previously seen with indiscriminate NPAS2 knockdown (Ozburn *et al*, 2015) in the NAc may be mediated in part through direct pathway mechanisms.

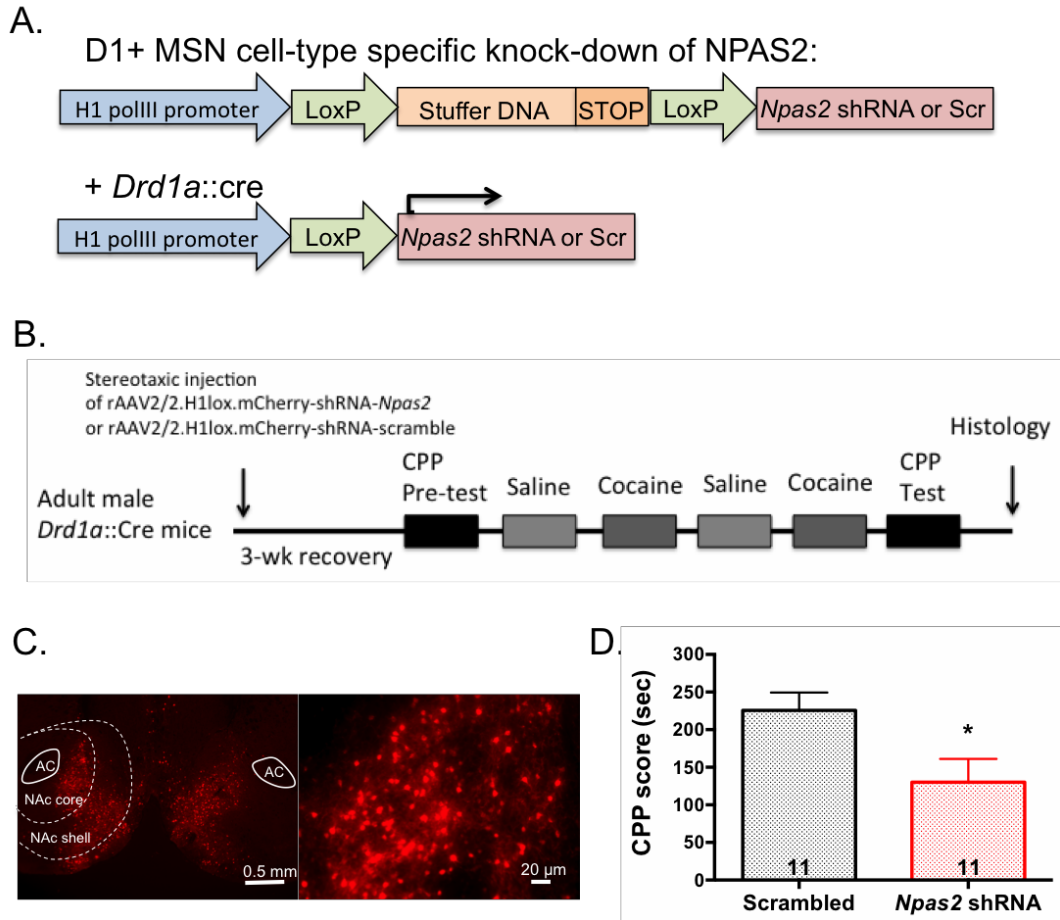


Figure 21. Viral-mediated knockdown of NPAS2 specifically in D1 MSNs reduces cocaine place preference. A) Schematic of Cre-inducible *Npas2* or scrambled shRNA constructs for cell-type specific reduction of NPAS2. B) timeline of viral injections, conditioning paradigm and histological verification. C) Representative micrograph of mCherry expression indicating presence and location of Cre-inducible shRNA virus within the NAc (left) and 20x image of virus expression within NAc cells (right). D) CPP score (test – pre-test time) for scramble and shRNA treated *Drd1a::Cre* mice. AC – anterior commissure.

3.4 DISCUSSION

The results of the current study provide preliminary evidence for the role of NPAS2 in regulating reward-related behavior potentially via synaptic mechanisms in accumbal D1 direct pathway circuitry. While circadian gene variants associate strongly with psychiatric illness including comorbid substance abuse, few studies have explored the regulatory function of these genes in mesolimbic regions and even fewer in specific circuits. We found that non-selective knockdown of NPAS2 in the NAc produced an overall increase in mEPSC amplitude indicative of either a higher density or conductance of postsynaptic AMPA receptors at individual synapses. A trend towards an increase in AMPAR/NMDAR ratio in a small number of cells further supports an increase in excitatory drive onto MSNs as a result of NPAS2 reduction. A strong trend towards an increase in the frequency of miniature currents at MSNs was also observed following NPAS2 knockdown compared with scrambled control. This implies a potential elevation in presynaptic release probability of glutamate at existing sites or an increase in the number of functional synaptic sites.

We hypothesized that the transcription of glutamate receptor subunit genes could be regulated by NPAS2, as previous ChIP-seq analysis revealed binding of the transcription factor to several of these genes. Using cDNA prepared from NAc tissue expressing either *Npas2* shRNA or control virus, we performed real-time quantitative PCR assays to measure transcript levels of the genes, *Gria1*, *Gria2*, *Grin2a* and *Grin2b*, which encode AMPA and NMDA receptor subunits respectively. We only detected a strong trend-level increase in mRNA expression of *Gria1* (GluA1) with NPAS2 knockdown. This, however, is a major subunit of AMPARs, which mediate fast excitatory neurotransmission. Adaptations in the expression or function of receptors containing this subunit most likely underlie the functional synaptic changes observed in our

electrophysiological recordings. ChIP-Seq results indicate NPAS2 binding within the *Gria1* gene, however direct transcriptional regulation of the gene by NPAS2 would have to be verified by identifying binding at a canonical or noncanonical E-box sequence within the promoter region. While not significant, a pattern of decrease in levels of *Gria2* with NPAS2 knockdown could indicate lowered expression of GluA2-containing calcium-impermeable AMPARs, however, this would have to be further tested with pharmacological methods. Collection of the whole NAc for gene expression measurements may be problematic if, as it has been previously shown, *Npas2* expression is largely restricted to a particular population of NAc neurons. However, these preliminary results point to at least one transcriptional mechanism that could underlie the function of NPAS2 as a negative regulator of excitatory synaptic transmission in the NAc, and should be expanded upon further.

In a previous study from our group, *Drd1a*-tdTomato mice were used to isolate D1 MSNs from other cells of the NAc (mostly D2+ MSNs) via fluorescence activated cell sorting (FACS) followed by qPCR. *Npas2* expression was found to be elevated approximately 80-fold in this population (Ozburn *et al*, 2015). Therefore, we were interested to find whether potentiation of excitatory synaptic transmission as a result of NPAS2 reduction would be specific to D1 cells. Here we found that in fact, D1 MSNs showed increased AMPAR mEPSC amplitude and frequency relative to control virus expression and compared with D2 cells. Additionally, the AMPAR/NMDAR ratio was significantly elevated exclusively in D1 cells. In our previous experiment, we saw a trend-level increase in this measure in NPAS2-deficient MSNs, possibly because we were sampling both D1 and D2 cells indiscriminately for recording. These results suggest that perhaps NPAS2 exerts influence on excitatory synaptic transmission and reward behavior in the NAc through adaptations in D1R-containing MSNs.

The interaction of NPAS2, NAc neuronal activity and modulation by cocaine is of particular interest to us. Cocaine is a highly reinforcing psychostimulant drug that is capable of rewiring reward circuitry through dynamic regulation of intracellular signaling and plasticity-related mechanisms in NAc neurons. Cocaine and other drugs of abuse also alter the expression of circadian genes in reward circuits (Falcon *et al*, 2009, 2013; Lynch *et al*, 2008). We therefore sought to address the question of whether NPAS2 is involved in cocaine-induced structural alterations on MSN dendritic spines. Chronic cocaine exposure followed by short or long withdrawal can up-regulate the number of spines on secondary and tertiary dendrites of NAc shell MSNs (Graziane *et al*, 2016). In a pilot study we exposed WT and NPAS2 KO mice to one week of a high dose (20mg/kg) of cocaine and labeled MSNs with a lipophilic dye that filled dendrites and spines for full visualization. Our analysis in a small group of animals revealed a strong trend towards reduced spine density in KO mice compared with WT mice following cocaine treatment. While we are in the process of repeating this experiment with saline controls, we find that spine density in cocaine treated WT mice, as we have measured, is similar to that reported (Graziane *et al*, 2016). These preliminary findings are supportive of our hypothesis that NPAS2 may mediate structural plasticity within NAc circuitry whereby, inhibition of NPAS2 function can occlude cocaine-induced spine changes on MSN dendrites. One possible mechanism that could underlie the action of NPAS2 is its potential association with the transcription factor, nuclear factor kappa B (NfκB), an important mediator of reward behavior in the NAc. NfκB signaling is increased in the accumbens after chronic cocaine and inhibition of NfκB specifically in the NAc reduces the conditioned response to cocaine. Furthermore, NfκB inhibition also prevents the increase in dendritic spines after chronic cocaine (Russo *et al*, 2009). The circadian paralog of NPAS2, CLOCK, has recently been shown to positively regulate NfκB-mediated transcription (Spengler *et*

al, 2012), therefore, it is possible that NPAS2 may associate in a similar manner with this important transcription factor to regulate reward-related mechanisms.

Tools to genetically target specific cell-types within the brain help to elucidate molecular mechanisms contributing to abnormal reward behavior. In this study, we employed a novel viral-mediated approach to selectively knockdown NPAS2 in D1-MSNs of the NAc. The Cre-dependent AAV backbone has been described (Arango-Lievano *et al*, 2014) and we have modified it for our use. We found that reducing NPAS2 expression only in D1 neurons was sufficient to decrease the expression of cocaine CPP, similar to the effect seen with non-specific knockdown in the NAc as well as *Npas2* mutation (Ozburn *et al*, 2015). Together, our results begin to shed light on molecular and cellular mechanisms underlying the regulation of reward by NPAS2.

3.5 FUTURE DIRECTIONS

The preliminary findings here are part of a more comprehensive study aimed at understanding how the forebrain-enriched circadian transcription factor, NPAS2, modulates NAc neuronal activity at baseline and in response to cocaine. We find quite striking cell-type specific adaptations in glutamatergic transmission as a result of NPAS2 disruption in drug naïve animals, however, it will be important to investigate these mechanisms in animals exposed to cocaine which has been shown to specifically increase expression of *Npas2* in the NAc (Falcon *et al*, 2013). We plan to follow up our experiments by recording miniature and evoked EPSCs in virus expressing *Drd1a*-tdTomato following chronic or acute cocaine administration. These experiments could reveal differential actions of NPAS2 at baseline compared with when the circuit undergoes adaptation by cocaine.

D1 and D2 excitatory signaling is altered by cocaine in varying manners, therefore we may find that NPAS2 function is more critical in mediating cocaine's effects in one pathway over the other.

Identifying the direct transcriptional targets of NPAS2 in the NAc is of great interest to us as we explore mechanisms of its action in this brain region. ChIP-Seq analysis has yielded a list of all sequences bound by NPAS2 in the striatum across the light/dark cycle. For added specificity, we are currently optimizing a protocol for the isolation of *Npas2*-containing or deficient D1 and D2 MSNs using fluorescence activated cell sorting (FACS) (figure 22). RNA extracted from the collected cell populations will be used for sequencing. Comparing the results of ChIP-Seq with RNA-Seq will allow us to determine genes both bound and directly regulated by NPAS2 in D1 MSNs of the NAc.

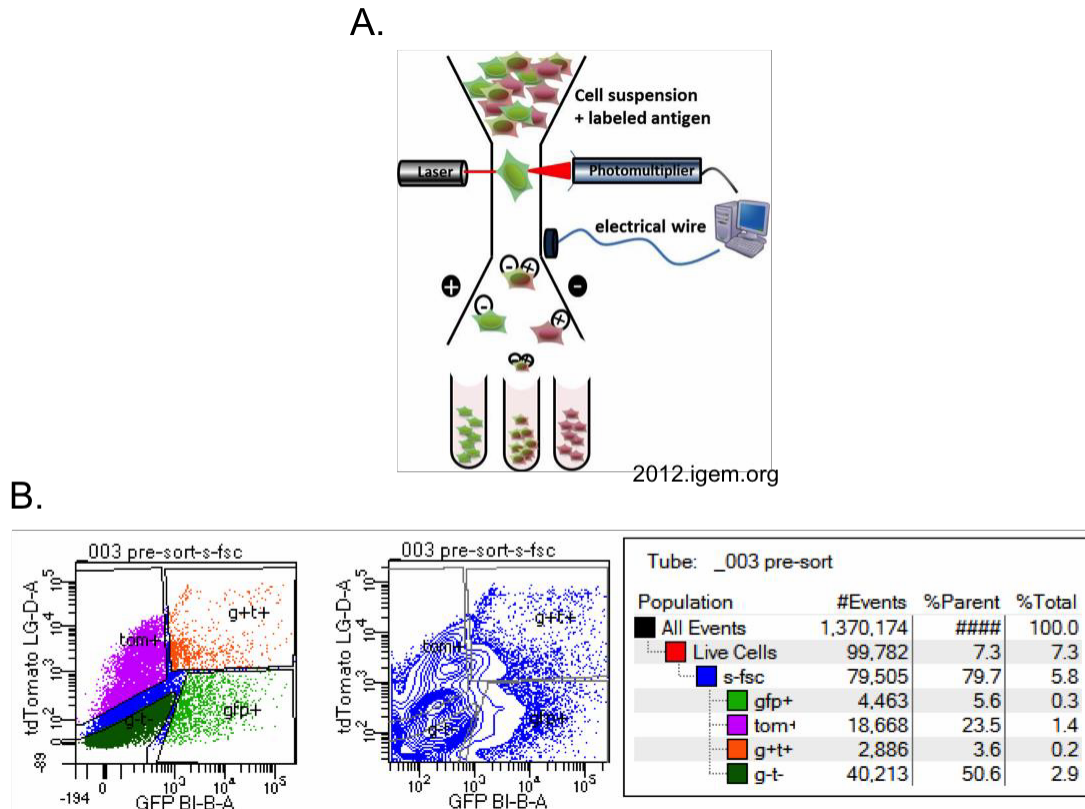


Figure 22. FACS-RNaseq for the identification of gene targets regulated by NPAS2 in D1 and D2 MSNs. A) Schematic diagram of the flow cytometry method to sort and isolate populations of cells from suspension by fluorescent signals. B) Results from a single sort of NAc tissue pooled from 3 *Drd1a*-tdTomato mice expressing *Npas2* shRNA. Cells are differentiated by signal intensity and gates are set for collection. Numbers of live cell events detected for each population are shown at the right. RNA can be extracted from these samples.

Drd1a-tdTomato mice expressing GFP-tagged *Npas2* shRNA or scrambled control viruses will be sacrificed and tissue dissociated as described (Lobo *et al*, 2006). Cells in suspension will be sorted into GFP+, tdTomato +, GFP-/tdTomato-, and GFP+/tdTomato+ populations. Cells are sorted into Trizol LS and RNA can be extracted and purified from these samples for RNA-sequencing. We have been successful in isolating these groups of MSNs from pooled NAc tissue

and have begun to optimize RNA extraction to meet the concentration and purity standards for sequencing. From samples containing ~2000- ~5000 dual-labeled cells, we are able to harvest ~200ng of total RNA. We are confident that this method will allow us to determine genes that are directly regulated by NPAS2 and that may influence direct and indirect pathway activity. Additionally, we plan to sample at multiple time points to map our results onto the ChIP-Seq data we have previously obtained. It is likely that genes involved in synaptic plasticity and dopaminergic and glutamatergic signaling in the NAc may be under circadian regulation by NPAS2. We have previously identified the dopamine D3 receptor as a direct and unique binding target of NPAS2 in the striatum. Furthermore, we can investigate how NPAS2 transcriptional activity changes in D1 and D2 cells as a result of cocaine exposure.

Cocaine induced up-regulation of dendritic spines in the NAc appears to be specific to D1 MSNs (Lee *et al*, 2006). We have attempted to identify D1 MSNs with NPAS2 knocked down for DiI labeling in order to determine whether cocaine-induced structural plasticity is only blocked by NPAS2 disruption in D1 neurons, however, we have faced some technical challenges. We were unable to isolate cells that both expressed shRNA virus and were dye labeled for analysis due to the necessity of sparse dye application to prevent oversaturation. It is thought that the incubation of cocaine craving is in part mediated by the generation of silent synapses in the NAc (synapses which contain very few functional AMPARs) (Huang *et al*, 2009; Lee *et al*, 2013). Morphologically, stubby or thin immature spines are associated with silent synapses (Holtmaat and Svoboda, 2009). Our analysis of spine density can be extended to include a characterization of spine morphology. Graziane and colleagues classified four types of spines found on MSN dendrites following chronic cocaine or morphine administration. The density of thin and filopodia-like spines was increased after cocaine compared with saline treatment (Graziane *et al*, 2016). Moreover, chronic cocaine selectively induced silent synapses in

D1 MSNs, which were measured using electrophysiological methods (Graziane *et al*, 2016; Huang *et al*, 2009). Turning to electrophysiological characterization of silent synapses in *Drd1a*-tdTomato mice expressing shRNA or scramble virus may be the preferred option for addressing the question of whether NPAS2 is important for cocaine-induced alterations of MSN dendritic spines in D1 neurons specifically.

4.0 GENERAL DISCUSSION

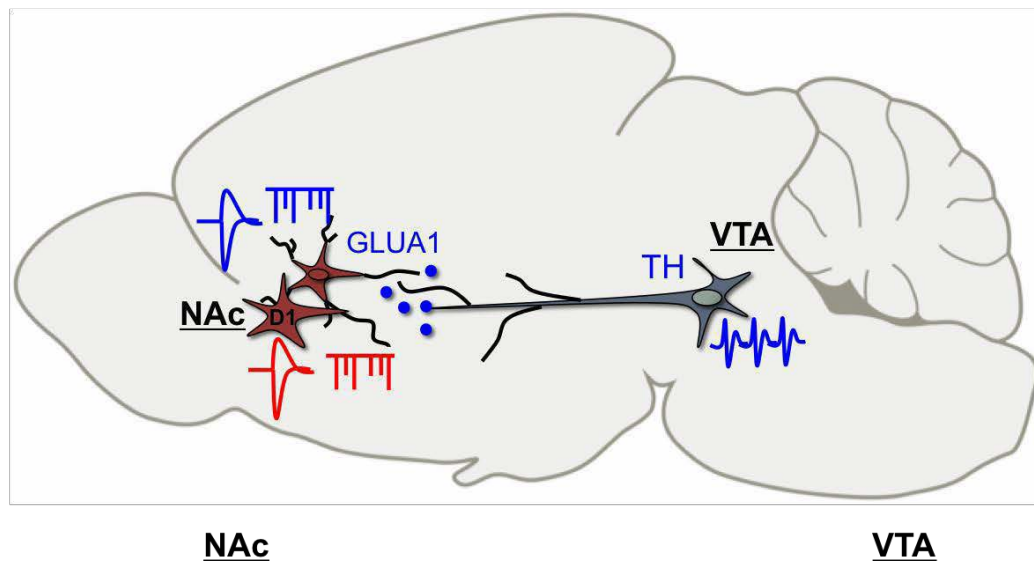
Through these studies, we set out to better understand how circadian genes and proteins regulate neural activity and consequently mood and reward-related behavior in extra-SCN brain regions. In particular, we focused on the nucleus accumbens as a critical integrator of signals encoding sensorimotor, emotional and motivational information to generate goal-directed actions. This complex structure serves as a hub of connections between forebrain and limbic regions. Bipolar disorder and substance abuse disorders, which are often comorbid, are associated with aberrant activity within mesolimbic circuitry. Circadian rhythm disruption on a behavioral or molecular level can be one of many symptoms or causal factors in the development or progression of these disorders. Mapping the cascade of molecular, circuit-level and network-level consequences of psychiatric disease-relevant genetic abnormalities is an overarching goal of our work. The hope is to be able to understand the precise ways in which systems are perturbed in order to restore balance where possible.

For our first study, we utilized a validated genetic mouse model of bipolar mania with a circadian gene disruption to study how *CLOCK* regulates excitatory synaptic activity of NAc MSNs. We performed measurements across the light/dark cycle in order to capture a more comprehensive profile of neural activity in this brain region which has not been previously interrogated. We expected however, that we might uncover diurnal differences in synaptic transmission, receptor expression, and/or intrinsic excitability, as it is evident that circadian

fluctuations exist in structural morphology and functional plasticity in other brain regions. These variations have been described in invertebrate and vertebrate synapses including the expression of hippocampal long-term potentiation (LTP) and changes in dendritic branching, spinogenesis and even the size and distribution of synaptic vesicles (Wardlaw *et al*, 2014; Perez-Cruz *et al*, 2010; Ikeda *et al*, 2015; Jasinska *et al*, 2015). Circadian or diurnal activity-dependence of synaptic protein expression has also been shown. In the hippocampus, striatum and cortex, levels of the synaptic protein, Shank3, are influenced by circadian/melatonin rhythms and wheel-running activity (Sarowar *et al*, 2016). Rhythms in circulating hormones can also modify synaptic connections in a dynamic manner. Liston and colleagues have demonstrated that endogenous glucocorticoid oscillations modulate postsynaptic dendritic spine formation in the mouse cortex associated with skill learning (Liston *et al*, 2013). Excessive or abnormally high levels of glucocorticoids eliminated learning associated new spines and disrupted memories, indicating that these mechanisms may be part of the pathophysiology of stress-related disorders. Therefore, it is important to continue to investigate and consider diurnal or circadian variation on aspects of physiology, behavior, therapeutic efficacy and the activation or inactivation of circuits.

The importance of cell-type and brain region specificity is further underscored by our results. Previous work from our lab has extensively characterized the role of CLOCK in the VTA for regulating aspects of dopaminergic neuronal activity and transmission, however, local disruption of CLOCK in the NAc does not significantly affect behavior or, as we have demonstrated here, excitatory drive onto MSNs. In contrast, the homologous circadian transcription factor, NPAS2 appears to exert its influence on plasticity and behavior predominantly in the NAc where it is highly expressed and perhaps specifically in D1R-containing MSNs. While CLOCK and NPAS2 have been thought to have overlapping function in the brain due to their high structural and functional similarity, we have characterized important differences in how they

regulate neural activity and mood and reward-related behavior. Our findings are summarized below.



- | | | |
|--|---|---|
| <p>CLOCK negatively regulates:</p> <ul style="list-style-type: none"> • DA synthesis and levels <p>CLOCK indirectly regulates:</p> <ul style="list-style-type: none"> • Excitatory transmission • MSN excitability • GluA1 expression • Network activity? | <p>NPAS2 negatively regulates:</p> <ul style="list-style-type: none"> • Excitatory transmission in D1 MSNs <p>NPAS2 positively regulates:</p> <ul style="list-style-type: none"> • Reward behavior • GABA_AR expression • Inhibitory transmission | <p>CLOCK negatively regulates:</p> <ul style="list-style-type: none"> • DA cell firing • TH mRNA/protein • Mood and reward behavior |
|--|---|---|

Figure 23. Summary of the differential roles of CLOCK and NPAS2 in the regulation of neural activity and behavior. Findings from the studies presented here along with previous work from our lab serve to provide a more comprehensive understanding of the functions of CLOCK and NPAS2 within mesolimbic circuitry.

APPENDIX A

ANTI-MANIC EFFICACY OF A NOVEL Kv3 POTASSIUM CHANNEL MODULATOR

Parekh PK*, Sidor, MM*, Gillman A, Bettelini L, Arban R, Alvaro GS, Zambello E, Mutanelli C, Huang Y, Large CH, and McClung CA. (Under revision for *Neuropsychopharmacology*).

* denotes equal contribution.

Kv3.1 and Kv3.2 voltage-gated potassium channels are expressed on parvalbumin-positive GABAergic interneurons in corticolimbic brain regions and contribute to high frequency neural firing. The channels are also expressed on GABAergic neurons of the basal ganglia, substantia nigra, and ventral tegmental area (VTA) where they regulate firing patterns critical for movement control, reward, and motivation. Modulation of Kv3.1 and Kv3.2 channels may therefore have potential in the treatment of disorders in which these systems have been implicated, such as bipolar disorder. Following the recent development of a potassium channel modulator, AUT1 - an imidazolidinedione compound which increases currents mediated by Kv3.1 and Kv3.2 channels in recombinant systems - we report that the compound is able to reverse “manic-like” behavior in two mouse models: amphetamine-induced hyperactivity and *Clock* Δ 19 mutants. AUT1 completely prevented amphetamine-induced hyperactivity in a dose-dependent manner, similar to the atypical antipsychotic, clozapine. Similar efficacy was observed in Kv3.2 knockout mice. In contrast,

AUT1 was unable to prevent amphetamine-induced hyperactivity in mice lacking Kv3.1 channels. Notably, Kv3.1 null mice displayed baseline hyperlocomotion, greater exploratory drive, and antidepressant-like behavior. In *Clock* Δ 19 mice, AUT1 reversed hyperactivity. Furthermore, AUT1 application modulated firing frequency and action potential properties of *Clock* Δ 19 VTA dopamine neurons potentially through network effects. Kv3.1 protein levels in the VTA of *Clock* Δ 19 mice were significantly increased, suggesting a possible compensation for the increased dopaminergic activity in this brain region. Taken together, these results suggest that the modulation of Kv3.1 channels may provide a novel approach to the treatment of bipolar-mania.

A.1 INTRODUCTION

Treatment of bipolar mania is currently based on a mixture of serendipitously discovered drugs, including the antipsychotic drug olanzapine, anticonvulsants such as valproate and lamotrigine, and lithium (Beaulieu and Caron, 2008; Geddes and Miklowitz, 2013; Tohen and Vieta, 2009). With the possible exception of lithium, these drugs primarily treat the symptoms and not necessarily the underlying disease pathology. Furthermore, many pharmacological treatment options in use today are associated with significant safety and tolerability issues that ultimately limit their utility. There is a desperate need for novel approaches that target the primary pathophysiological mechanisms thought to underlie bipolar disorder.

Some, if not all, symptoms of bipolar mania may be caused by an imbalance in the reward and motor circuits of the mesolimbic system and basal ganglia (Caseras *et al*, 2013; Phillips and Swartz, 2014; Salvatore *et al*, 2010). Behavioral abnormalities similar to symptoms of bipolar mania can be induced in mice by interventions that alter activity of the nigrostriatal and mesolimbic

dopamine pathways. Two such approaches involve acute amphetamine administration (Lyon, 1991; Martinowich *et al*, 2009) and genetic mutation of the *Clock* gene in mice (McClung *et al*, 2005; Mukherjee *et al*, 2010; Roybal *et al*, 2007b). Previous studies found that the *Clock* Δ 19 mice have an increase in dopamine cell firing and bursting in the ventral tegmental area (VTA), which appear to underlie many of their manic-like phenotypes, including hyperactivity (Coque *et al*, 2011; McClung *et al*, 2005; Roybal *et al*, 2007b). Psychiatrists have used antipsychotic interventions to reduce the "over-activity" of the dopamine system by inhibiting post-synaptic dopamine receptors, but this approach necessarily leads to significant adverse effects. An alternative approach may be to consider the activity of GABAergic output neurons of the basal ganglia and mesolimbic system that control movement and reward.

Kv3.1 channels have been implicated in the maintenance of high-frequency firing of GABA output neurons in the globus pallidus (Hernandez-Pineda *et al*, 1999) and substantia nigra (Ding *et al*, 2011), areas critical to maintaining inhibitory control over motor output. Although function of Kv3 channels in the mesolimbic system has not yet been demonstrated, distribution studies confirm the presence of Kv3.1 channels in the VTA and striatum (Lenz *et al*, 1994), so an analogous mechanism of control over reward and motivation could be proposed. Activation of Kv3.1 channels may help enhance the fast firing of GABAergic neurons in these systems to re-establish the balance of inhibitory control in patients with bipolar disorder without resorting to blockade of the dopamine system. To this end, we have investigated the efficacy of a novel class of drug that modulates Kv3.1 channels (Rosato-Siri *et al*, 2016) in two models of mania-like hyperactivity associated with imbalance of the mesolimbic system in mice: acute amphetamine treatment and the *Clock* Δ 19 genetic mutation.

A.2 MATERIALS AND METHODS

A.2.1 Animals.

Male *Clock* Δ 19 mutant mice were created by N-ethyl-N-nitrosurea mutagenesis that produces a dominant-negative CLOCK protein defective in transcriptional activity (King *et al*, 1997) and were obtained from J. Takahashi (UT Southwestern). For all behavioral experiments using *Clock* Δ 19 mutants, adult male mutants (*Clock/Clock*) were compared with wild-type (+/+) littermate controls (10-12wks), on a mixed BALBc x C57BL/6 background. *Clock* Δ 19 mice (4-6wks) were used for electrophysiological experiments. Kv3.1 null (Kv3.1 *-/-*) male mice (Ho *et al*, 1997) on a mixed C57BL/6 x 129 background were obtained from R. Joho (UT Southwestern) and het-het breeding was used to obtain both nulls and WT littermate controls; Kv3.2 null (Kv3.2 *-/-*) male mice were obtained from B. Rudy (New York University). CD1 outbred male mice (8-12wks) were purchased from Jackson labs. All mice were maintained on a 12/12-hr light dark cycle (lights on/off at 7:00/19:00) with food and water provided *ad libitum*. Mice were housed 2-4 per cage. All animal use was conducted in accordance with the National Institute of Health guidelines and approved by the Institutional Animal Care and Use Committees of the University of Pittsburgh and UT Southwestern Medical Center.

A.2.2 Drug Preparation.

AUT1 (structure: (5R)-5-ethyl-3-(6-{[4-methyl-3-(methoxy)phenyl]oxy}-3-pyridinyl)-2,4-imidazolidinedione; Autifony Therapeutics Limited, UK) was administered intraperitoneally (i.p.) or through oral gavage and prepared fresh in vehicle (AUT1-vehicle) consisting of 0.1% Tween20,

0.5% HPMC K15EP (Colorcon) and 12.5% Captisol in bacteriostatic saline. Freshly prepared AUT1 was administered 30 minutes prior to behavioral testing. D-amphetamine (2 mg/kg, i.p. or 4 mg/kg, i.p.) and clozapine (3 mg/kg, i.p.) (Sigma, St. Louis, MO) were prepared fresh in saline. All drugs were dosed at 10ml/kg. Lithium chloride was dissolved in drinking water (600 mg/L) and made available for 10 days as published previously (Roybal *et al*, 2007a). This treatment has been shown to produce a stable serum concentration in the low therapeutic range for humans (0.41 ± 0.06 mmol/L) with little to no adverse health consequence (Roybal *et al*, 2007a).

A.2.3 Behavioral Assays.

Mood-related behavioral assays were performed in a cohort of Kv3.1 null mice with at least one week between tests. Behavioral testing was conducted during the light cycle and mice were habituated to the environment for a minimum of 30 minutes.

Locomotor Activity. Mice were individually placed in novel, unexplored automated locomotor activity chambers equipped with apparatus-embedded infrared photobeams (San Diego Instruments, San Diego, CA and Kinderscientific Smart Cage Rack System; field dimensions: 9.5”x18.0”), which measured continuous horizontal locomotor activity for 60 min. Kv3.1 null mouse naïve locomotor behavior was assessed under red light conditions; all other locomotor behavior was measured under regular room lighting conditions.

Elevated plus maze. The plus maze consisted of two plastic open arms perpendicular to two closed arms (arms: 30 x 5 cm). Mice were habituated to the testing room for 30 min and then placed into the center of the plus-maze facing a closed arm under dim lighting conditions. The time spent on

the closed and open arms, as well as the number of explorations of open and closed arms were determined by video tracking software, Ethovision 3.0 (Noldus, Leesburg, Virginia) over a 5-minute period. The apparatus was cleaned and dried between animals.

Light/Dark Test. The dark/light apparatus consisted of a two-chambered box (25 cm x 26 cm for each side, Med Associates, St. Albans, Vermont). One side was kept dark while the light chamber had a fluorescent bulb placed horizontally across the top. Mice were initially habituated to the dark chamber for 2 min and then allowed free exploration of both light and dark chambers for an additional 10 minutes. The time spent in each chamber and total transitions were measured by Med Associates automated software.

Forced Swim Test. Mice were tested in the one-day modified forced swim test. Mice were placed into a 4L Pyrex glass beaker filled with 3L of water (23-26 °C) where the time spent struggling during the last 4 minutes of a 6-minute test (first 2 minutes are habituation) was videotaped and later measured by a blinded observer. Immobility was defined as all cessation of movement except those required for flotation.

A.2.4 VTA Slice preparation.

Clock Δ 19 mutant mice were anesthetized rapidly with isoflurane inhalation and decapitated. Brains were removed into ice-cold oxygenated (95% O₂/ 5% CO₂) modified aCSF containing (in mM): 93 N-methyl-D-glucamine, 2.5 KCl, 1.2 NaH₂PO₄, 30 NaHCO₃, 20 HEPES, 25 D-Glucose, 5 Sodium ascorbate, 2 Thiourea, 3 Sodium pyruvate, 10 MgSO₄•7H₂O, 0.5 CaCl₂•2H₂O; pH 7.3-7.4 adjusted with HCL; 300-310 mOsm. VTA-containing horizontal slices (250 μ m) were

sectioned with a vibratome (VT1200S; Leica, Wetzlar, Germany) and incubated for 12 minutes at 37°C in the same solution. Slices were then transferred to holding aCSF at room temperature until recording. Holding aCSF contained (in mM): 92 NaCl, 2.5 KCl, 1.2 NaH₂PO₄, 30 NaHCO₃, 20 HEPES, 25 D-Glucose, 5 Sodium ascorbate, 2 Thiourea, 3 Sodium pyruvate, 2 MgSO₄•7H₂O, 2 CaCl₂•2H₂O (pH 7.3-7.4; 300-310 mOsm).

A.2.5 Whole-cell patch-clamp recordings.

Slices were viewed by differential interference contrast (DIC) optics (Leica) and the VTA was localized medial to the optic tract. Recordings were made under visual guidance (40X objective). Slices were maintained at 30-32°C in oxygenated aCSF containing (in mM): 124 NaCl, 2.5 KCl, 1.2 NaH₂PO₄, 24 NaHCO₃, 5 HEPES, 13 D-Glucose, 2 MgSO₄•7H₂O, 2 CaCl₂•2H₂O (pH 7.3-7.4, 300-310 mOsm). Borosilicate glass pipettes (3-5MΩ) were filled with (in mM): 119 K-MeSO₄, 2 KCl, 1 MgCl₂, 1 EGTA, 0.1 CaCl₂, 10 HEPES, 2 Mg-ATP, 0.4 Na-GTP (pH 7.3 adjusted with KOH; 285-295 mOsm). Giga-Ohm seal was achieved and spontaneous sodium currents recorded in cell-attached mode to differentiate dopamine and non-dopamine neurons (Johnson and North, 1992). Cells were voltage clamped at -65mV and a hyperpolarizing voltage step protocol was applied (0mV to -100mV) to detect the presence of “h” current for further identification of neurons (Margolis *et al.*, 2006). For recordings, cells were current clamped and action potential (AP) firing was recorded in response to increasing current steps (-80pA to 200pA) in the presence of DMSO (0.1%) or 10μM AUT1 (dissolved in 0.1% DMSO; 30 + min. bath incubation), a dose previously confirmed to modulate Kv3.1 channels (Rosato-Siri *et al.*, 2016). All recordings were made using a MultiClamp 700B amplifier (Molecular Devices, Sunnyvale, CA). Signals were

filtered at 2.6-3 kHz and amplified 10 times, then digitized at 20 kHz with a Digidata 1332A analog-to-digital converter (Molecular Devices). Spike counts were tallied manually to produce input-output relationships. Using pClamp 10 software (Molecular Devices). AP half-width and amplitude of the negative peak of the first derivative were determined for each of the middle 5 APs in the train and averaged. Inter-event intervals were automatically determined and CV was calculated as the SD/mean.

A.2.6 Immunohistochemistry.

Free-floating tissue sections underwent antigen retrieval for 20 min at 80°C in 10 mM sodium citrate buffer pH 9 (pre-heated), followed by a 10 min cooling period at room temperature (RT) in the same buffer. Sections were permeabilized for 10 min at RT in 0.1 M phosphate buffered saline (PBS) + 0.1% Triton X-100, then washed (3 x 5 min) in 0.1 M PBS, and incubated for 60 min in 0.1 M PBS + 1% H₂O₂ (30%) at RT. Sections were blocked with 1% blocking buffer (Component D, supplied by tyramide signal amplification kit) for 60 min at RT and then incubated at 4 °C for 48 hours with rabbit anti-Kv3.1b (Sigma #P9732) diluted 1:500 in 1% blocking buffer. Following primary antibody incubation, sections were washed with 0.1 M PBS (3 x 5 min washes) and incubated at RT with a goat anti-rabbit HRP conjugated antibody prepared in 1% blocking buffer, followed by 3 x 10 min washes with 0.1 M PBS. For amplification of signal, sections were incubated for 10 min in freshly prepared tyramide working solution, consisting of diluted tyramide stock solution (1:100) in amplification buffer. Sections were washed for 3 x 10 min with 0.1 M PBS and mounted with Vectashield mounting medium for fluorescence (Vector Laboratories, Burlingame, CA).

A.2.7 Western Blotting.

SDS-PAGE and Western blots: Mice were placed in a plexiglass restrainer and euthanized by microwave irradiation aimed at the head (5 kW, 1.2 s, Murimachi Kikai Co., Ltd. Tokyo, Japan). Both ventral tegmental (VTA) and nucleus accumbens (NAc) tissue was dissected from 1-2 mm slices with a 16-gauge tissue punch and immediately frozen on dry ice for later use. For protein extraction, tissue samples were homogenized by sonication on wet ice in a buffer containing 320 mM sucrose, 5 mM HEPES, phosphatase inhibitor cocktail I and II (Sigma, St. Louis, MO), protease inhibitor (Sigma, St. Louis, MO), 5% SDS, and 50 mM NaF. Protein homogenate was spun at 12,000 RPM for 10 min at 4 °C and the supernatant carefully removed. DC assays (Biorad, Hercules, CA) were performed to quantitate protein levels. Aliquots of sample were combined in Laemmli SDS sample buffer (Bio-World, Dublin, OH), and heated at 65 °C for 20 min. Samples were loaded (VTA: 20 µg total protein per lane; NAc: 40 ug total protein per lane) and run on a pre-cast 4-15% Tris-glycine (TG) extended gel (Biorad, Hercules, CA) at 100V for 95 min in 1 x TGS buffer (Biorad, Hercules, CA). Proteins were transferred overnight at 4 °C onto Immobilon PVDF membranes (Millipore, Bedford, MA) at 30V in 1 x TG buffer. Membranes were re-wet briefly in a series of methanol, MilliQ water and 1 x PBS and blocked in Odyssey Blocking Buffer (LI-COR Biosciences, Lincoln, NE) for 1 hr at room temperature (RT). Membranes were incubated for 24 hrs at RT with the primary antibody, mKv3.1b (1:100, Abcam, UK #ab84823) and mouse anti-GAPDH (1:50,000, Fitzgerald, Acton, MA) diluted in blocking buffer + 0.2% Tween20. The following day, blots were washed in 1 x PBS + 0.1% Tween20 and incubated for 1 hour at RT with infrared (IR) Dye 680 conjugated goat anti-mouse antibody (1:5000, LI-COR Biosciences, Lincoln, NE) diluted in 0.2% Tween20 + 0.02% SDS. Blots were washed in 1 x PBS + 0.1% Tween20 with a final wash in 1 x PBS. Blots were scanned using the Odyssey Infrared

Imaging System (LI-COR Biosciences, Lincoln, NE) interfaced to a PC running Odyssey 2.1 software for quantification. To control for potential discrepancies in loading concentration, values are expressed as a ratio to the corresponding GAPDH integrated intensity. Values that were ± 1.5 standard deviations from the group mean were excluded from analyses.

A.2.8 Pharmacokinetics.

Blood aliquots were collected into micronic tubes (70 μ L blood + 130 μ L water with HEPES 0.1N), vortexed and stored at 4°C prior to the assay. Samples were vortexed and centrifuged at 3000rpm for 10 mins and diluted into 96 well plates for the assay (80 μ L water + 100 μ L supernatant). Brains were homogenized with 4.3 vol. di MeOH 50% and collected into tubes (200 μ L). Homogenates were then vortexed and centrifuged at 3000rpm for 10 minutes and the aliquots of the supernatant transferred to 96 well plates. High performance liquid chromatographic (HPLC) assays using mass spectrometric detection (LC-MS/MS with UV) for the determination of AUT1 were developed and validated to identify the compound in brain and blood matrices.

A.2.9 Statistical Analysis.

Data were analyzed using an unpaired Student's *t*-test while comparisons of three or more group means were conducted using an analysis of variance (ANOVA) followed by a Bonferroni or Dunnett post-hoc test for multiple comparisons. Analyses over time were conducted using a two-way repeated measures-ANOVA followed by a Bonferroni post-hoc test to control for multiple comparisons. In some instances, interactions that reached significance or trended towards significance were followed up with post-hoc student's *t*-tests and are indicated in the figure

legends. Analyses were conducted using the GraphPad Prism 5 statistical software for Windows. Data are presented as mean \pm standard error of the mean (SEM) with a two-tailed p-value ≤ 0.05 considered statistically significant.

A.3 RESULTS

A.3.1 AUT1 attenuates amphetamine-induced hyperactivity: importance of K_v3.1 channels.

The efficacy of AUT1 was first assessed in the amphetamine-induced hyperactivity model in the outbred CD1 mouse strain (figure 23). AUT1, administered 30 min prior to a single dose of amphetamine, was effective in preventing amphetamine-induced hyperactivity in a dose-dependent manner (figure 23a,c). One-way ANOVA revealed a significant difference between pre-treatment groups ($F_{5,57} = 2.96$, $p = 0.02$) Both 30 mg/kg and 60 mg/kg doses were effective in attenuating hyperactivity, whereas no significant effect was found with a 10 mg/kg AUT1 dose. Significant group differences were found in locomotor activity during the 60 minutes following amphetamine injection ($F_{5,54} = 13.17$, $p < 0.0001$) (figure 23c). Importantly, the higher (60 mg/kg) AUT1 dose was as effective as clozapine, an antipsychotic with demonstrated anti-manic efficacy, at preventing hyperactivity.

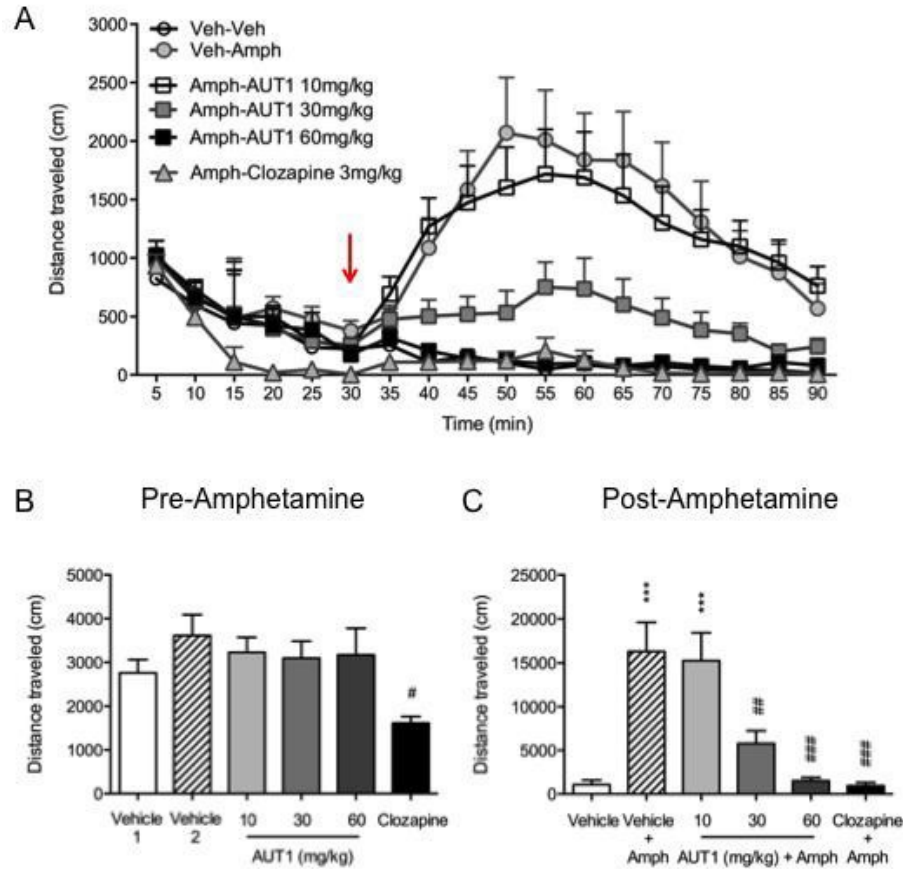


Figure 24. A Kv3.1 channel modulator (AUT1) prevents amphetamine-induced hyperactivity. (A) CD1 mice were pre-treated with AUT1 (10 mg/kg, 30 mg/kg or 60 mg/kg) or AUT1-vehicle 30 minutes prior to a single injection of 2 mg/kg amphetamine (indicated by red arrow). Locomotor behavior was assessed both before (B) and after (C) amphetamine injection. Clozapine was administered as a positive control. (A) Time course of locomotor activity following AUT1 administration at T=0min and after amphetamine injection at T=30min. (B) There was a significant difference in locomotor activity across pretreatment groups, with a specific reduction in locomotor activity within the clozapine group prior to amphetamine injection. Note that two vehicle groups are depicted to dissociate groups that subsequently received a second dose of a vehicle (vehicle group 1: vehicle + vehicle) vs. a dose of amphetamine (vehicle group 2: vehicle + amph). Importantly, AUT1 had no effect on locomotor activity prior to amphetamine injection. (C) As expected, amphetamine injection resulted in a significant increase in activity in vehicle pre-treated CD1 mice and in mice that were pre-treated with a low dose of AUT1 (10 mg/kg). Locomotor activity following amphetamine injection was significantly lower in mice that were pretreated with higher doses of AUT1 (30 mg/kg and 60mg/kg) relative to vehicle pre-treated mice, i.e. locomotor activity following amphetamine injection in AUT1 pre-treated mice was not significantly different than mice who did not receive amphetamine (saline injection). The highest dose of AUT1 was as effective as clozapine pre-treatment at preventing amphetamine-induced hyperactivity (clozapine vs. vehicle + amph). Vehicle group = AUT1-vehicle pretreatment + saline injection. Vehicle + amph = AUT1-vehicle pre-treatment + amphetamine. Treatment group vs. vehicle ***p<0.001; treatment group vs.

amphetamine: ##p<0.01, ###p<0.001. Amph = amphetamine. Red arrow indicates time of amphetamine administration. n=10/group.

Pharmacokinetic analyses were conducted to measure the systemic exposure and brain penetration of differing doses of AUT1 (10, 30 and 60 mg/kg) in male CD1 mice at 30 min (blood concentration) and 90 minutes (blood and brain concentration measured following locomotor testing) post-administration (Table 4). Overall, brain penetration was high and consistent among the doses. The mean brain-to-blood concentration ratio for AUT1 was ca. 1.6. Importantly, sufficient brain penetration was observed at all doses tested and was concurrent with behavioral effects seen during efficacy testing.

Table 3. Bioavailability of AUT1 with oral administration.

Dose (mg/kg)	Time (min)	Blood conc. ng/ml (μM)	Unbound blood conc. ng/ml (μM)	Brain conc. ng/ml (μM)	Unbound brain conc. ng/ml (μM)
10	30	1055 (2.39)	86.5 (0.25)	783 (2.29)	45.4 (0.13)
	90	497 (1.46)	40.8 (0.12)		
30	30	4827 (14.1)	396 (1.16)	4658 (13.6)	270 (0.79)
	90	2858 (8.36)	234 (0.69)		
60	30	8853 (25.9)	726 (2.13)	12405 (36.3)	719 (2.11)
	90	7725 (22.6)	633 (1.85)		

To test the specificity of this effect to Kv3.1 channels, separate cohorts of Kv3.1 null mice and their WT littermates were administered three different doses of AUT1 (or vehicle) 30 min prior to a single injection of amphetamine or vehicle (figure 24). Both WT and Kv3.1 null mice

exhibited the expected increase in locomotor activity following a single amphetamine injection (figure 24b). WT mice, however, that received AUT1 prior to amphetamine, exhibited attenuation in amphetamine-induced hyperactivity with the effects most notable at the 60 mg/kg and 100 mg/kg doses. Two-way ANOVA revealed a significant main effect of treatment on locomotor activity ($F_{4,67} = 22.37$, $p < 0.0001$) and a genotype x treatment interaction ($F_{4,67} = 2.28$, $p = 0.07$) (figure 24b).

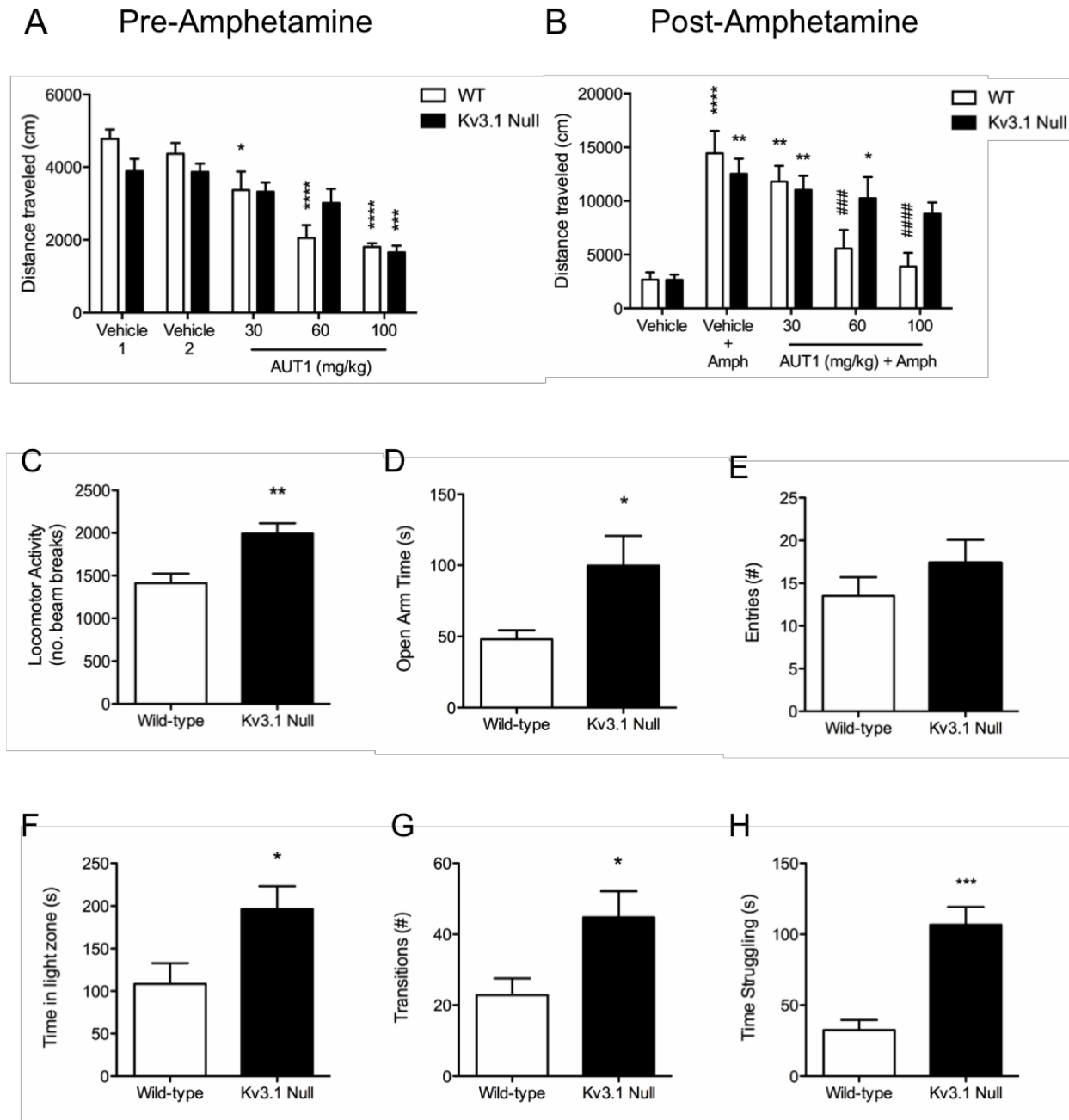


Figure 25. AUT1 does not attenuate amphetamine-induced hyperactivity in Kv3.1 null mice and these mice exhibit manic-related behaviors. (A) Cohorts of mice were pre-treated with AUT1 (30 mg/kg, 60 mg/kg or 100 mg/kg, i.p.) or AUT-vehicle prior to amphetamine injection (4 mg/kg, i.p.) at T=30min. Bonferroni post-hoc analyses revealed that wild-type (WT) mice decreased locomotor activity in response to AUT administration in a dose-dependent manner relative to vehicle-treated WT mice. In Kv3.1 null mice, only AUT1 at the highest dose of 100 mg/kg significantly reduced activity relative to vehicle treated Kv3.1 mice. Note that two vehicle groups are depicted to dissociate groups that subsequently received a second dose of a vehicle (vehicle group 1: vehicle + vehicle) vs. a dose of amphetamine (vehicle group 2: vehicle + amph). (B) Bonferroni post-hoc analyses revealed that amphetamine

injection lead to a significant increase in locomotor activity in both vehicle pre-treated WT and Kv3.1 null mice and in mice pre-treated with the lower 30 mg/kg dose of AUT1. AUT1 administered at 60 mg/kg and 100 mg/kg, however, prevented amphetamine-induced hyperactivity in WT mice, leading to a significant reduction in locomotor behavior relative to vehicle pre-treated mice administered amphetamine (WT AUT1 vs. amph). In contrast, AUT1 was not effective at preventing amphetamine-induced hyperactivity in Kv3.1 null mice, with significant increases in locomotion observed following amphetamine injection at 30 mg/kg (Kv3.1 AUT1 vs. vehicle) and 60 mg/kg but not at 100 mg/kg. AUT1 vs. vehicle: * $p < 0.05$, ** $p < 0.01$, *** $p < 0.001$, **** $p < 0.0001$; AUT1 vs. vehicle + Amph: ### $p < 0.001$. Amph = amphetamine. $n = 6-10$ /group. (C) Kv3.1 null mice exhibited a significant increase in total locomotor activity over a 1-hour test in novel locomotor chambers. Anxiety-like behaviors were decreased in Kv3.1 null mice as demonstrated by significant increases in (D) time spent exploring the open arms of the elevated plus maze (no difference in entries into open arm [E]) and in (F and G) time spent in, and transitions into, the light chamber of the light:dark test. (H) Furthermore, Kv3.1 mice exhibited a significant increase in time spent struggling in the forced swim test. WT vs. Kv3.1: * $p < 0.05$, ** $p < 0.01$, *** $p < 0.001$ $n = 8$ /genotype.

At the highest dose of 100 mg/kg, AUT1 significantly decreased locomotor activity in both WT and Kv3.1 null mice prior to amphetamine injection, possibly indicating a non-specific sedative effect at this dose (figure 24a). AUT1, however, was not effective at reducing amphetamine-induced hyperactivity in mice lacking Kv3.1 channels, even at these high doses (figure 24b.), which argues against a purely sedative effect. This suggests that functional Kv3.1 channels are required for the effects of AUT1 on amphetamine-induced hyperactivity. Notably, this was confirmed by repeating the experiment using Kv3.2 knock-out mice where AUT1 was as effective at preventing hyperactivity as in WT mice ($F_{2,24} = 12.73$, $p = 0.0002$) (figure 25). Collectively, this suggests that Kv3.1 channels (and not Kv3.2) are necessary for AUT1's mechanism of action in this model.

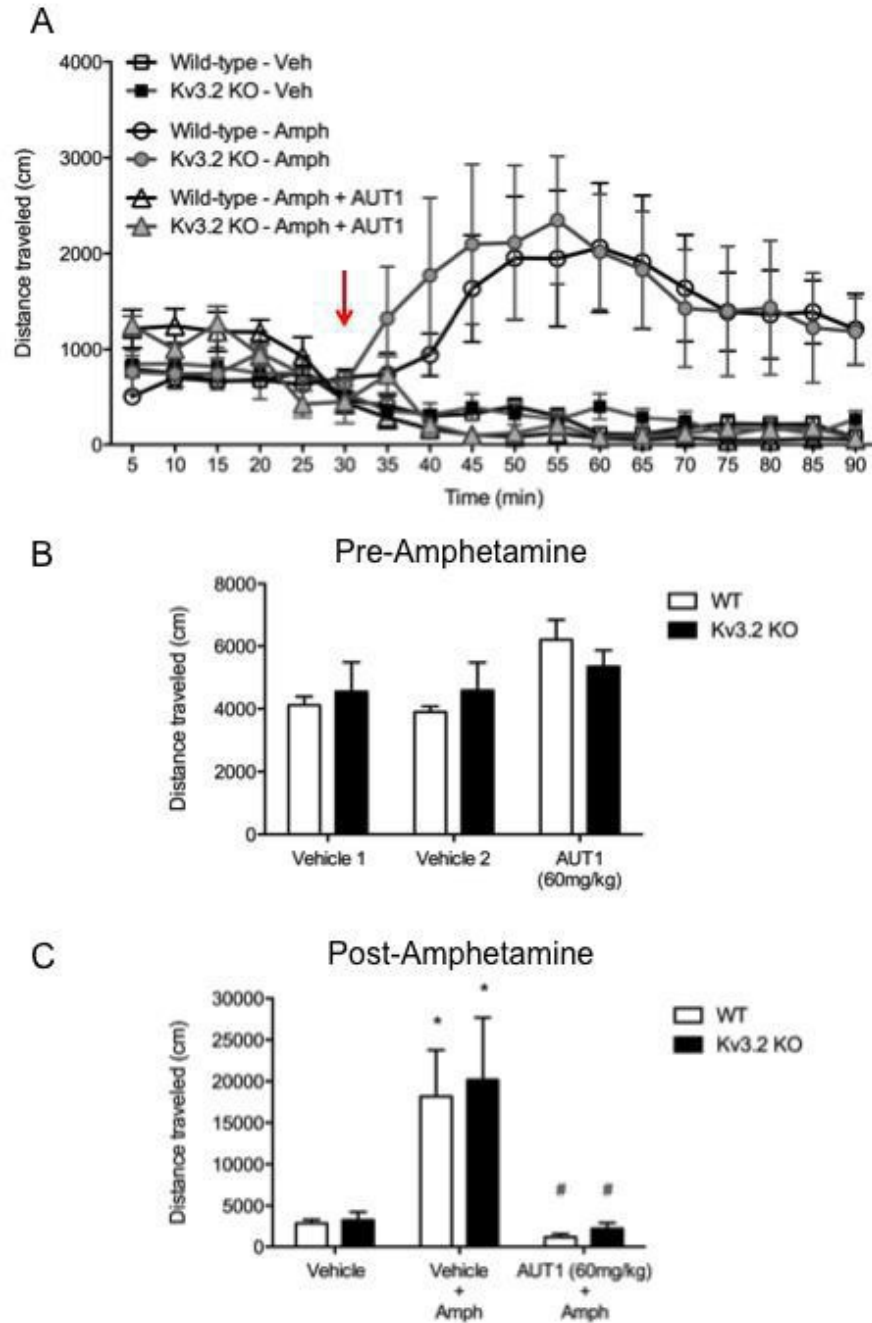


Figure 26. AUT1 prevents amphetamine-induced hyperactivity in Kv3.2 KO mice. (A) Time course of locomotor activity in wild-type (WT) and Kv3.2 knock-out (KO) mice that received pre-treatment with AUT1 (60 mg/kg, p.o.) or vehicle at T=0min followed by an injection of amphetamine (2 mg/kg, i.p.) at T=30min (injection time indicated by red arrow). (B) There was no significant difference in locomotor activity following AUT1 administration prior to amphetamine injection. Note that two vehicle groups are depicted to dissociate groups that subsequently received a second dose of a vehicle (vehicle group 1: vehicle + vehicle) vs. a dose of amphetamine (vehicle group 2: vehicle + amph). (C) Two-way ANOVA revealed a significant main effect of treatment on locomotor activity following

amphetamine injection. Bonferroni post-hoc analyses confirmed that amphetamine led to a significant increase in activity in both WT and Kv3.2 vehicle pre-treated mice. AUT1 pre-treatment was effective at preventing amphetamine-induced hyperactivity in both WT and Kv3.2 mice, with no significant difference from vehicle pre-treated mice. Locomotor activity in AUT1 pre-treated mice was significantly lower than mice that received amphetamine injection alone. Treatment group vs. vehicle: * $p < 0.05$; treatment group vs. amphetamine: # $p < 0.05$. Amph = amphetamine. Red arrow indicates time of amphetamine administration. $n = 5$ /group.

A.3.2 Kv3.1 null mice exhibit manic-like behaviors.

To further establish an association between Kv3.1 channels and mood-related behaviors, mice lacking Kv3.1 channels were tested in a behavioral battery to assess features of manic-like behavior including exploratory, anxiety- and depressive-like behaviors. Kv3.1 null mice exhibited a hyperactive phenotype during a 1-hr locomotor test ($t_{12} = 3.55$, $p < 0.01$) (figure 24c). Kv3.1 null mice also exhibited an increase in exploration of the open arms of the elevated plus maze (figure 24d-e) and light chamber of the light-dark test (figure 24f-g), indicating an overall decrease in anxiety-like behaviors (time: $t_{12} = 2.43$, $p = 0.032$; transitions: $t_{13} = 2.42$, $p = 0.031$). In the forced swim test, Kv3.1 null mice exhibited antidepressant-like behavior as evidenced by increased time spent struggling relative to WT littermate controls ($t_{14} = 5.11$, $p = 0.0002$) (figure 24h).

A.3.3 Effects of AUT1 on hyperactivity in the *Clock* Δ 19 mutant mouse model of mania.

The ability of AUT1 to attenuate hyperactivity was additionally tested in the well-validated *Clock* Δ 19 mutant mouse model of mania (Roybal *et al*, 2007b). As expected, vehicle treated *Clock* Δ 19 mice exhibited hyperactivity compared to WT littermate controls throughout the duration of locomotor testing ($p < 0.01$) (figure 26). *Clock* Δ 19 mutant mice that received acute

administration of AUT1, however, exhibited a reduction in locomotor activity at both a 30 mg/kg ($F_{1,27} = 14.67$, $p = 0.0007$, genotype effect; $F_{1,27} = 6.11$, $p = 0.02$, treatment effect) (figure 26a,b) and 60 mg/kg dose (figure 26c,d), with the higher 60 mg/kg dose completely reversing hyperactivity to WT levels with a significant main effect of treatment ($F_{1,25} = 9.023$, $p = 0.006$) and a trend for a main effect of genotype ($F_{1,25} = 3.84$, $p = 0.062$). Importantly, AUT1 did not impact locomotion in WT controls at these doses.

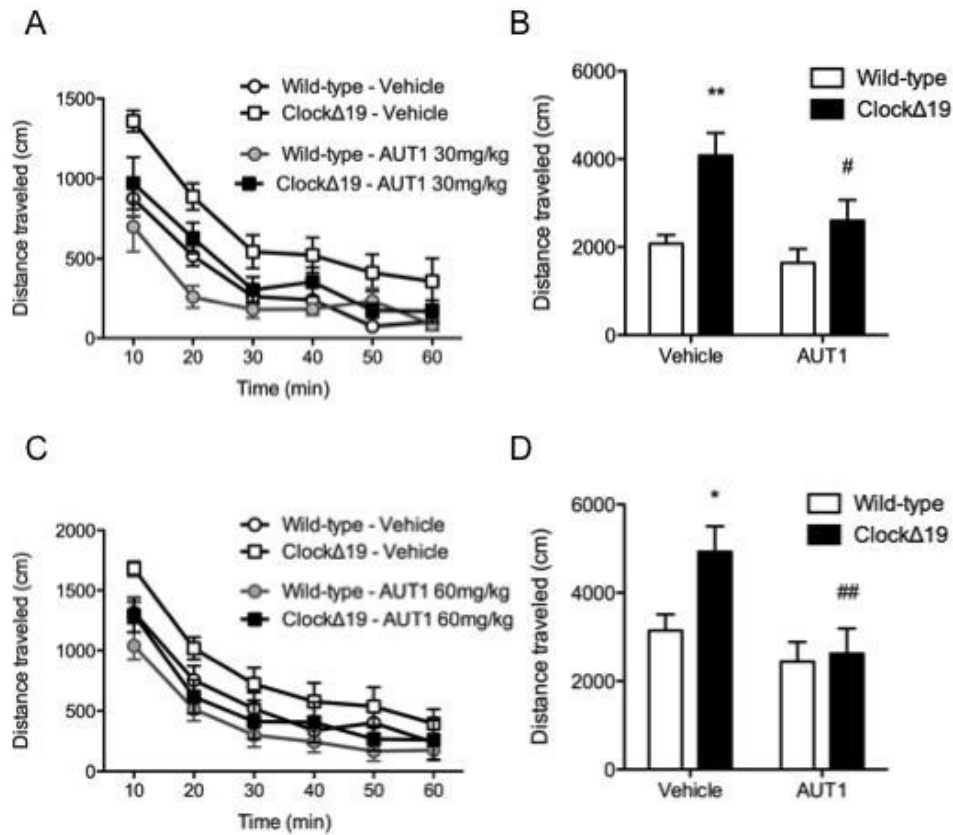


Figure 27. AUT1 reverses hyperactivity in the *ClockΔ19* mutant mouse model of mania. (A, C) Time course of locomotor activity in wild-type (WT) and *ClockΔ19* administered a (A, B) 30 mg/kg or (C, D) 60 mg/kg dose of AUT1 or vehicle (AUT1-vehicle) at T=0min. (B). As expected, Bonferroni post-hoc analyses revealed that vehicle-treated *ClockΔ19* mice exhibited a significant increase in locomotor activity relative to WT mice. *ClockΔ19* mice administered 30 mg/kg AUT1 exhibited a significant reduction in locomotor activity compared with vehicle treatment. (D) The ability of AUT1 to reduce hyperactivity in *ClockΔ19* mutants was additionally tested at a 60 mg/kg dose. Hyperactivity was seen in vehicle treated *ClockΔ19* vs. WT and a complete reversal of this phenotype with 60 mg/kg AUT1 administration (*ClockΔ19* AUT1 vs. vehicle). Genotype effects: * $p < 0.05$, ** $p < 0.01$; treatment effects: # $p < 0.05$, ## $p < 0.01$. $n = 7-8$ /genotype.

A.3.4 AUT1 differentially modulates *ClockΔ19* VTA neuronal activity.

Given the effect of AUT1 in attenuating hyperactivity in *ClockΔ19* mice, we focused on the VTA as a region of interest to further explore the underlying mechanism. In an *ex vivo* preparation, we

tested the ability of AUT1 to modulate firing and action potential (AP) properties of *Clock* Δ 19 dopamine and non-dopamine (putatively GABAergic) neurons (figure 27). The identity of cell types was confirmed by standard electrophysiological signatures including morphology, spontaneous firing rate and the presence of an HCN channel-mediated hyperpolarization-activated current (I_h) (figure 27a,b). As measured by whole-cell current clamp, AUT1 bath application (10 μ M) significantly decreased DA neuron AP firing compared with DMSO (0.1%) specifically at higher current injections ($F_{(1,31)} = 4.049$, $p = 0.0530$ treatment effect; $F_{(10, 310)} = 392.5$, $p < 0.0001$ current effect; $F_{(10, 310)} = 2.994$, $p = 0.0013$ interaction) (figure 27c). AUT1 appeared to increase the rate of firing in non-DA neurons, but this effect did not reach significance ($F_{(1,10)} = 0.5848$, $p = 0.4621$ treatment effect; $F_{(10, 100)} = 179.3$, $p < 0.0001$ current effect) (figure 27d).

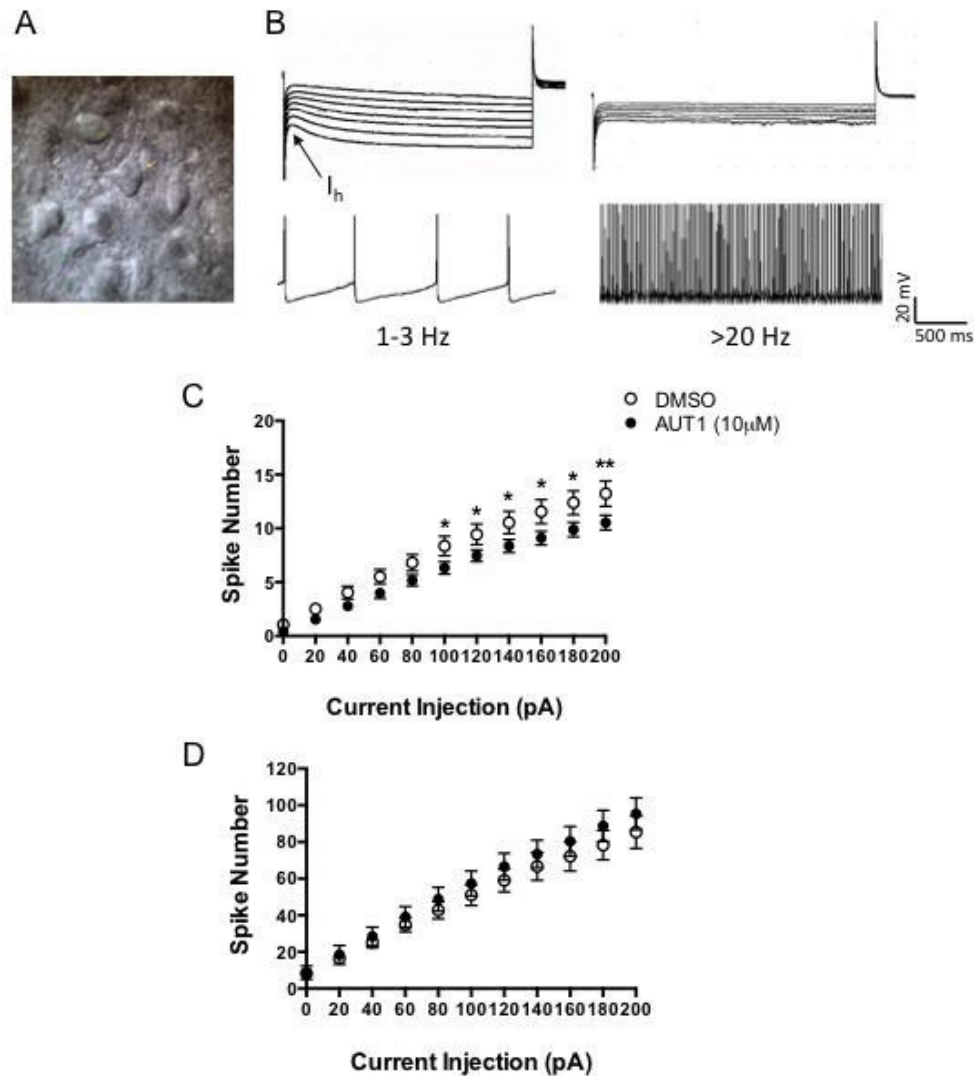


Figure 28. The firing rate of *Clock* Δ 19 VTA dopamine neurons is attenuated by AUT1. (A) Micrograph of VTA dopamine neurons in a brain slice from *Clock* Δ 19 mutant mice. (B) DA neurons exhibit a characteristic I_h -mediated “sag” response to hyperpolarizing voltage steps and spontaneous activity in the range of 1-3Hz (left) while putative GABAergic neurons in the VTA lack I_h current and fire at a rate higher than 20Hz (right). (C) AUT1 reduced the firing of DA neurons compared with DMSO specifically at higher current steps; n=14 DMSO, n=19 AUT1 (D) AUT1 application did not significantly alter the firing of GABAergic cells in a small sample group; n=6 DMSO, n=6 AUT1. *p<0.05, **p<0.01.

Furthermore, we examined the effects of AUT1 application on several action potential properties of DA and non-DA neurons in *ClockΔ19* VTA. We analyzed the half width, amplitude of the negative phase of the first derivative, coefficient of variation (CV) of the inter-event interval and amplitude of spikes at 100pA and 200pA current steps (figure 28a). Here we found that AP half width of *ClockΔ19* mutant DA cells was significantly increased ($F_{(1,27)} = 6.306$, $p = 0.0183$ treatment effect; $F_{(1,27)} = 43.05$, $p < 0.0001$ current effect) as was the CV ($F_{(1,26)} = 7.520$, $p = 0.0109$ treatment effect; $F_{(1,26)} = 40.11$, $p < 0.0001$ current effect). The first derivative was significantly reduced in the presence of AUT1 ($F_{(1,27)} = 6.602$, $p = 0.0160$ treatment effect; $F_{(1,27)} = 46.98$, $p < 0.0001$ current effect). AP amplitude remained unchanged ($F_{(1,26)} = 1.254$, $p = 0.2730$ treatment effect; $F_{(1,26)} = 66.24$, $p < 0.0001$ current effect) (figure 28b-e). These data indicate that AUT1 broadens individual APs, decreases the rate of repolarization and increases irregularity of APs within the spike train.

When we recorded from putative GABAergic neurons, we did not find significant changes in AP half width ($F_{(1,7)} = 0.2994$, $p = 0.6013$ treatment effect; $F_{(1,7)} = 6.060$, $p = 0.0434$ current effect), first derivative ($F_{(1,7)} = 1.773$, $p = 0.2248$ treatment effect; $F_{(1,7)} = 185.5$, $p < 0.0001$ current effect) and amplitude ($F_{(1,7)} = 0.3100$, $p = 0.5950$ treatment effect; $F_{(1,7)} = 23.30$, $p = 0.0019$ current effect). However, AUT1 significantly decreased the CV at both current steps ($F_{(1,7)} = 10.44$, $p = 0.0144$ treatment effect; $F_{(1,7)} = 1.809$, $p = 0.2206$ current effect) (figure 28f-i). Together, our results suggest that AUT1 may exert its effects on reducing *ClockΔ19* hyperactivity through a subtle augmentation of GABAergic neuronal firing properties that may lead to an inhibition of DA neuronal firing and spike fidelity.

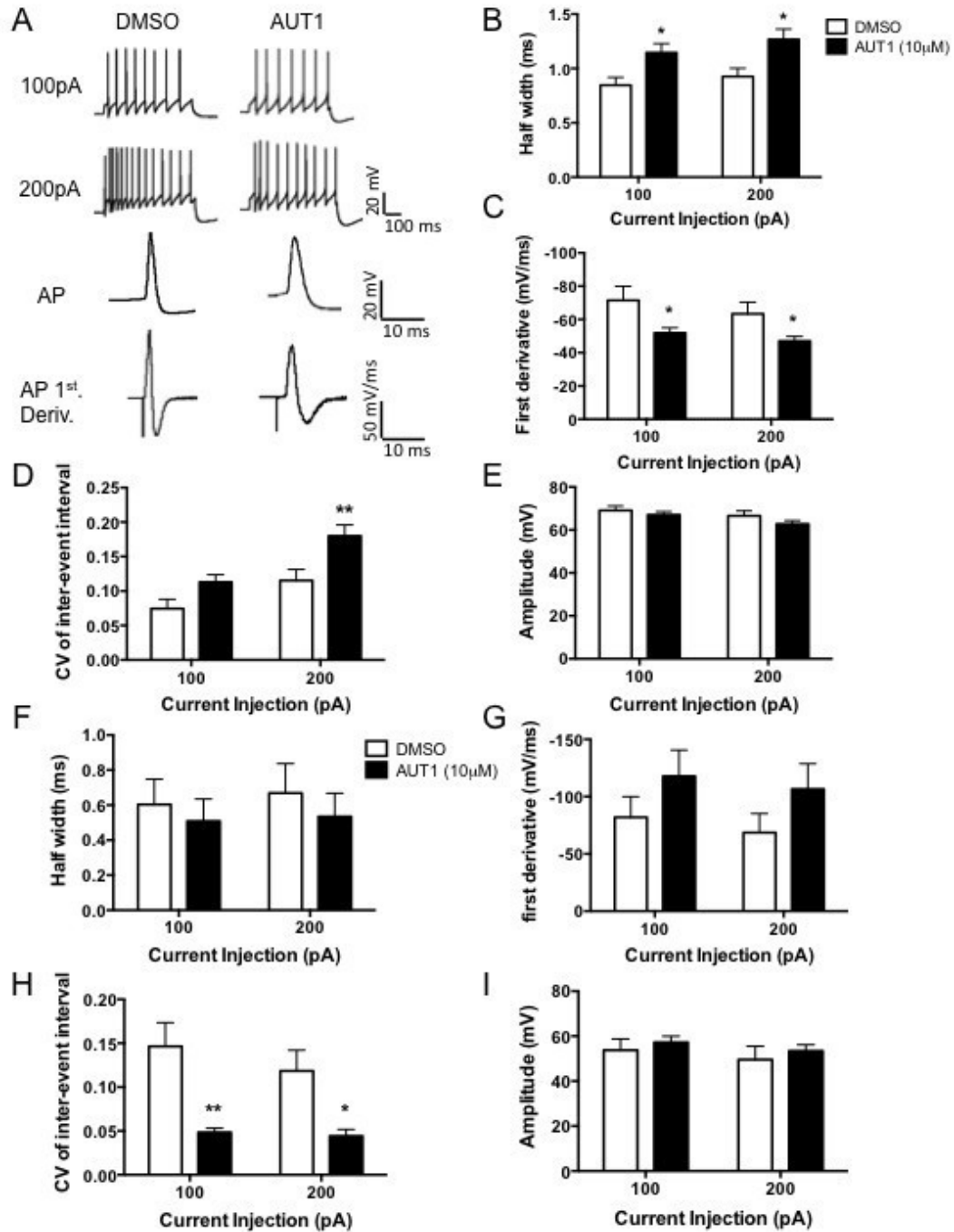


Figure 29. AUT1 modulates action potential properties of *Clock* Δ 19 dopamine and GABAergic neurons. (A) Representative spike trains and individual action potentials from DMSO and AUT1 treated DA neurons. Middle APs were chosen for analysis of half width, first derivative negative phase amplitude, and spike amplitude. (B) Application of AUT1 increased the AP half width of DA neurons at 100pA and 200pA. (C) The first derivative of APs was significantly decreased by AUT1 at both 100pA and 200pA current steps. (D) AUT1 incubation increased the CV of

the inter-event interval. (E) Lastly, we did not identify an effect of AUT1 on the AP amplitude of DA neurons compared with DMSO. (F) Analysis of AP properties of GABAergic revealed no significant effect of AUT1 on AP half width. (G) Similarly, AUT1 incubation failed to alter the first derivative compared with DMSO. (H) *ClockΔ19* GABAergic neurons however responded to AUT1 application with a significant decrease in the CV of the inter-event interval at both current steps. (I) AP amplitude was unaffected by AUT1 incubation. * $p < 0.05$, ** $p < 0.01$.

A.3.5 Kv3.1 channels are targets of mood stabilizer treatment in *ClockΔ19* mutant mice

Immunohistochemistry confirmed the presence of Kv3.1b channels in various dopaminergic rich regions of the brain, including the caudate putamen (figure 29a), Islands of Calleja (figure 29b), VTA (figure 29c) and substantia nigra (figure 29d). Based on previous work demonstrating the importance of both the VTA and NAc to manic-related behaviors in *ClockΔ19* mutant mice (Coque *et al*, 2011; Dzirasa *et al*, 2010; McClung *et al*, 2005; Mukherjee *et al*, 2010), we used Western blotting to quantitate levels of Kv3.1b protein (an alternative splice form of the Kv3.1 subunit) specifically in these mesolimbic brain regions. Analysis revealed an increase in Kv3.1b channel protein in the VTA of *ClockΔ19* mutant mice compared to WT controls ($p = 0.056$) (figure 28e), with no differences in the NAc (figure 28f). Interestingly, lithium, which reverses manic-like behavior in *ClockΔ19* mutant mice and restores normal dopaminergic activity (Roybal *et al*, 2007; Coque *et al*, 2011), also restored Kv3.1 protein to WT levels in the VTA ($p < 0.05$) with a trend for an interaction in the effect of lithium treatment on Kv3.1b protein in *ClockΔ19* mice compared with WT littermate controls ($F_{(1,18)} = 3.38$, $p = 0.08$) (figure 29e).

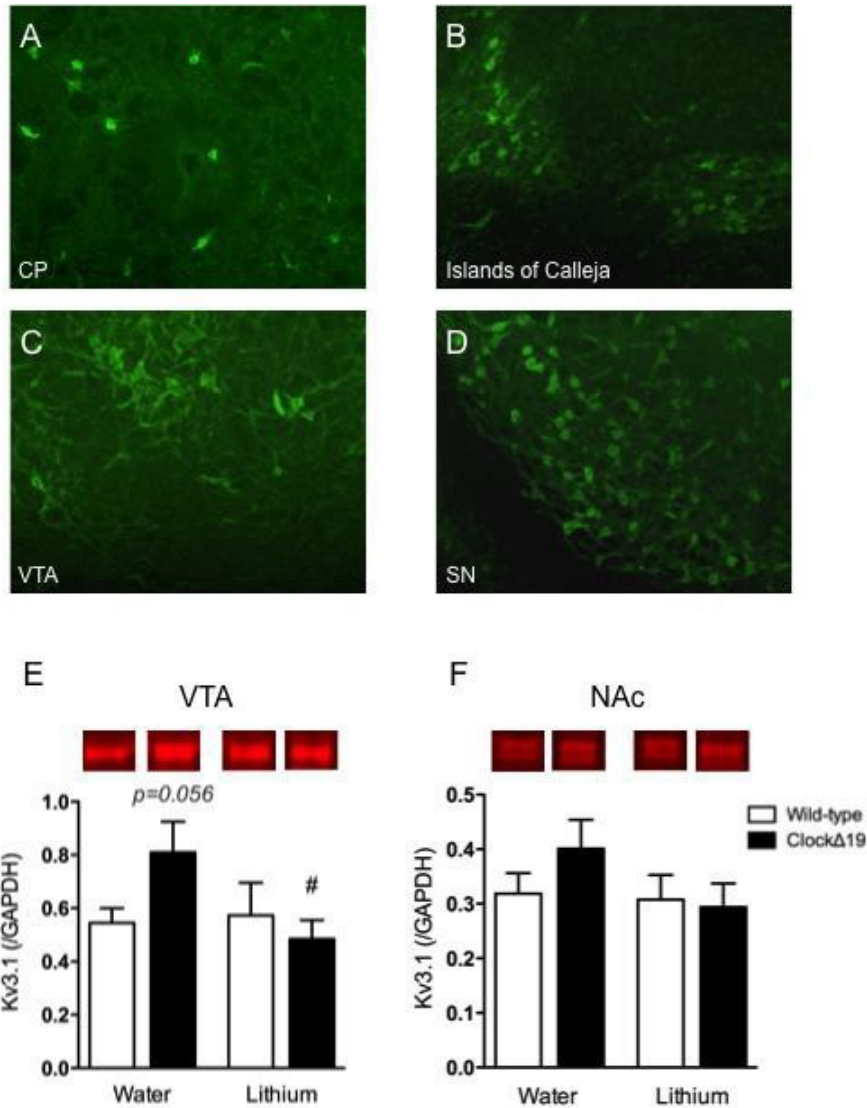


Figure 30. Lithium restores abnormal Kv3.1b protein levels in a mouse model of mania. Kv3.1b immunopositive cells (green) were detected in various dopamine-rich areas of the brain including the (A) caudate putamen (CP), (B) Islands of Calleja, (C) ventral tegmental area (VTA), and (D) substantia nigra (SN). (E) Post-hoc analyses revealed an increase in Kv3.1b protein in the VTA of vehicle-treated *ClockΔ19* mice that decreased to WT levels after 10 days of lithium treatment. (F) No significant genotype or treatment effects were found in the nucleus accumbens (NAc). *ClockΔ19* water vs. lithium treatment: # $p < 0.05$. $n = 5-6$ /genotype.

A.4 DISCUSSION

The current study tested the efficacy of a novel modulator of Kv3-family voltage-gated potassium channels (AUT1) in two separate animal models associated with imbalance of the mesolimbic system: the amphetamine-induced hyperactivity model and the *Clock* Δ 19 mutant mouse model of mania. Furthermore, Kv3.1 null mice were used to test for behavioral abnormalities in mice lacking Kv3.1 channels. Kv3.1 null mice were found to exhibit both increased exploratory drive and reduced depressive-like behaviors, combined with hyperactivity. A similar behavioral phenotype is present in the *Clock* Δ 19 model of mania, though we have not yet determined if Kv3.1 null mice share other features of mania including increases in the reward value for drugs of abuse, motivated behavior, and impulsivity. The current findings extend previous studies that have also shown similar behavioral abnormalities in Kv3.1 knockout mice, most notably hyperactivity (Espinosa *et al*, 2004; Joho *et al*, 2006). It should be noted that these mice also have highly disrupted daily activity rhythms (Kudo *et al*, 2011), with increased activity during the day (light cycle) and reduced sleep time, similar to that seen in *Clock* Δ 19 mice and human manic patients (Espinosa *et al*, 2004; Joho *et al*, 2006; Naylor *et al*, 2000).

In the amphetamine-induced hyperactivity model, we found that AUT1 successfully prevented hyperactivity in outbred mice. Importantly, AUT1 was unable to prevent amphetamine-induced hyperactivity in Kv3.1 null mice, demonstrating the importance of Kv3.1 channels to AUT1's mechanism of action. Notably, this effect was specific to Kv3.1 channels, as AUT1 successfully prevented hyperactivity in mice lacking Kv3.2 channels. Additionally, AUT1 also reversed hyperactivity in the *Clock* Δ 19 mutant mouse model of mania, where we found background alterations in the expression of Kv3.1 channels in dopamine-rich mesolimbic regions. Specifically, Kv3.1b protein levels were increased in the VTA of *Clock* Δ 19 mutant mice. Based

on the manic-like behavioral profile observed in mice lacking functional Kv3.1 channels, one might expect a decrease in Kv3 channels in the VTA of *Clock* Δ 19 mutants. However, the increase might reflect a compensatory mechanism that attempts to normalize the increased VTA dopamine neural activity present in *Clock* Δ 19 mutants (Coque *et al*, 2011; Roybal *et al*, 2007b). A similar compensatory effect has been proposed for the observed decrease in levels of glutamate-receptor 1 (GLUA1) protein in the NAc of *Clock* Δ 19 mutant mice (Dzirasa *et al*, 2010). It is also possible that these channels are not optimally functional in the *Clock* Δ 19 mice leading to an attempt at rescue through increased expression. Regardless of the directionality of the effect, the current results suggest an association between Kv3.1 channels and mania-related behaviors possibly through its action on dopaminergic neural activity. Indeed, given that previous studies have shown that Kv3.1 channels are present in dopaminergic-rich CNS regions and given that we found evidence of protein expression in various dopamine-rich areas, it is likely that Kv3.1 channels indirectly contribute to dopaminergic neural activity through modulation of GABAergic interneuron activity. With regards to the current findings, it should be noted that 30% of VTA neurons are GABAergic (Sesack and Grace, 2010).

Rosato-Siri and colleagues have demonstrated AUT1-induced modulation of PV interneuron firing in the somatosensory cortex of mice when potassium channel activity is pharmacologically impaired (Rosato-Siri *et al*, 2016). Our results showed significant effects of AUT1 on the action potential characteristics of *Clock* Δ 19 DA and putative GABAergic neurons in the VTA. The most robust effect of the drug was to reduce the CV of firing of GABAergic neurons. This effect may be associated with the reduced AP half-width and increased rate of repolarization that was observed following AUT1 application; these parameters showed only a trend towards reduction and increase, respectively. However, AP half-width and rate of

repolarization prior to AUT1 application were already very short and fast, respectively, thus further positive modulation would be limited by other ion channels mechanisms. The combination of effects of AUT1 observed in GABAergic neurons is entirely consistent with Kv3.1 positive modulation. We suggest that observed effects of AUT1 on the AP characteristics of the recorded DA neurons may be secondary to alterations in the firing properties of the GABAergic neurons that synapse onto them. This would be consistent with the presence of Kv3.1 channels on GABAergic neurons, but not DA neurons (Kudo *et al*, 2011). However, we cannot exclude the possibility that the significant changes in DA cell AP characteristics seen with AUT1 might be due to action of the drug on other ion channels directly on the DA cells.

Moreover, we found that the levels of Kv3.1 channel protein were normalized in the *Clock* Δ 19 mice in response to lithium, which is known to decrease dopaminergic activity in these animals (Coque *et al*, 2011). The decrease in Kv3.1 levels could occur as a response to normalization of dopamine levels, or it could be involved more directly in the actions of lithium on neural activity. A critical aspect of this study was the ability to compare concentrations of AUT1 that were active *in vivo* with those concentrations that have been shown to modulate Kv3 channels. *In vitro*, concentrations in the range of 1–10 micromolar were found to modulate Kv3.1 and Kv3.2 channels (Rosato-Siri *et al*, 2016). In the present study, we found that doses of 30 and 60 mg/kg of AUT1 produced significant effects on behavior in the mouse models tested. These oral doses were associated with free brain concentrations in the range of 1 – 2 micromolars over the time-course of behavioral testing. These concentrations are therefore consistent with effects mediated by Kv3 channels.

A recent study confirmed the importance of Kv3.1 channels to additional psychiatric disorders. Kv3.1 channels were reduced in patients with schizophrenia and normalized with

antipsychotic treatment (Yanagi *et al*, 2014). Here, the authors focused on the importance of these channels located on cortical parvalbumin (PV) interneurons and the role of these neurons in maintenance of cortical gamma oscillations and synchrony (Sohal *et al*, 2009), which are disrupted in schizophrenia, bipolar disorder and in severe cases of unipolar depression (Uhlhaas *et al*, 2011). A direct role for Kv3.1 channels in the generation of thalamocortical gamma oscillations has been described in the Kv3.1 null mice (Joho *et al*, 1999), demonstrating a link between Kv3.1 channels and the maintenance of fast spiking neural activity required for gamma synchronization. Moreover, AUT1 was able to restore normal levels of activity of the PV-positive interneurons in the somatosensory cortex (Rosato-Siri *et al*, 2016). Thus, Kv3.1 channels may play a role in the development of different classes of psychiatric diseases. As novel medications for psychiatric diseases are greatly needed, we propose that compounds like AUT1, which directly target and modulate Kv3 channels, may be beneficial for the treatment of disorders associated with abnormal neural activity. In particular, this may prove to be a useful strategy for restoring dopaminergic function without the side effects associated with dopamine blockade. Further studies will be needed to understand the exact role these channels play in the development of psychiatric disease.

APPENDIX B

REGULATION OF ANXIETY-LIKE BEHAVIOR AND GABA_A RECEPTORS BY NPAS2

Ozburn AR, Kern J, Parekh PK, Logan RW, Liu Z, Falcon E, Becker-Krail D, Purohit K, Edgar NM, Huang Y, and McClung CA. (Submitted to *Biological Psychiatry*)

Abnormal circadian rhythms are strongly associated with several psychiatric disorders. NPAS2 is a core component of the molecular clock that acts as a transcription factor and is highly expressed in reward- and stress-related brain regions such as the nucleus accumbens (NAc). Variations in *Npas2* are associated with seasonal affective disorder and major depressive disorder. However, the mechanisms by which NPAS2 is involved in mood-related behaviors is still unclear. We determined the effect of a chronic stress paradigm on NAc *Npas2* expression, characterized the behavioral phenotype of mice with a null mutation in *Npas2* and mice with reduced NAc *Npas2* expression (via RNAi). Further, we identified and validated GABA_A subunits as novel transcriptional targets of NPAS2, and assessed the effects of NAc *Npas2* knockdown on inhibitory neurotransmission. Chronic unpredictable mild stress significantly increased *Npas2* expression in the NAc. *Npas2* mutants exhibited decreased anxiety-like behaviors (in elevated plus maze, light/dark box, and open field assay) as compared with WT mice. NAc *Npas2* knockdown was sufficient to reduce anxiety-like behaviors and alter

inhibitory neurotransmission (decrease mIPSC amplitude). Additionally, *Npas2* mutants were resistant to the motor incoordinating effects of diazepam. Furthermore, we found that NPAS2 binds to and regulates specific *Gabra* genes and *Npas2* knockdown rendered MSNs insensitive to diazepam. We provide strong evidence that the circadian transcription factor, NPAS2, modulates anxiety-like behaviors and GABA_A receptors using a combination of molecular and behavioral approaches. These findings suggest a mechanism by which stress increases NPAS2 dependent transcription of specific GABA_A receptor subunits, thus altering the function of the receptors and ultimately inhibitory neurotransmission.

B.1 INTRODUCTION

Psychiatric disorders are among the most devastating diseases and rank among the top factors involved in loss of productivity, quality of life, and reduced life span. Clinical and pre-clinical studies provide strong evidence that circadian rhythms and the genes that make up the molecular clock play a key role in the expression of mood-related symptoms in psychiatric disorders (Karatsoreos, 2014; Landgraf *et al*, 2014; Logan *et al*, 2014; Falcon and McClung, 2009). In fact, nearly all psychiatric disorders involve some disruption to the normal sleep/wake cycle and this is often one of the criteria used for diagnosis (McClung, 2013).

Circadian rhythms are regulated by a set of transcriptional/translational feedback loops that make up the molecular clock. The core feedback loop consists of transcription factors Circadian Locomotor Output Cycles Kaput (CLOCK), or Neuronal PAS Domain Protein 2 (NPAS2), and Brain and Muscle ARNT like Protein 1 (BMAL1) forming heterodimers, binding to E-box (CACGTG) sequences and positively regulating the transcription of Period (*Per1*, *Per2*, and *Per3*)

and Cryptochrome (*Cry1* and *Cry2*) genes. PER and CRY proteins are phosphorylated by casein kinase epsilon 1 (CKE1), form homomers or heteromers, and translocate to the nucleus where they can inhibit CLOCK:BMAL1 or NPAS2:BMAL1-mediated transcription (Lowrey and Takahashi, 2000; Mohawk and Takahashi, 2011; Wang *et al*, 2007). While the circadian genes that drive these molecular rhythms are found in the master pacemaker (the suprachiasmatic nucleus), elements of the molecular clock are expressed throughout the brain and periphery.

Studies have revealed that circadian genes and rhythms significantly contribute to mood, anxiety and depression, as well as reward and motivation (Logan *et al*, 2014; McClung, 2013; Ozburn *et al*, 2012; Ozburn *et al*, 2015; Parekh *et al*, 2015; Spencer *et al*, 2013; Roybal *et al*, 2007; Ozburn *et al*, 2013). Abnormal rhythms are strongly associated with psychiatric diseases like seasonal affective disorder, bipolar disorder, major depression, and drug addiction (Hasler *et al*, 2012; Li *et al*, 2013; McCarthy *et al*, 2013; McClung, 2011; Mukherjee *et al*, 2010; Salgado-Delgado *et al*, 2011). Increased agitation and anxiety are key symptoms commonly associated with these disorders, and are the focus of the studies presented here. Moreover, many of the therapies used to treat these disorders are known to modulate the circadian clock (Bunney and Bunney, 2013). Additionally, single nucleotide polymorphisms (SNP) in a number of circadian genes have been associated with mood disorders (Benedetti *et al*, 2004; Desan *et al*, 2000; Kishi *et al*, 2008; Kripke *et al*, 2009; Lavebratt *et al*, 2010a-b; Nievergelt *et al*, 2006). SNPs in *Npas2* are associated with seasonal affective disorder and major depressive disorder (Partonen *et al*, 2007; Soria *et al*, 2010). However, the role of NPAS2 in these mood-related behaviors is unclear.

Our present research focuses on identifying mechanisms by which the circadian gene, *Npas2*, regulates anxiety-like behaviors. *Npas2* is highly expressed in reward- and stress-related brain regions such as the nucleus accumbens (NAc) (Garcia *et al*, 2000). The NAc, primarily composed of GABAergic medium spiny neurons (MSNs), is a significant point of convergence for

this circuitry where it receives dopaminergic input from the VTA, as well as glutamatergic inputs from a number of other brain regions (such as the pre-frontal cortex, amygdala, and hippocampus). Previously we found that NPAS2 expression in the NAc is localized specifically to dopamine receptor 1 (*Drd1a*) containing neurons of the so-called “direct” pathway (Ozburn *et al*, 2015). This circuit is thought to underlie positive or rewarding associations with salient events. We performed ChIP Seq (chromatin immunoprecipitation followed by deep sequencing) on striatal tissue to identify DNA sequences bound to NPAS2 and identified many novel gene targets, including GABA_Aalpha (1, 2, 3, 4 and 5), beta (1, 2, 3), gamma (1, 2,3), epsilon, and pi subunits (Ozburn *et al*, 2015). In the current studies, we determine how stress and anxiety alter *Npas2* in the NAc and how *Npas2* regulates anxiety-like behavior and inhibitory neurotransmission using a combination of qPCR, RNA interference, pharmacological, behavioral, and electrophysiological methods. We hypothesize that stress and anxiety alter NPAS2-dependent transcription of specific GABAergic subunits that selectively alter phasic inhibitory neurotransmission (perhaps specifically in *Drd1a* containing medium spiny neurons of the NAc).

B.2 MATERIALS AND METHODS

B.2.1 Animal use.

Npas2 (C57BL/6:129S6) mutant mice (Garcia *et al*, 2000) were tested as homozygotes. Wild type littermate controls were utilized as a control for this mutation. Male C57BL/6J mice (The Jackson Laboratory, Bar Harbor, Maine) were utilized for *Npas2* knockdown, gene expression following unpredictable chronic mild stress, and ChIP studies. All mice were housed in a 12:12 light/dark

cycle (lights on at 7am, lights off at 7pm) with food and water *ad libitum*. All animal use was approved by the University of Texas Southwestern Medical Center, the University of Pittsburgh, and the Portland VA Medical Center Institutional Animal Care and Use Committees.

B.2.2 Unpredictable Chronic Mild Stress(UCMS).

Mice were group housed and exposed to six weeks of UCMS or control handling (N=36 mice per group). UCMS treated mice were subjected to a randomized schedule of 1-2 mild stressors per day, seven days per week. Stressors included forced bath (~4cm of water in a rat-sized cage for 15 min), wet bedding, aversive smell (1h exposure to fox urine), dirty bedding (rotate mice into previously occupied “dirty” cages), tilt cages (45° tilt), restraint (50ml tube for 15 min), reduced cage space, no bedding, and bedding change (replaced soiled bedding with clean bedding). Two or three stressors were intermittently used simultaneously to contribute to the random nature of the paradigm. No light/dark manipulations were used. Fur rating and body weights were measured weekly to track the progression of the “UCMS syndrome”. Control animals were housed in the same room as the UCMS exposed animals and only handled for fur ratings and body weight measurements. To ensure UCMS treated mice exhibited increased anxiety-like behaviors associated with UCMS syndrome, mice were subjected to elevated plus maze and light/dark box testing (on two separate days) during the 5th week of UCMS, and thus did not receive randomized stressors on these days. Stressors were purposely conducted at random times throughout the day to avoid potential non-specific circadian effects of acute stressors. Immediately after 6 weeks of UCMS or control handling, mice were sacrificed by cervical dislocation and rapid decapitation every 4 hours over the next 24-hour period (6 time points). Whole brains were dissected and flash frozen on dry ice, sectioned on a cryostat at 200um, and NAc tissue was collected using a 1mm

core tissue puncher.

B.2.3 Quantitative Real-time RT-PCR.

For UCMS tissue: Total RNA was extracted using an RNeasy Micro Kit (Qiagen, Germantown, MD) and converted to cDNA using the Superscript III First Strand Synthesis Kit (Life Technologies, Grand Island, NY). cDNA was mixed with SYBR Green master mix (Applied Biosystems, ABI) and specific primers for *Npas2* or *Gapdh*. Prior to the experiment primer sets were tested thoroughly to determine reaction efficiency, specificity, and the absence of primer-dimers [2]. Primer sequences for *Npas2* were (forward) 5'-GACACTGGAGTCCAGACGCAA-3' and (reverse) 5'-AATGTATACAGGGTGCGCCAAA-3' and for *Gapdh* (forward) 5'-AACGACCCCTTCATTGAC-3' and (reverse) 5'-TCCACGACATACTCAGCAC-3'. Quantitative real-time RT-PCR reactions were assessed by SYBR green fluorescence signal (Power SYBR Green PCR Master Mix, Life Technologies) using a 7900HT Fast Real-Time PCR System (Applied Biosystems, Grand Island, NY).

For *Npas2* shRNA and Scramble shRNA transduced NAc tissue: Tissue was collected, RNA was isolated, and cDNA synthesis was performed as described (Ozburn *et al*, 2015). Following cDNA synthesis, multiplex polymerase chain reaction (PCR) was used to measure relative gene expression of multiple gamma-aminobutyric acid receptor (type A) subunits of interest (and housekeeping gene *Gapdh*) in the same sample. In brief, cDNA was mixed with SsoAdvanced™ Universal Probes Supermix (Bio-Rad Laboratories; Hercules, CA) and all five probes for genes of interest: *Gapdh*: Cy5.5 reporter, Cat# 10031237; *Gabrg1*: FAM reporter, Cat# 10031228; *Gabrg2*: HEX reporter, Cat# 10031231; *Gabra1*: TEX 615, Cat# 10031234, and *Gabra2*: Cy5 reporter, Cat# 12001950. Reactions were carried out in a Bio-Rad CFX96 Touch™ Real-Time PCR Detection System using the Bio-Rad CFX Manager 3.1 software (Bio-rad

Laboratories). Scan mode was set to ‘all channels’ to allow for detection of each of the five fluorophore reporters. For all reactions: Samples were run in duplicate and ΔCT values were determined by normalizing to the reference gene *Gapdh*. Relative expression values were calculated based on the following: $\Delta\Delta\text{CT}=(\Delta\text{CT}_{\text{highest value across groups}} - \Delta\text{CT}_{\text{sample}})$ then relative expression $((2^{-\Delta\Delta\text{CT}}_{\text{sample}} / 2^{-\Delta\Delta\text{CT}}_{\text{highest value across groups}})*100)$ was calculated as described in (Landgraf *et al*, 2014).

B.2.4 Behavioral Assays.

Locomotor Response to Novelty: Mice were individually placed in a novel environment inside automated locomotor activity chambers equipped with infrared photobeams (San Diego Instruments, San Diego, CA) and measurements began immediately. Activity was continuously measured and the data was collected in 5-minute bins over a period of two hours. Distance traveled was measured. An initial exploratory bout of increased activity that decreases over the two-hour testing period is typically seen and represents habituation to the novel environment.

Elevated Plus Maze: The maze consisted of two open arms and two arms with raised walls. The mice were placed into the center of the maze, and their movement and time spent in each arm was tracked using Noldus EthoVision video tracking software. Each test lasted ten minutes. Number of entries into the open and closed arms were measured, as well as time spent in the open arms. More time spent in the open arms, and more open arm entries are both indicative of reduced anxiety-like behavior.

Light/Dark Box: A locomotor box was partitioned into a dark chamber and a light chamber. The

mice were placed into the dark chamber for 1 min prior to beginning data collection. Recording began when the gates were opened and the number of beam breaks in both chambers were recorded over the course of 10 minutes. Latency to enter and time spent in the light side of the apparatus were measured. Reduced latency to enter the light portion of the apparatus indicates reduced anxiety-like behavior.

Open Field: The open field arena consisted of a square plexiglass arena with a clear floor and solid black walls (61 x 61 cm). Mice were placed in the center of the open field and allowed to freely explore for 10 minutes. Anxiety-like behavior was assessed using the following: time spent in the center of the arena, distance traveled and velocity of movement in the center. Locomotor activity was measured by total distance traveled. Behaviors were recorded and scored using Ethovision XT. Increased time spent in the center and distance traveled in the center of the arena indicated reduced anxiety-like behavior.

Accelerating Rotarod Assay: The rotarod test was performed to evaluate motor coordination. *Npas2* knockout and WT mice (n=7/genotype) were placed on immobile cylinders, which ramped up from 0 to 45 rotations/min (IITC, USA). The timer was stopped when the mouse fell off the cylinder or did a whole turn with it. This procedure was repeated for four consecutive days. The first two days consisted of training on the accelerating rotarod. On the last two days, mice were injected with either saline or 3 mg/kg diazepam (in a counterbalanced manner) 30 minutes prior to rotarod testing. For each genotype, latency to fall was compared under diazepam and saline treatment conditions. A reduction in the latency to fall indicates sensitivity to the motor incoordinating effects of diazepam.

B.2.5 Stereotaxic surgery.

Bilateral stereotaxic injections of 1 μ l of purified high titer AAV2 encoding a scrambled sequence with no known target (scramble shRNA) or *Npas2* shRNA was injected into the NAc (from bregma: angle 10°, AP +1.5 mm, Lat +1.5, DV -4.4). Mice recovered for 3-4 weeks in their home cage to allow for full viral expression before behavioral testing began. At the completion of behavioral testing, viral injection placement verification was carried out using immunohistochemical methods.

B.2.6 Immunohistochemistry.

Mice were deeply anesthetized with a mixture of ketamine (225mg/kg) and xylazine (22.5mg/kg) and transcardially perfused with phosphate buffered saline (PBS) and then 4% paraformaldehyde in PBS. The brains were incubated in 4% paraformaldehyde for 24 hours and then placed in 1X PBS-30% glycerol for an additional 24 hours. Tissue sections (30 μ m) containing the NAc were obtained using a freezing microtome (Leica, Wetzlar, Germany). Immunofluorescence detection was carried out using a primary antibody for GFP (ab290, AbCam, Cambridge, MA) and a secondary anti-rabbit antibody conjugated with Alexa-488 (Molecular Probes, Carlsbad, CA) using standard procedures (Mukherjee *et al.*, 2010, Ozburn *et al.*, 2015). Brain sections were mounted onto glass slides using Vectashield mounting media with DAPI (H-1200, Vector Labs, Burlingame, CA) and observed with an epifluorescence microscope with a 10x objective. Data from mice were excluded from study if the viral infection spread was not localized to the NAc (with spillover to adjacent areas) or if there was a significantly disproportionate amount of infection between both hemispheres.

B.2.7 Chromatin Immunoprecipitation(ChIP).

Chromatin immunoprecipitation was carried out as previously described (Ozburn *et al*, 2015). ChIP Seq was performed at 6 times of day and identified novel DNA binding targets of NPAS2. Here, we performed a separate ChIP experiment using an NPAS2 antibody (H20X, Santa Cruz Biotechnology, Santa Cruz, CA) to confirm findings that NPAS2 binds to several genes encoding subunits of the GABA_A receptor. As a control, we also incubated samples with Anti-acetyl-Histone H3 (Upstate) or non-immune rabbit IgG (Upstate). PCR products were visualized and size verified using agarose gel electrophoresis. Primer sets used for PCR verification of ChIP Seq results include: *Gabra1* Forward 5' GCT CTA AAA GCT GGA GAG TAG CAC C, Reverse 5' CCC AGT CCT TCT TTA TAG GCA CCG C; *Gabra2* Forward 5' TGG GAA GAT TGT AAC CCG TCC CCC, Reverse 5' CCT GTC ATA GCC CTG TGA GCC ACC; *Gabra4* Forward 5' GCC CTG CTT CCA CAG CAA CAC AC, Reverse 5' GCC AAA TAC CTG GCC TCA GCA GC; *Gabra5* Forward 5' CCC AGA CAA GCA AGG GCT GAC CC, Reverse 5' AGC CCA AGG AGA GTC CAG ACT GAT T; *Gabrb1* Forward 5' ACT GCA CAG CAC AGT GAG AGA GAG T, Reverse 5' ACA CAC ACA CTC ACA CAC ACA CAG A; *Gabrb2* Forward 5' ATC ACT GAC TGC TAG GAT GCG ACT, Reverse 5' GAG TCC TAT TGC CCG ATG CAA GGC; *Gabrb3* Forward 5' GGG AGG AGA GTG TAT TGT CCT GGT, Reverse 5' ACA GTG CTA ACG GAG CAG AGC CA; *Gabre* Forward 5' GGG CTC TGA TTT CAT CTC TGG CTC, Reverse 5' AAC CGG AGC CCC ATC CCC A; *Gabrg1* (SET 1) Forward 5' AAA AGG CAT GCA CAT GGT TGG GTG A, Reverse 5' CCT CAG CTG CAT CCC TGA CCC TC; and *Gabrg1* (SET 2) Forward 5' TCC CTC GGG AAC CCG ACT CTC A, Reverse 5' TCA CAC CGG GTG GAT GCG GC.

B.2.8 NAc slice preparation and electrophysiological recordings.

Three weeks after stereotaxic injection of AAV *Npas2* or scramble shRNA into the NAc, mice were anesthetized with isoflurane and decapitated. Brains were removed into ice-cold oxygenated (95% O₂/5% CO₂) modified aCSF containing (in mM): 135 *N*-methyl-D-glucamine, 1 KCl, 1.2 KH₂PO₄, 1.5 MgCl₂, 0.5 CaCl₂, 70 choline bicarbonate, and 10 D-glucose; pH 7.4 adjusted with HCL; pH 7.4 adjusted with HCl). Coronal slices (250 μm) containing the NAc were sectioned with a vibratome (VT1200S; Leica) and incubated for 30 minutes at 37°C in oxygenated aCSF containing (in mM): 119 NaCl, 26 NaHCO₃, 2.5 KCl, 1 NaH₂PO₄, 2.5 CaCl₂, 1.3 MgCl₂, 11 D-glucose. Slices were kept at room temperature until recording at which point they were perfused with aCSF heated to 30-32°C. Whole-cell patch-clamp recordings of identified MSNs with viral expression (as indicated by GFP fluorescence) were made under visual guidance with 40x objective and DIC optics. Borosilicate glass pipettes (3-5 MΩ) were filled with (in mM): 15 Cs-MeSO₃, 120 CsCl, 10 HEPES, 0.5 EGTA, 8 NaCl, 5 TEA-Cl, 2 Mg-ATP, 0.3 Na-GTP, 5 QX-314; 290mOsm; pH 7.3 adjusted with CsOH.

For miniature IPSC (mIPSC) and evoked IPSC experiments, D-APV (50 μM) and NBQX (5 μM) were included to block ionotropic glutamate receptors and TTX (1 μM) was used to prevent action potential generation in mIPSC recordings. Drugs were bath applied. Cells were voltage-clamped at -70 mV and held for at least 10 minutes prior to data collection. A constant-current isolated stimulator (DS3; Digitimer) was used to stimulate inhibitory afferents through a monopolar electrode at 0.1 Hz using 0.1 μs single pulses. After establishing a stable baseline of mIPSCs or IPSCs, 10 μM diazepam-containing aCSF was bath applied at a consistent flow rate over 10 minutes. Synaptic currents were recorded with a MultiClamp 700B amplifier (Molecular

Devices). Signals were filtered at 2.6-3 kHz and amplified 5-10 times, then digitized at 20 kHz with a Digidata 1322A analog-to-digital converter (Molecular Devices). Series resistance for all recordings was $<20\text{M}\Omega$ and was monitored continuously. Cells with a change in series resistance beyond 20% were excluded from data analysis. For mIPSC analysis, an event template was obtained by averaging at least 50 single events and used for template search with a threshold of 4. Events from each cell underwent visual inspections. Scoring was performed blind to treatment. The amplitude and frequency of miniature events were analyzed offline with Clampfit software (Molecular Devices). Peak amplitude of evoked IPSCs was measured and averaged across baseline and treatment conditions. All data is presented as Mean \pm S.E.M., with n representing the number of cells/animals.

B.2.9 Data analysis.

Two-way analysis of variance (ANOVA) was performed to analyze 1) *Npas2* gene expression data after UCMS (treatment x time factors), 2) locomotor activity in response to a novel environment for NAc *Npas2* shRNA and Scramble shRNA treated mice (viral treatment x time), and 3) electrophysiological measurements of mIPSC amplitude, mIPSC frequency, and IPSC decay time in NAc MSNs with *Npas2* shRNA or Scramble shRNA treated mice (viral treatment x drug treatment). Student's t-test (two tailed, unpaired) was performed to analyze data from anxiety-like behavioral testing (elevated plus maze, light/dark box, and open field assays) in WT or *Npas2* mutant mice, and NAc *Npas2* shRNA or Scramble shRNA treated mice. Student's t-test (two tailed, unpaired) was performed to analyze change in IPSC amplitude with diazepam treatment (percent change from baseline) in NAc *Npas2* shRNA or Scramble shRNA treated mice. Data are presented as mean \pm SEM and $p < 0.05$ is considered statistically significant.

B.3 RESULTS

B.3.1 *Npas2* expression is increased in the NAc in response to UCMS.

We sought to determine whether expression of *Npas2* changes in response to a paradigm known to alter mood-related behaviors, we employed a 6 week UCMS paradigm which in our hands reliably induces an increase in anxiety and depressive-like behavior (Logan *et al*, 2014). We found that UCMS resulted in a robust and significant increase in diurnal *Npas2* expression in the NAc compared to control mice (figure 30; two way ANOVA, main effect of treatment group $F(1,68)=163.45$, $p < 0001$; main effect of time $F(6,68)=2.94$, $p < 0.05$), suggesting that NPAS2 might be involved in the response to chronic stress.

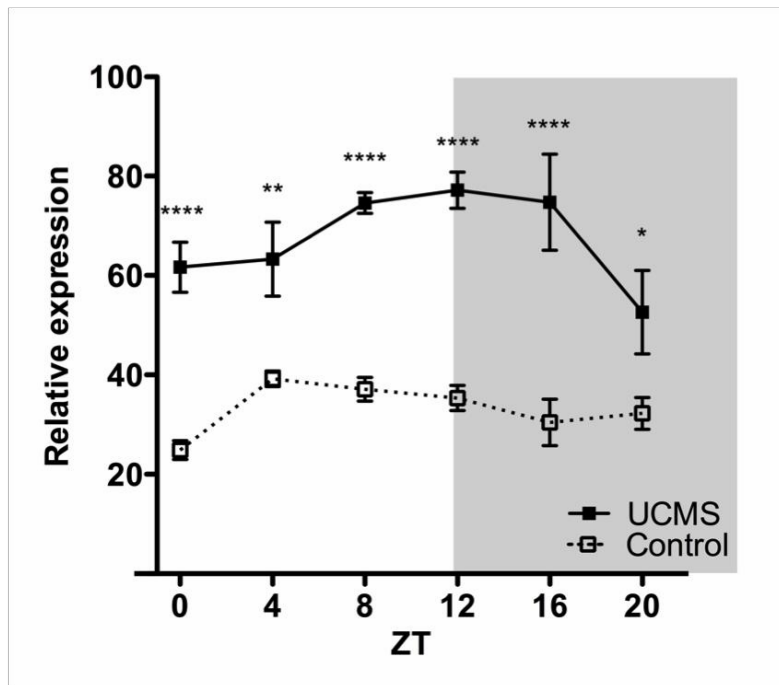


Figure 31. Chronic unpredictable mild stress results in a robust and significant increase in diurnal NAc *Npas2* expression as compared with control mice. Two way ANOVA, main effect of treatment group $F(1,68)=163.45$, $p < 0.0001$; main effect of time $F(6,68)=2.94$, $p < 0.05$. ZT=zeitgeber time, ZT0=lights on, ZT12=lights off. $n=5-6/\text{treatment}/\text{ZT}$. Bonferroni post-hoc * $p < 0.05$, ** $p < 0.01$, ***** $p < 0.0001$.

B.3.2 *Npas2* mutant mice have reduced anxiety-like behaviors and reduced sensitivity to diazepam.

In order to determine if functional NPAS2 is important for anxiety-like behavior, we assayed *Npas2* mutant mice and their wild-type littermates in a battery of behavioral tests. Compared with wild-type mice, *Npas2* mutant mice exhibited reduced anxiety-like behavior as seen by the increased percent time spent in the open arms of the elevated plus maze (figure 31a, Student's t-test, $t=2.454$, $p < 0.05$; with a trend for increased number of open arm entries, $t=1.505$, $p=0.14$),

reduced latency to explore the light side of the light/dark box (figure 31b, $t=2.739$, $p < 0.05$) and increased distance traveled in the center of the open field arena (figure 31c, $t=2.822$, $p < 0.01$). Additionally, we observed that WT, but not *Npas2* mutant, mice are sensitive to the motor incoordinating effects of diazepam (3mg/kg; a GABA_A receptor positive allosteric modulator) as determined by the rotorod test (Student's t-test, WT saline vs diazepam $t=3.134$, $p < 0.01$; *Npas2* mutant saline vs diazepam $t=0.3451$, n/s).

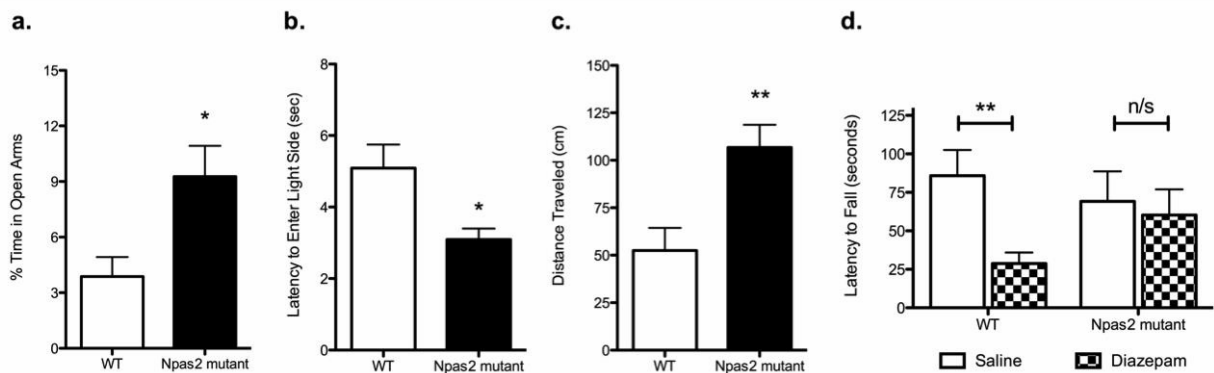


Figure 32. *Npas2* mutant mice exhibit reduced anxiety-like behavior. A) Percent time spent in the open arms of the elevated plus maze (n=16-24/genotype; Student's t-test, $t=2.454$, * $p < 0.05$). B) Latency to explore the light side of the light/dark box (n=16/genotype; Student's t-test, $t=2.739$, * $p < 0.05$). C) Distance traveled in the center of the open field arena (n=12-25/genotype; Student's t-test, $t=2.822$, * $p < 0.05$). D) Latency to fall on accelerating rotarod assay in response to saline or diazepam (n=7/treatment/genotype; Student's t-test, WT saline vs diazepam $t=3.134$, ** $p < 0.01$; *Npas2* mutant saline vs diazepam $t=0.3451$, n/s).

B.3.3 NAc knockdown of *Npas2* results in reduced anxiety-like behaviors.

Because *Npas2* expression in the NAc is highly responsive to the anxiogenic paradigm, UCMS, and the NAc is an important site of neural integration for salient events, we determined if reducing *Npas2* expression in the NAc via viral mediated RNAi (*Npas2* knockdown) was sufficient for a reduction in anxiety-related behaviors. We first assessed the effects of NAc specific *Npas2*

knockdown on locomotor response to a novel environment where analysis revealed a small, but significant treatment x time interaction (figure 32a, two-way ANOVA, $F(23,805)=2.12$, $p < 0.01$). As expected, there was a significant main effect of time ($F(23,805)=63.61$, $p < 0.0001$), indicative of locomotor habituation over the two hour testing period. These results reveal that NAc *Npas2* knockdown did not have the same effect over the times measured, suggestive of altered habituation over time. We note that the effect is modest, with increased exploration in response to the novel environment during the first 30 minutes of the assay, and reduced exploration in the last 10 minutes of the assay. NAc *Npas2* shRNA treated mice exhibited reduced anxiety-like behavior (as compared with scramble shRNA treated mice) in several behavioral measures. *Npas2* knockdown in the NAc resulted in a significant increase in the number of open arm entries (figure 32b, Student's t-test, $t=2.097$, $p < 0.05$) in the elevated plus maze, with a trend towards a significant increase in time spent in the open arms ($t=1.798$, $p = 0.08$, data not shown). *Npas2* knockdown in the NAc resulted in a reduced latency to explore the light side of the light/dark box (figure 32c, $t=2.243$, $p < 0.05$). The effects of NAc *Npas2* knockdown were less robust on behaviors in the open field test. *Npas2* knockdown resulted in a trend towards an increase in the distance traveled in the center of the open field arena that did not reach statistical significance (figure 32d, $t=1.591$, $p = 0.12$).

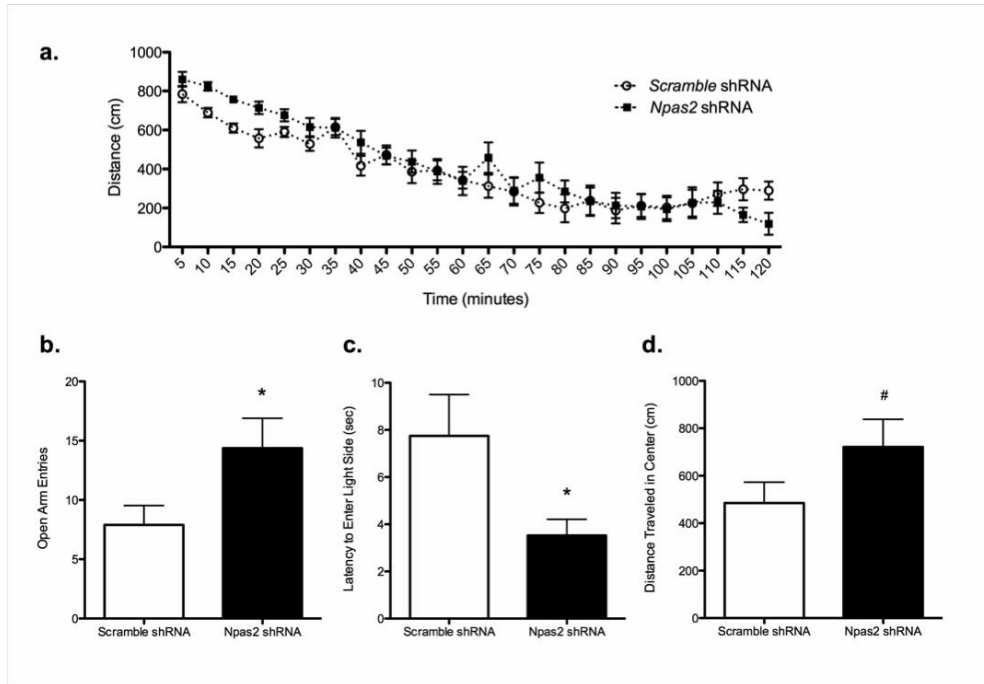


Figure 33. NAc *Npas2* knockdown results in reduced anxiety-like behavior. A) locomotor response to a novel environment (two-way ANOVA, treatment x time interaction $F(23,805)=2.12$, $p < 0.01$; main effect of time ($F(23,805)=63.61$, $p < 0.0001$), B) number of open arm entries in elevated plus maze (Student's t-test, $t=2.097$, $p < 0.05$), C) latency to explore the light side of the light/dark box (Student's t-test, $t=2.243$, $p < 0.05$), and D) amount of time spent in the center of the open field arena (Student's t-test, $t=1.591$, $p = 0.12$). $n=10-13$ /treatment.

B.3.4 NPAS2 regulates expression of GABA_A subunits.

Altered GABA_A subunit composition and possibly altered inhibitory synaptic transmission may occur with reductions in *Npas2* because NPAS2 mutant mice have reduced diazepam sensitivity. NPAS2 is a transcription factor, and in a previous study we performed ChIP Seq on striatal tissue to identify DNA sequences bound to NPAS2 and identified many novel gene targets, including GABA_A alpha (1, 2, 3, 4 and 5), beta (1, 2, 3), gamma (1, 2, 3), epsilon, and pi subunits (Ozburn *et al*, 2015). Here we replicated these findings using ChIP followed by PCR, and we found that

indeed NPAS2 binds genes encoding the GABA_A subunits alpha 1, 2, 4, and 5, beta 2 and 3, and gamma 1 (data not shown)

We next wanted to determine whether NPAS2 mediates expression of GABA_A subunits that mediate responses to diazepam, or that could indicate synaptic or extra-synaptic localization (*Gabra1*, *Gabra2*, *Gabrg1*, and *Gabrg2*). Following viral-mediated knockdown of *Npas2* in the NAc, expression of GABA_A subunits at two time points (ZT16 (lights off) and ZT4 (lights on)) were measured via qPCR. Interestingly, *Npas2* knockdown significantly reduced *Gabra1* expression at both time points measured, suggesting NPAS2 mediates positive regulation of *Gabra1* transcription (figure 33; two way ANOVA - main effect of knockdown, $F(1,24)=4.81$, $p < 0.05$). *Gabra2* exhibited diurnal expression, but was not changed with knockdown (data not shown). Intriguingly, the effect of *Npas2* knockdown on *Gabrg1* expression had different effects depending on time of day, suggesting factors play a role in its transcriptional regulation (data not shown). Lastly, *Gabrg2* expression was unaltered with *Npas2* knockdown as expected since it was not identified via ChIP-Seq. We assayed for this gene to ascertain whether it exhibited diurnal variation, and to determine whether *Npas2* knockdown resulted compensatory changes in expression of this subunit; data not shown).



Figure 34. Effect of *Npas2* knockdown on diurnal expression of GABA α alpha 1 (*Gabra1*) subunit in the NAc.

Two way ANOVA – significant knockdown x time of day (ZT) interaction, $F(1,24)=4.81$, $p<0.05$.

B.3.5 *Npas2* knockdown prevents diazepam-induced potentiation of IPSC amplitude in NAc MSNs

In order to assess the effect of *Npas2* knockdown on inhibitory synaptic activity of MSNs, we performed whole-cell patch-clamp recordings in NAc-containing brain slices. We recorded baseline inhibitory miniature currents (mIPSCs) from scramble shRNA and *Npas2* shRNA infected cells to determine effects of knockdown on current amplitude and frequency (indicating alterations in postsynaptic and presynaptic mechanisms, respectively; representative trace shown in Figure 34a). Analysis of mIPSC amplitude revealed a significant main effect of viral treatment (figure 34b; two way ANOVA, $F(1,46)=6.26$, $p<0.05$) but no main effect of diazepam and no significant interaction. Analysis of mIPSC frequency revealed no significant shRNA treatment by diazepam interaction and no main effect of either shRNA or drug. These results suggest that *Npas2* knockdown in the NAc alters postsynaptic responses but not presynaptic release of GABA onto

MSNs (figure 34c).

However, because we found that mice lacking a functional *Npas2* gene display behavioral insensitivity to diazepam (figure 31d) and NPAS2 binds to genes encoding GABA_A subunits important for pharmacological actions of diazepam, we tested whether this insensitivity could be identified at the cellular level. Therefore, we measured the peak amplitude of the evoked IPSC at baseline and following 10 minutes of diazepam bath application (10 μM) in both scramble shRNA and *Npas2* shRNA treated MSNs. We found that diazepam application reliably increased the average IPSC peak amplitude in scramble control cells by approximately 20% while this increase in current amplitude was noticeably absent in *Npas2* shRNA infected cells (figures 33d,e; Student's *t*-test, $t_{20}=2.152$, $p < 0.05$; $n = 10$ scrambled, $n = 12$ shRNA). Additionally, we measured the decay kinetics of IPSCs from both groups under baseline and diazepam conditions. We found that there is a significant main effect of diazepam to prolong the decay time of the GABA_A receptor-mediated IPSCs (two way ANOVA, $F(1,34)=4.90$, $p < 0.05$). However, it does so to a similar extent in both scramble- and *Npas2* shRNA treated cells (decay time constants for Scramble shRNA: baseline 13.8 +/- 1.7, diazepam 19.4 +/- 2.5; decay time constants for *Npas2* shRNA: baseline 16.8 +/- 3.4, diazepam 24.6 +/- 5.0; $n = 10$ baseline scrambled, $n = 13$ baseline shRNA, $n = 7$ diazepam scrambled, $n = 12$ diazepam shRNA), suggesting that the effects of *Npas2* knockdown are specific to the change in current amplitude by diazepam.

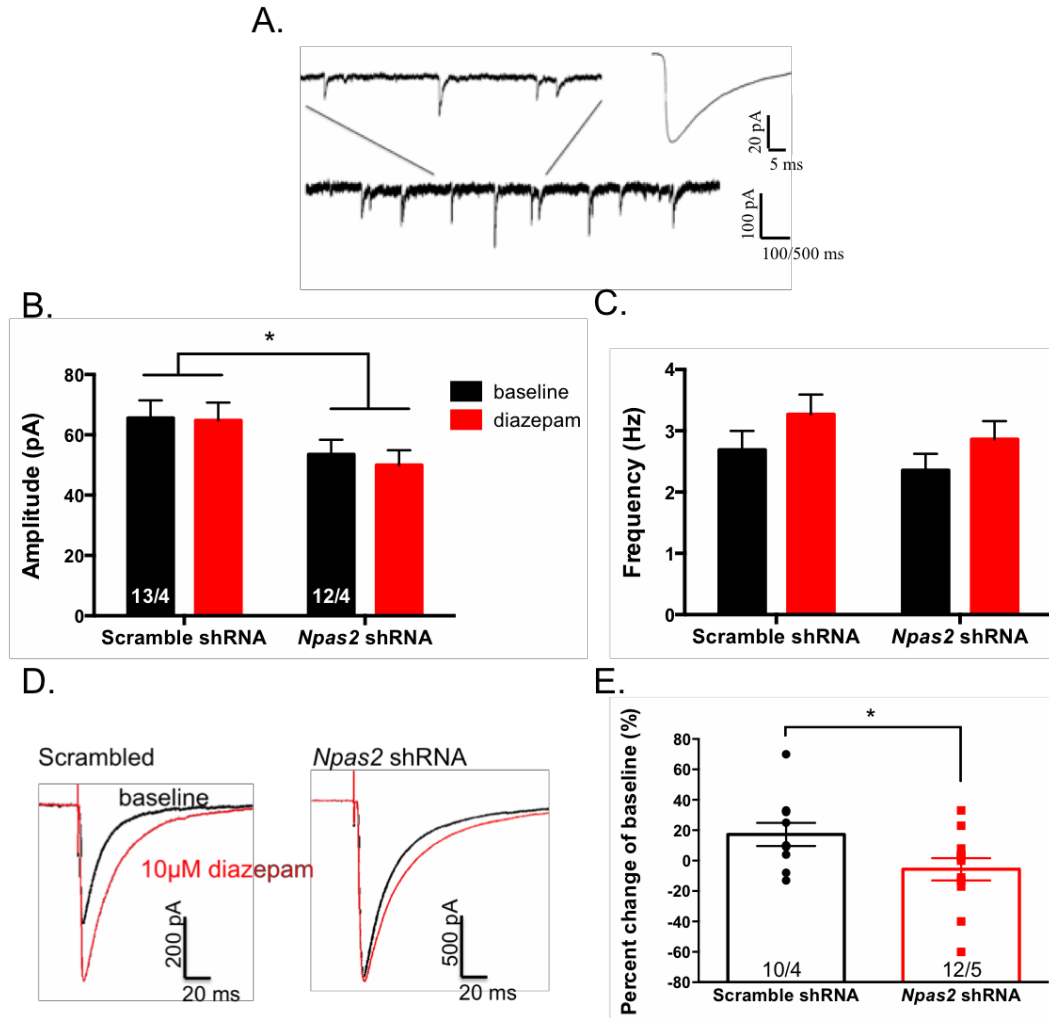


Figure 35. *Npas2* knockdown prevents diazepam-induced potentiation of IPSC amplitude in NAc MSNs. A) Representative traces of baseline mIPSCs from AAV-scramble shRNA and -*Npas2* shRNA infected cells, B) mIPSC amplitude (two way ANOVA, $F(1,46)=6.26$, $* p < 0.05$), C) mIPSC frequency (n/s), D) peak amplitude of the evoked IPSC at baseline and following 10 minutes of diazepam bath application (10 μ M) in both scramble shRNA and *Npas2* shRNA treated MSNs (Student's t-test, $t=2.152$, $* p < 0.05$), and E) representative traces of evoked IPSC at baseline and following 10 minutes of diazepam from AAV-scramble shRNA and -*Npas2* shRNA infected cells. n = cells/animals.

B.4 DISCUSSION

Circadian rhythms and the genes that make up the molecular clock play an important role in the expression of mood-related symptoms in psychiatric disorders. Here we link *Npas2* to responses to stressful and anxiogenic stimuli, expression of anxiety-like behavior, regulation of specific GABAA subunit expression, and inhibitory neurotransmission in the nucleus accumbens in response to anxiolytic medication.

Chronic unpredictable mild stress (UCMS) results in a robust increase in levels of *Npas2* expression in the NAc. To examine the effects of this stressful and anxiogenic paradigm on rhythmic circadian gene expression, tissue samples were collected over a 24 hour period. Individuals with mood disorders experience perturbations in a myriad of rhythmic processes, therefore, this result was surprising in that we had hypothesized that chronic stress would decrease or completely disrupt *Npas2* gene expression rhythms. Interestingly, we found that UCMS treatment resulted in an approximate 4-hour phase delay in the peak expression of *Npas2* and as indicated by the significant main effect of time which might contribute to the development of anxiety-like phenotype following UCMS.

To determine if *Npas2* is important for the expression of anxiety-like behaviors, we subjected mice lacking functional *Npas2* to a battery of behavioral tests. *Npas2* mutant mice exhibited decreased anxiety-like behaviors as compared with wild-type mice. *Npas2* mutants exhibited an increased percent time in open arms of the elevated plus maze, reduced latency to explore the light side of the light/dark box, and an increase in the distance traveled in the center of the open field arena. Further, *Npas2* mutant mice were resistant to the motor incoordinating effects of diazepam, suggesting these mice may have altered GABA_A receptor subunit composition and reduced synaptic localization. This phenotype is the opposite of the *Per1*^{-/-}/*Per2*^{-/-} double mutant,

which exhibit increased anxiety-like behavior (Spencer *et al*, 2013). Because *Per1* and *Per2* negatively regulate NPAS2/BMAL1 transcription, this further supports a role for NPAS2 in the regulation of anxiety-like behaviors. WT and *Npas2* mutant mice were evaluated in tests of sucrose preference and locomotor response to novelty, with no differences observed (Ozburn *et al*, 2015). Although CLOCK and NPAS2 are homologous transcription factors, these mutants exhibit opposing reward-related phenotypes. Previously we found that *Npas2* mutant mice exhibit reduced sensitivity to the rewarding effects of cocaine, whereas *Clock* Δ 19 mutant mice exhibit increased sensitivity (Ozburn *et al*, 2015). Observed differences in sensitivity to the rewarding properties of cocaine in *Clock* Δ 19 and *Npas2* mutants are likely due to brain region (and cell-type) specific expression differences, as well as differences in transcriptional targets (Ozburn *et al*, 2012). For example, *Npas2* is highly expressed in limbic and forebrain regions (Garcia *et al*, 2000). Furthermore, *Npas2* expression has been shown to be specific to dopamine receptor 1 (D1) containing MSNs in the NAc, which are thought to underlie positive or rewarding associations with salient events (Ozburn *et al*, 2012).

Selective knockdown of *Npas2* in the NAc results in reduced anxiety-like behavior, similar to *Npas2* mutant mice. AAV-mediated knockdown of *Npas2* specifically in the NAc results in increased percent time in the open arms of the elevated plus maze, reduced latency to explore the light side of the light/dark box, and an increase in the velocity of movement in the center of the open field arena. NAc *Npas2* knockdown also resulted in a small, but significant difference in locomotor response to novelty, where *Npas2* shRNA treated mice exhibited an initial increased exploratory behavior that decreased more quickly (habituation) than scramble shRNA treated mice. Together, these findings suggest that knocking down NAc expression of *Npas2* recapitulates the reduced anxiety-like behaviors seen in the *Npas2* mutant mice. Previous reports, in conjunction

with the studies presented here, support a model whereby VTA *Clock* is important for negatively regulating reward and anxiety and NAc *Npas2* is important for positively regulating reward and anxiety (Ozburn *et al*, 2012; Mukherjee *et al*, 2010; Coque *et al*, 2011; Sidor *et al*, 2015).

We further examined genes that are under the transcriptional control of NPAS2 to identify a mechanism by which NPAS2 could positively regulate reward and anxiety. Using ChIP Seq, gene expression and behavioral assays, we found that the direct regulation of Dopamine receptor 3 (*Drd3*) by NPAS2 in the NAc is important for regulating reward (Ozburn *et al*, 2015). Genetic manipulation of *Drd3* in mice has not yielded reports of consistent effects on anxiety-like behavior (Morago-Amaro *et al*, 2014; Steiner *et al*, 1997; Xing *et al*, 2013). These studies separate the role of NPAS2 regulation of *Drd3* in reward from the role of NPAS2 in measures of anxiety-related behavior and suggest a separate mechanism by which these processes are regulated. Based on our current findings that *Npas2* mutant mice are insensitive to diazepam, we explored the possibility that NPAS2 may act as a positive regulator for the transcription of GABA_A subunits. We performed ChIP assays on striatal tissue to isolate DNA bound to NPAS2 and used this DNA as a template for PCR with primers targeting various GABA_A subunit genes. We confirmed that NPAS2 binds genes encoding the GABA_A subunits alpha 1, 2, 4, and 5, beta 2 and 3, and gamma 1 and plays an important role in the positive regulation of the GABA_Aalpha 1 subunit. The binding site for diazepam requires the pentameric subunit composition of the GABA_A receptor to contain two alpha subunits (1,2,3 or 5) in combination with two beta and one gamma subunit. Thus, the reduced sensitivity to diazepam in *Npas2* mutant mice is likely mediated by a reduction in alpha 1 subunit expression. GABA_A alpha1 is thought to be important for the sedative effect of benzodiazepines, whereas alpha 2 and 3 confer the anxiolytic effects. This novel finding indicates

that chronic stress increases *Npas2* and via NPAS2 mediated transcription of specific GABA_A subunits, likely altering inhibitory neurotransmission in the NAc.

Lastly, we tested the functional consequences of *Npas2* knockdown on GABAergic neurotransmission in MSNs of the NAc using ex-vivo slice electrophysiology. We found that *Npas2* shRNA infected cells had a reduction in mIPSC amplitude, but not frequency. This finding suggests that *Npas2* knockdown may result in postsynaptic modification of MSNs resulting in decreased mIPSC amplitude, but does not affect presynaptic release of GABA onto MSNs. The lack of diazepam's effect on this measure is not entirely surprising, as it is thought that the effects of diazepam are seen only with evoked IPSCs in this preparation. Further, we found that mice lacking *Npas2* were insensitive to diazepam, and this insensitivity persists at the cellular level in *Npas2* shRNA infected cells. Diazepam has been shown to potentiate GABA_A-receptor mediated currents by binding specific subunit combinations of synaptic GABA_A receptors and promoting the binding of GABA, which in turn increases total conductance of chloride. We found that diazepam application reliably increased the average IPSC peak amplitude in scramble control cells by approximately 20% while this increase in current amplitude was noticeably absent in *Npas2* shRNA infected cells. This result suggests that knockdown of *Npas2* in NAc MSNs abolishes the cellular response to diazepam as measured by a change in inhibitory synaptic signaling. These results provide functional evidence for the regulation of GABA_A receptor subunit expression by NPAS2.

We propose that expression of the circadian transcription factor, *Npas2*, is important for stress responses and anxiety-related behaviors and regulates GABAergic inhibitory neurotransmission in MSNs of the NAc. Taken together, these findings support the existence of a homeostatic mechanism by which stress and anxiety increase NPAS2-dependent transcription of

specific GABAergic subunits that selectively alter phasic, synaptic inhibitory neurotransmission (perhaps specifically in *Drd1a* containing medium spiny neurons of the NAc). Future work will focus on testing the efficacy of pharmacotherapeutics (that target the molecular clock and/or its targets) in ameliorating these adaptations to improve our understanding of and treatments for anxiety-related disorders.

BIBLIOGRAPHY

- Alamilla J, Granados-Fuentes D, Aguilar-Roblero R (2015). The anterior Paraventricular Thalamus Modulates Neuronal Excitability in the Suprachiasmatic Nuclei of the Rat. *The European journal of neuroscience* doi:10.1111/ejn.13088.
- Anand A, Barkay G, Dzemidzic M, Albrecht D, Karne H, Zheng Q-HH, *et al.* (2011): Striatal dopamine transporter availability in unmedicated bipolar disorder. *Bipolar Disord* **13**: 406–13.
- Angeles-Castellanos M, Salgado-Delgado R, Rodríguez K, Buijs RM, Escobar C (2008). Expectancy for food or expectancy for chocolate reveals timing systems for metabolism and reward. *Neuroscience* **155**: 297–307.
- Anguelova M, Benkelfat C, Turecki G (2003). A systematic review of association studies investigating genes coding for serotonin receptors and the serotonin transporter: II. Suicidal behavior. *Mol Psychiatry* **8**: 646–53.
- Arango-Lievano M, *et al.* (2014). Cell-type specific expression of p11 controls cocaine reward. *Biological Psychiatry*. **76**(10): 794-801.
- Arey RN, Enwright JF, Spencer SM, Falcon E, Ozburn AR, Ghose S, *et al* (2014). An important role for cholecystokinin, a CLOCK target gene, in the development and treatment of manic-like behaviors. *Mol Psychiatry* **19**: 342–50.
- Aston-Jones G, Chen S, Zhu Y, Oshinsky ML (2001). A neural circuit for circadian regulation of arousal. *Nat Neurosci* **4**: 732–8.
- Aston-Jones G, Smith RJ, Moorman DE, Richardson KA (2009). Role of lateral hypothalamic orexin neurons in reward processing and addiction. *Neuropharmacology* **56 Suppl 1**: 112–21.
- Bachtell RK, Choi K-HH, Simmons DL, Falcon E, Monteggia LM, Neve RL, Self DW (2008): Role of GluR1 expression in nucleus accumbens neurons in cocaine sensitization and cocaine-seeking behavior. *Eur J Neurosci* **27**: 2229–40.
- Baik J-HH (2013). Dopamine signaling in reward-related behaviors. *Front Neural Circuits* **7**: 152.
- Ballard IC, Murty VP, Carter RM, MacInnes JJ, Huettel SA, Adcock RA (2011). Dorsolateral prefrontal cortex drives mesolimbic dopaminergic regions to initiate motivated behavior. *J Neurosci* **31**: 10340–6.
- Beaulieu JM, Caron MG (2008). Looking at lithium: molecular moods and complex behaviour. *Mol Interv* **8**(5): 230-241.

- Bedrosian TA, Nelson RJ (2013). Influence of the modern light environment on mood. *Mol Psychiatry* **18**: 751–7.
- Ben-Hamo M, Larson TA, Duge LS, Sikkema C, Wilkinson CW, Iglesia HO de la, *et al* (2016). Circadian Forced Desynchrony of the Master Clock Leads to Phenotypic Manifestation of Depression in Rats. *eNeuro* **3**: 237-16.
- Benedetti F, *et al.* (2004). A single nucleotide polymorphism in glycogen synthase kinase 3-beta promoter gene influences onset of illness in patients affected by bipolar disorder. *Neurosci Lett* **355**(1-2): 37-40.
- Benedetti F, Dallaspezia S, Colombo C, Pirovano A, Marino E, Smeraldi E (2008). A length polymorphism in the circadian clock gene Per3 influences age at onset of bipolar disorder. *Neurosci Lett* **445**: 184–7.
- Benedetti F, Dallaspezia S, Fulgosi MC, Lorenzi C, Serretti A, Barbini B, *et al* (2007). Actimetric evidence that CLOCK 3111 T/C SNP influences sleep and activity patterns in patients affected by bipolar depression. *Am J Med Genet B Neuropsychiatr Genet* **144B**: 631–5.
- Benedetti F, Serretti A, Colombo C, Barbini B, Lorenzi C, Campori E, *et al* (2003). Influence of CLOCK gene polymorphism on circadian mood fluctuation and illness recurrence in bipolar depression. *Am J Med Genet B Neuropsychiatr Genet* **123B**: 23–6.
- Beneyto M, Meador-Woodruff JH (2006). Lamina-specific abnormalities of AMPA receptor trafficking and signaling molecule transcripts in the prefrontal cortex in schizophrenia. *Synapse* **60**: 585–598.
- Berridge KC, Robinson TE (1998). What is the role of dopamine in reward: hedonic impact, reward learning, or incentive salience? *Brain Res Brain Res Rev* **28**: 309–69.
- Beurrier C, Malenka RC (2002): Enhanced inhibition of synaptic transmission by dopamine in the nucleus accumbens during behavioral sensitization to cocaine. *J Neurosci* **22**: 5817–22.
- Boudreau AC, Milovanovic M, Conrad KL, Nelson C, Ferrario CR, Wolf ME (2012): A protein cross-linking assay for measuring cell surface expression of glutamate receptor subunits in the rodent brain after in vivo treatments. *Curr Protoc Neurosci* Chapter 5: Unit5.30.1–19.
- Boudreau AC, Wolf ME (2005): Behavioral sensitization to cocaine is associated with increased AMPA receptor surface expression in the nucleus accumbens. *J Neurosci* **25**: 9144–51.
- Bourdy R, Barrot M (2012). A new control center for dopaminergic systems: pulling the VTA by the tail. *Trends Neurosci* **35**: 681–90.
- Boyce-Rustay JM, Holmes A (2006): Genetic inactivation of the NMDA receptor NR2A subunit has anxiolytic- and antidepressant-like effects in mice. *Neuropsychopharmacology* **31**: 2405–14.

- Britt JP, Benaliouad F, McDevitt RA, Stuber GD, Wise RA, Bonci A (2012). Synaptic and behavioral profile of multiple glutamatergic inputs to the nucleus accumbens. *Neuron* **76**: 790–803.
- Broms U, Kaprio J, Hublin C, Partinen M, Madden PA, Koskenvuo M (2011). Evening types are more often current smokers and nicotine-dependent—a study of Finnish adult twins. *Addiction* **106**: 170–7.
- Broms U, Pitkäniemi J, Bäckmand H, Heikkilä K, Koskenvuo M, Peltonen M, *et al* (2014). Long-term consistency of diurnal-type preferences among men. *Chronobiol Int* **31**: 182–8.
- Bunney BG, Bunney WE (2013). Mechanisms of rapid antidepressant effects of sleep deprivation therapy: clock genes and circadian rhythms. *Biol Psychiatry* **73**(12):1164–71.
- Bunning E (1935). Zur kenntnis der erblichen tagesperiodizität bei den primarblättern von *Phaseolus multiflorus*. *Jahrb. Wiss. Bot.* **81**: 411.
- Carlezon WA, Thomas MJ (2009): Biological substrates of reward and aversion: a nucleus accumbens activity hypothesis. *Neuropharmacology* **56 Suppl 1**: 122–32.
- Carpen JD, Archer SN, Skene DJ, Smits M, Schantz M von (2005). A single-nucleotide polymorphism in the 5'-untranslated region of the hPER2 gene is associated with diurnal preference. *J Sleep Res* **14**: 293–7.
- Carpen JD, Schantz M von, Smits M, Skene DJ, Archer SN (2006). A silent polymorphism in the PER1 gene associates with extreme diurnal preference in humans. *J Hum Genet* **51**: 1122–5.
- Caseras X, Lawrence NS, Murphy K, Wise RG, Phillips ML (2013). Ventral striatum activity in response to reward: differences between bipolar I and II disorders. *Am J Psychiatry* **170**(5): 533–541.
- Castañeda TR, Prado BM de, Prieto D, Mora F (2004). Circadian rhythms of dopamine, glutamate and GABA in the striatum and nucleus accumbens of the awake rat: modulation by light. *J Pineal Res* **36**: 177–85.
- Chandrashekar MK (1998). Biological rhythms research: A personal account. *J. Biosci.* **23**: 545.
- Cho K, Ennaceur A, Cole JC, Suh CK (2000). Chronic jet lag produces cognitive deficits. *J Neurosci* **20**: RC66.
- Ciarleglio CM, Resuehr HE, McMahon DG (2011). Interactions of the serotonin and circadian systems: nature and nurture in rhythms and blues. *Neuroscience* **197**: 8–16.
- Coogan AN, Thome J (2011). Chronotherapeutics and psychiatry: setting the clock to relieve the symptoms. *World J Biol Psychiatry* **12 Suppl 1**: 40–3.

- Colavito V, Tesoriero C, Wirtu AT, Grassi-Zucconi G, Bentivoglio M (2015). Limbic thalamus and state-dependent behavior: The paraventricular nucleus of the thalamic midline as a node in circadian timing and sleep/wake-regulatory networks. *Neuroscience and biobehavioral reviews* **54**: 3–17.
- Conrad KL, Tseng KY, Uejima JL, Reimers JM, Heng L-JJ, Shaham Y, *et al.* (2008): Formation of accumbens GluR2-lacking AMPA receptors mediates incubation of cocaine craving. *Nature* **454**: 118–21.
- Coque L, Mukherjee S, Cao J-LL, Spencer S, Marvin M, Falcon E, *et al.* (2011): Specific role of VTA dopamine neuronal firing rates and morphology in the reversal of anxiety-related, but not depression-related behavior in the Clock Δ 19 mouse model of mania. *Neuropsychopharmacology* **36**: 1478–88.
- Cousins DA, Butts K, Young AH (2009). The role of dopamine in bipolar disorder. *Bipolar Disord* **11**: 787–806.
- Craig LA, McDonald RJ (2008). Chronic disruption of circadian rhythms impairs hippocampal memory in the rat. *Brain Res Bull* **76**: 141–51.
- Dallaspezia S, Suzuki M, Benedetti F (2015). Chronobiological Therapy for Mood Disorders. *Curr Psychiatry Rep* **17**: 95.
- Damiola F, Minh N Le, Preitner N, Kornmann B, Fleury-Olela F, Schibler U (2000). Restricted feeding uncouples circadian oscillators in peripheral tissues from the central pacemaker in the suprachiasmatic nucleus. *Genes Dev* **14**: 2950–61.
- Danel T, Jeanson R, Touitou Y (2003). Temporal pattern in consumption of the first drink of the day in alcohol-dependent persons. *Chronobiol Int* **20**: 1093–102.
- Doi M, Hirayama J, Sassone-Corsi P (2006). Circadian regulator CLOCK is a histone acetyltransferase. *Cell* **125**: 497–508.
- Dayas CV, McGranahan TM, Martin-Fardon R, Weiss F (2008). Stimuli linked to ethanol availability activate hypothalamic CART and orexin neurons in a reinstatement model of relapse. *Biol Psychiatry* **63**: 152–7.
- De Bartolomeis A, Buonaguro EF, Iasevoli F, Tomasetti C (2014): The emerging role of dopamine-glutamate interaction and of the postsynaptic density in bipolar disorder pathophysiology: Implications for treatment. *J Psychopharmacol (Oxford)* **28**: 505–526.
- DeBruyne JP, Weaver DR, Reppert SM (2007). CLOCK and NPAS2 have overlapping roles in the suprachiasmatic circadian clock. *Nat Neurosci* **10**: 543–5.
- Desan PH, *et al.* (2000). Genetic polymorphism at the CLOCK gene locus and major depression. *Am J Med Genet* **96**(3): 418-21.

- Ding S, Matta SG, Zhou FM (2011). Kv3-like potassium channels are required for sustained high-frequency firing in basal ganglia output neurons. *J Neurophysiol* **105**(2):554-570.
- Domínguez-López S, Howell RD, López-Canúl MG, Leyton M, Gobbi G (2014). Electrophysiological characterization of dopamine neuronal activity in the ventral tegmental area across the light-dark cycle. *Synapse* **68**: 454–67.
- Du J, Gray NA, Falke CA, Chen W, Yuan P, Szabo ST, *et al.* (2004): Modulation of synaptic plasticity by antimanic agents: the role of AMPA glutamate receptor subunit 1 synaptic expression. *J Neurosci* **24**: 6578–89.
- Dudley CA, Erbel-Sieler C, Estill SJ, Reick M, Franken P, Pitts S, *et al* (2003). Altered patterns of sleep and behavioral adaptability in NPAS2-deficient mice. *Science* **301**: 379–83.
- Dunn H, Anderson MA, Hill PD (2010). Nighttime lighting in intensive care units. *Crit Care Nurse* **30**: 31–7.
- Dzirasa K, Coque L, Sidor MM, Kumar S, Dancy EA, Takahashi JS, *et al.* (2010): Lithium ameliorates nucleus accumbens phase-signaling dysfunction in a genetic mouse model of mania. *J Neurosci* **30**: 16314–23.
- Easton A, Arbuzova J, Turek FW (2003): The circadian Clock mutation increases exploratory activity and escape-seeking behavior. *Genes Brain Behav* **2**: 11–9.
- Edgar N, McClung CA (2013). Major depressive disorder: a loss of circadian synchrony? *Bioessays* **35**: 940–4.
- Edwards S, Koob GF. (2010). Neurobiology of dysregulated motivational systems in drug addiction. *Future Neurol* **5**: 393–401.
- Enkhuizen J van, Geyer MA, Young JW (2013). Differential effects of dopamine transporter inhibitors in the rodent Iowa gambling task: relevance to mania. *Psychopharmacology (Berl)* **225**: 661–74.
- Enkhuizen J van, Henry BL, Minassian A, Perry W, Milienne-Petiot M, Higa KK, *et al* (2014). Reduced dopamine transporter functioning induces high-reward risk-preference consistent with bipolar disorder. *Neuropsychopharmacology* **39**: 3112–22
- Enkhuizen J van, Geyer MA, Minassian A, Perry W, Henry BL, Young JW (2015). Investigating the underlying mechanisms of aberrant behaviors in bipolar disorder from patients to models: Rodent and human studies. *Neurosci Biobehav Rev* **58**: 4–18.
- Enkhuizen J van, Minassian A, Young JW (2013): Further evidence for Clock Δ 19 mice as a model for bipolar disorder mania using cross-species tests of exploration and sensorimotor gating. *Behav Brain Res* **249**: 44–54.
- Espinosa F, Marks G, Heintz N, Joho RH (2004). Increased motor drive and sleep loss in mice lacking Kv3-type potassium channels. *Genes Brain Behav* **3**(2): 90-100.

- Etain B, Jamain S, Milhiet V, Lajnef M, Boudebessé C, Dumaine A, *et al* (2014). Association between circadian genes, bipolar disorders and chronotypes. *Chronobiol Int* **31**: 807–14.
- Falcon E, McClung CA (2009). A role for the circadian genes in drug addiction. *Neuropharmacology* **56 Suppl 1**: 91-6.
- Falcon E, Ozburn A, Mukherjee S, Roybal K, McClung CA (2013). Differential regulation of the period genes in striatal regions following cocaine exposure. *PLoS ONE* **8**: e66438.
- Faure A, Richard JM, Berridge KC (2010): Desire and dread from the nucleus accumbens: cortical glutamate and subcortical GABA differentially generate motivation and hedonic impact in the rat. *PLoS ONE* **5**: e11223.
- Ferris MJ, España RA, Locke JL, Konstantopoulos JK, Rose JH, Chen R, *et al* (2014). Dopamine transporters govern diurnal variation in extracellular dopamine tone. *Proc Natl Acad Sci USA* **111**: E2751–9.
- Forbes EE, Dahl RE, Almeida JR, Ferrell RE, Nimgaonkar VL, Mansour H, *et al* (2012). PER2 rs2304672 polymorphism moderates circadian-relevant reward circuitry activity in adolescents. *Biol Psychiatry* **71**: 451–7.
- Gallerani M, Manfredini R, Monte D Dal, Calò G, Brunaldi V, Simonato M (2001). Circadian differences in the individual sensitivity to opiate overdose. *Crit Care Med* **29**: 96–101.
- Garcia JA, Zhang D, Estill SJ, Michnoff C, Rutter J, Reick M, *et al* (2000). Impaired cued and contextual memory in NPAS2-deficient mice. *Science* **288**: 2226–30.
- Geddes JR, Miklowitz DJ (2013). Treatment of bipolar disorder. *Lancet* **381**(9878): 1672-1682.
- Gekakis N, Staknis D, Nguyen HB, Davis FC, Wilsbacher LD, King DP, *et al*. (1998): Role of the CLOCK protein in the mammalian circadian mechanism. *Science* **280**: 1564–9.
- Gerfen CR, Engber TM, Mahan LC, Susel Z, Chase TN, Monsma FJ, *et al* (1990). D1 and D2 dopamine receptor-regulated gene expression of striatonigral and striatopallidal neurons. *Science* **250**: 1429–32.
- Gill S, Panda S (2015). A Smartphone App Reveals Erratic Diurnal Eating Patterns in Humans that Can Be Modulated for Health Benefits. *Cell Metab* **22**: 789–98.
- Gompf HS, Aston-Jones G (2008). Role of orexin input in the diurnal rhythm of locus coeruleus impulse activity. *Brain research* **1224**: 43–52.
- Gillman AG, Kosobud AE, Timberlake W (2010). Effects of multiple daily nicotine administrations on pre- and post-nicotine circadian activity episodes in rats. *Behav Neurosci* **124**: 520–31.
- Gipson CD, Kupchik YM, Kalivas PW (2014). Rapid, transient synaptic plasticity in addiction. *Neuropharmacology* **76 Pt B**: 276–86.

- González MMM, Aston-Jones G (2006). Circadian regulation of arousal: role of the noradrenergic locus coeruleus system and light exposure. *Sleep* **29**: 1327–36.
- Goto Y, Grace AA (2008). Limbic and cortical information processing in the nucleus accumbens. *Trends Neurosci* **31**: 552–8.
- Gould TJ, Keith RA, Bhat RV (2001). Differential sensitivity to lithium's reversal of amphetamine-induced open-field activity in two inbred strains of mice. *Behav Brain Res* **118**: 95–105.
- Graziane NM, *et al.* (2016). Opposing mechanisms mediate morphine- and cocaine-induced generation of silent synapses. *Nat Neurosci* **19**: 915-925.
- Green NH, Jackson CR, Iwamoto H, Tackenberg MC, McMahon DG (2015). Photoperiod programs dorsal raphe serotonergic neurons and affective behaviors. *Curr Biol* **25**: 1389–94.
- Greenwood TA, Schork NJ, Eskin E, Kelsoe JR (2006). Identification of additional variants within the human dopamine transporter gene provides further evidence for an association with bipolar disorder in two independent samples. *Molecular psychiatry* **11**: 125–133, 115.
- Groenewegen HJ, Galis-de Graaf Y, Smeets WJ (1999). Integration and segregation of limbic cortico-striatal loops at the thalamic level: an experimental tracing study in rats. *J Chem Neuroanat* **16**: 167–85.
- Grueter BA, Robison AJ, Neve RL, Nestler EJ, Malenka RC (2013). Δ FosB differentially modulates nucleus accumbens direct and indirect pathway function. *Proc Natl Acad Sci USA* **110**: 1923–8.
- Guilding C, Hughes AT, Piggins HD (2010). Circadian oscillators in the epithalamus. *Neuroscience* **169**: 1630–9.
- Hagenauer MH, Lee TM (2012). The neuroendocrine control of the circadian system: adolescent chronotype. *Front Neuroendocrinol* **33**: 211–29.
- Hampp G, Ripperger JAA, Houben T, Schmutz I, Blex C, Perreau-Lenz S, *et al* (2008). Regulation of monoamine oxidase A by circadian-clock components implies clock influence on mood. *Curr Biol* **18**: 678–83.
- Hardin PE, Yu W (2006). Circadian transcription: passing the HAT to CLOCK. *Cell* **125**: 424–6.
- Hasler BP, *et al.* (2012). Circadian rhythms, sleep, and substance abuse. *Sleep Med Rev* **16**(1): 67–81.
- Hasler BP, Clark DB (2013). Circadian misalignment, reward-related brain function, and adolescent alcohol involvement. *Alcohol Clin Exp Res* **37**: 558–65.

- Hasler BP, Dahl RE, Holm SM, Jakubcak JL, Ryan ND, Silk JS, *et al* (2012). Weekend-weekday advances in sleep timing are associated with altered reward-related brain function in healthy adolescents. *Biol Psychol* **91**: 334–41.
- Hasler BP, Soehner AM, Clark DB (2015). Sleep and circadian contributions to adolescent alcohol use disorder. *Alcohol* **49**: 377–87.
- Hattar S, Kumar M, Park A, Tong P, Tung J, Yau K-WW, *et al* (2006). Central projections of melanopsin-expressing retinal ganglion cells in the mouse. *J Comp Neurol* **497**: 326–49.
- Haynes PL, Gengler D, Kelly M (2016). Social Rhythm Therapies for Mood Disorders: an Update. *Curr Psychiatry Rep* **18**: 75.
- Henriksen TE, Skrede S, Fasmer OB, Schoeyen H, Leskauskaite I, Bjørke-Bertheussen J, *et al* (2016). Blue-blocking glasses as additive treatment for mania: a randomized placebo-controlled trial. *Bipolar Disord* **18**: 221–32.
- Hernandez-Pineda R, Chow A, Amarillo Y, Moreno H, Saganich M, Vega-Saenz de Miera EC, *et al* (1999). Kv3.1-Kv3.2 channels underlie a high-voltage-activating component of the delayed rectifier K⁺ current in projecting neurons from the globus pallidus. *J Neurophysiol* **82**(3): 1512-1528.
- Ho CS, Grange RW, Joho RH (1997). Pleiotropic effects of a disrupted K⁺ channel gene: reduced body weight, impaired motor skill and muscle contraction, but no seizures. *Proc Natl Acad Sci U S A* **94**(4): 1533-1538.
- Holtmaat and Svoboda (2009). Experience-dependent structural synaptic plasticity in the mammalian brain. *Nat Rev Neurosci.* **10**(9): 647-58.
- Horne JA, Ostberg O (1976). A self-assessment questionnaire to determine morningness-eveningness in human circadian rhythms. *Int J Chronobiol* **4**: 97–110.
- Huang YH, *et al.* (2009). *In vivo* cocaine exposure generates silent synapses. *Neuron.* **63**(1): 40-7.
- Hyman SE (2005). Addiction: a disease of learning and memory. *Am J Psychiatry* **162**: 1414–22.
- Ikeda M, Hojo Y, Komatsuzaki Y, Okamoto M, Kato A, Takeda T *et al.* (2015). Hippocampal spine changes across the sleep-wake cycle: corticosterone and kinases. *The Journal of endocrinology* **226**: M13–27.
- Jasinska M, Grzegorzczak A, Woznicka O, Jasek E, Kossut M, Barbacka-Surowiak G *et al.* (2015). Circadian rhythmicity of synapses in mouse somatosensory cortex. *The European journal of neuroscience*
- Johnson CH, Elliott JA, Foster R (2003). Entrainment of circadian programs. *Chronobiol Int* **20**: 741–74.

- Johnson SW and North RA (1992). Two types of neurone in the rat ventral tegmental area and their synaptic inputs. *J Physiol.* **450**(1): 455-468.
- Joho RH, Ho CS, Marks GA (1999). Increased gamma- and decreased delta-oscillations in a mouse deficient for a potassium channel expressed in fast-spiking interneurons. *J Neurophysiol* **82**(4): 1855-1864.
- Joho RH, Marks GA, Espinosa F (2006). Kv3 potassium channels control the duration of different arousal states by distinct stochastic and clock-like mechanisms. *Eur J Neurosci* **23**(6): 1567-1574.
- Juarez B, Han M-H (2016). Diversity of Dopaminergic Neural Circuits in Response to Drug Exposure. *Neuropsychopharmacology* **41**: 2424-46.
- Karatsoreos IN (2014). Links between Circadian Rhythms and Psychiatric Disease. *Front Behav Neurosci* **8**: 162.
- Katz G, Durst R, Zislin Y, Barel Y, Knobler HY (2001). Psychiatric aspects of jet lag: review and hypothesis. *Med Hypotheses* **56**: 20-3.
- Katzenberg D, Young T, Finn L, Lin L, King DP, Takahashi JS, *et al* (1998). A CLOCK polymorphism associated with human diurnal preference. *Sleep* **21**: 569-76.
- Kauer JA, Malenka RC (2007). Synaptic plasticity and addiction. *Nat Rev Neurosci* **8**: 844-58.
- King DP, Vitaterna MH, Chang AM, Dove WF, Pinto LH, Turek FW, *et al* (1997). The Mouse Clock Mutation Behaves as an Antimorph and Maps Within the W(19H) Deletion, Distal of Kit. *Genetics* **146**(3): 1049-1060.
- King DP, Zhao Y, Sangoram AM, Wilsbacher LD, Tanaka M, Antoch MP, *et al.* (1997): Positional cloning of the mouse circadian clock gene. *Cell* **89**: 641-53.
- Kirouac GJ (2015). Placing the paraventricular nucleus of the thalamus within the brain circuits that control behavior. *Neuroscience and biobehavioral reviews* **56**: 315-29.
- Kishi T, *et al.* (2009). Association analysis of nuclear receptor Rev-erb alpha gene (NR1D1) with mood disorders in the Japanese population. *Neurosci Res* **62**(4): 211-5.
- Kripke DF, *et al.* (2009). Circadian polymorphisms associated with affective disorders. *J Circadian Rhythms* **7**: p. 2.
- Ko CH, Takahashi JS (2006). Molecular components of the mammalian circadian clock. *Hum Mol Genet* **15 Spec No 2**: R271-7.
- Kolaj M, Zhang L, Rønnekleiv OK, Renaud LP (2012): Midline thalamic paraventricular nucleus neurons display diurnal variation in resting membrane potentials, conductances, and firing patterns in vitro. *J Neurophysiol* **107**: 1835-44.

- Konttinen H, Kronholm E, Partonen T, Kanerva N, Männistö S, Haukkala A (2014). Morningness-eveningness, depressive symptoms, and emotional eating: a population-based study. *Chronobiol Int* **31**: 554–63.
- Koob GF, Volkow ND (2010). Neurocircuitry of addiction. *Neuropsychopharmacology* **35**: 217–38.
- Koob GF, Volkow ND (2016). Neurobiology of addiction: a neurocircuitry analysis. *Lancet Psychiatry* **3**: 760–73.
- Kosobud AE, Gillman AG, Leffel JK, Pecoraro NC, Rebec GV, Timberlake W (2007). Drugs of abuse can entrain circadian rhythms. *ScientificWorldJournal* **7**: 203–12.
- Kovanen L, Kaunisto M, Donner K, Saarikoski ST, Partonen T (2013). CRY2 genetic variants associate with dysthymia. *PLoS ONE* **8**: e71450.
- Kovanen L, Saarikoski ST, Haukka J, Pirkola S, Aromaa A, Lönnqvist J, *et al* (2010). Circadian clock gene polymorphisms in alcohol use disorders and alcohol consumption. *Alcohol Alcohol* **45**: 303–11.
- Kravitz AV, Owen SF, Kreitzer AC (2013). Optogenetic identification of striatal projection neuron subtypes during in vivo recordings. *Brain Res* **1511**: 21–32.
- Kripke DF, Elliott JA, Welsh DK, Youngstedt SD (2015). Photoperiodic and circadian bifurcation theories of depression and mania. *F1000Res* **4**: 107.
- Kristiansen LV, Meador-Woodruff JH (2005). Abnormal striatal expression of transcripts encoding NMDA interacting PSD proteins in schizophrenia, bipolar disorder and major depression. *Schizophr Res* **78**: 87–93.
- Kudo T, Loh DH, Kuljis D, Constance C, Colwell CS (2011). Fast delayed rectifier potassium current: critical for input and output of the circadian system. *J Neurosci* **31**(8): 2746-2755.
- Lam RW, Levitan RD (2000). Pathophysiology of seasonal affective disorder: a review. *J Psychiatry Neurosci* **25**: 469–80.
- Landgraf D, Joiner WJ, McCarthy MJ, Kiessling S, Barandas R, Young JW, *et al* (2016). The mood stabilizer valproic acid opposes the effects of dopamine on circadian rhythms. *Neuropharmacology* **107**: 262–70.
- Landgraf D, Long JE, Proulx CD, Barandas R, Malinow R, Welsh DK (2016). Genetic Disruption of Circadian Rhythms in the Suprachiasmatic Nucleus Causes Helplessness, Behavioral Despair, and Anxiety-like Behavior in Mice. *Biol Psychiatry* **80**: 827–835.
- Landgraf D, McCarthy MJ, Welsh DK (2014). Circadian clock and stress interactions in the molecular biology of psychiatric disorders. *Curr Psychiatry Rep* **16**(10): p. 483.

- Landgraf D, McCarthy MJ, Welsh DK (2014). The role of the circadian clock in animal models of mood disorders. *Behav Neurosci* **128**: 344–59.
- Landgraf D, Wang LL, Diemer T, Welsh DK (2016). NPAS2 Compensates for Loss of CLOCK in Peripheral Circadian Oscillators. *PLoS Genet* **12**: e1005882.
- Larson EB, *et al.* (2011). Overexpression of CREB in the nucleus accumbens shell increases cocaine reinforcement in self-administering rats. *J Neurosci* **31**: 16447-16457.
- Lavebratt C, *et al.* (2010). CRY2 is associated with depression. *PLoS One* **5**(2): e9407.
- Lavebratt C, *et al.* (2010). PER2 variantion is associated with depression vulnerability. *Am J Med Genet B Neuropsychiatr Genet* **153B**(2): 570-81.
- Lecca S, Melis M, Luchicchi A, Muntoni AL, Pistis M (2012). Inhibitory inputs from rostromedial tegmental neurons regulate spontaneous activity of midbrain dopamine cells and their responses to drugs of abuse. *Neuropsychopharmacology* **37**: 1164–76.
- Lee BR, *et al.* (2013). Maturation of silent synapses in amygdala-accumbens projection contributes to incubation of cocaine craving. *Nat Neurosci.* **16**(11): 1644-51.
- Lee KW, *et al.* (2006). Cocaine-induced dendritic spine formatin in D1 and D2 dopamine-receptor containing neurons in nucleus accumbens. *Proc Natl Acad Sci U S A.* **103**(9): 3399-404.
- Lee E, Kim EY (2014). A role for timely nuclear translocation of clock repressor proteins in setting circadian clock speed. *Exp Neurobiol* **23**: 191–9.
- Lee HM, Chen R, Kim H, Etchegaray J-PP, Weaver DR, Lee C (2011). The period of the circadian oscillator is primarily determined by the balance between casein kinase 1 and protein phosphatase 1. *Proc Natl Acad Sci USA* **108**: 16451–6.
- Lee HJ, Weitz AJ, Bernal-Casas D, Duffy BA, Choy M, Kravitz AV, *et al* (2016). Activation of Direct and Indirect Pathway Medium Spiny Neurons Drives Distinct Brain-wide Responses. *Neuron* **91**: 412–24.
- Lenz JD, *et al.* (2013). Optogenetic insights into striatal function and behavior. *Behavioural brain research.* **255**:44-54.
- Lenz S, Perney TM, Qin Y, Robbins E, Chesselet MF (1994). GABA-ergic interneurons of the striatum express the Shaw-like potassium channel Kv3.1. *Synapse* **18**(1): 55-66.
- Li JZ, *et al.* (2013). Circadian patterns of gene expression in the human brain and disruption in major depressive disorder. *Proc Natl Acad Sci U S A* **110**(24): 9950-5.
- Li J-DD, Hu W-PP, Zhou Q-YY (2012). The circadian output signals from the suprachiasmatic nuclei. *Prog Brain Res* **199**: 119–27.

- Lobo MK, *et al.* (2006). FACS-array profiling of striatal projection neuron subtypes in juvenile and adult mouse brains. *Nat Neurosci.* **9**(3): 443-52.
- Lobo MK, Covington HE, Chaudhury D, Friedman AK, Sun H, Damez-Werno D, *et al* (2010). Cell type-specific loss of BDNF signaling mimics optogenetic control of cocaine reward. *Science* **330**: 385–90.
- Logan RW, McClung CA (2016). Animal models of bipolar mania: The past, present and future. *Neuroscience* **321**: 163–88.
- Logan RW, Williams WP, McClung CA (2014): Circadian rhythms and addiction: mechanistic insights and future directions. *Behav Neurosci* 128: 387–412.
- Lois G, Linke J, Wessa M. (2014). Altered Functional Connectivity between Emotional and Cognitive Resting State Networks in Euthymic Bipolar I Disorder Patients. *PLoS ONE* **9**: e107829.
- Lowrey PL, Takahashi JS (2011). Genetics of circadian rhythms in Mammalian model organisms. *Adv Genet* **74**: 175–230.
- Lu XY, Ghasemzadeh MB, Kalivas PW (1998). Expression of D1 receptor, D2 receptor, substance P and enkephalin messenger RNAs in the neurons projecting from the nucleus accumbens. *Neuroscience* **82**: 767–80.
- Lucas G, Rymar VV, Du J, Mnie-Filali O, Bisgaard C, Manta S, *et al* (2007). Serotonin(4) (5-HT(4)) receptor agonists are putative antidepressants with a rapid onset of action. *Neuron* **55**: 712–25.
- Lüscher C, Malenka RC (2011): Drug-evoked synaptic plasticity in addiction: from molecular changes to circuit remodeling. *Neuron* 69: 650–63.
- Lynch WJ, Girgenti MJ, Breslin FJ, Newton SS, Taylor JR (2008). Gene profiling the response to repeated cocaine self-administration in dorsal striatum: a focus on circadian genes. *Brain Res* **1213**: 166–77.
- Lyon M (1991). Animal Models for the Symptoms of Mania. In: Boulton A, Baker G, Martin-Iverson M (eds). *Animal Models in Psychiatry, I*. Humana Press. Vol 18, pp 197-244.
- Mackey SR (2007). Biological Rhythms Workshop IA: molecular basis of rhythms generation. *Cold Spring Harb Symp Quant Biol* **72**: 7–19.
- Magnusson A, Boivin D (2003). Seasonal affective disorder: an overview. *Chronobiol Int* **20**: 189–207.
- Mansour, *et al.* (2006). Association study of eight circadian genes with bipolar I disorder, schizoaffective disorder and schizophrenia. *Genes, Brain, Behav.* **5**: 150.

- Mansour HA, Talkowski ME, Wood J, Chowdari KV, McClain L, Prasad K, *et al* (2009). Association study of 21 circadian genes with bipolar I disorder, schizoaffective disorder, and schizophrenia. *Bipolar Disord* **11**: 701–10.
- Margolis EB, Lock H, Hjelmstad GO, Fields HL (2006). The ventral tegmental area revisited: is there an electrophysiological marker for dopaminergic neurons? *J Physiol*. **577**(3): 907–924.
- Martinowich K, Schloesser RJ, Manji HK (2009). Bipolar disorder: from genes to behavior pathways. *J Clin Invest* **119**(4): 726–736.
- Martucci L, Wong AH, De Luca V, Likhodi O, Wong GW, King N *et al.* (2006). N-methyl-D-aspartate receptor NR2B subunit gene GRIN2B in schizophrenia and bipolar disorder: Polymorphisms and mRNA levels. *Schizophr Res* **84**: 214–221.
- Masubuchi S, Honma S, Abe H, Ishizaki K, Namihira M, Ikeda M, *et al* (2000). Clock genes outside the suprachiasmatic nucleus involved in manifestation of locomotor activity rhythm in rats. *Eur J Neurosci* **12**: 4206–14.
- Matzeu A, Zamora-Martinez ER, Martin-Fardon R (2014). The paraventricular nucleus of the thalamus is recruited by both natural rewards and drugs of abuse: recent evidence of a pivotal role for orexin/hypocretin signaling in this thalamic nucleus in drug-seeking behavior. *Front Behav Neurosci* **8**: 117.
- McCarthy MJ, *et al.* (2013). Genetic and clinical factors predict lithium's effects on PER2 gene expression rhythms in cells from bipolar disorder patients. *Transl Psychiatry* **3**: p. e318.
- McCarthy MJ, Fernandes M, Kranzler HR, Covault JM, Welsh DK (2013a). Circadian clock period inversely correlates with illness severity in cells from patients with alcohol use disorders. *Alcohol Clin Exp Res* **37**: 1304–10.
- McCarthy MJ, Nievergelt CM, Kelsoe JR, Welsh DK (2012). A survey of genomic studies supports association of circadian clock genes with bipolar disorder spectrum illnesses and lithium response. *PLoS ONE* **7**: e32091.
- McCarthy MJ, Wei H, Marnoy Z, Darvish RM, McPhie DL, Cohen BM, *et al* (2013b). Genetic and clinical factors predict lithium's effects on PER2 gene expression rhythms in cells from bipolar disorder patients. *Transl Psychiatry* **3**: e318.
- McCarthy MJ, Welsh DK (2012). Cellular circadian clocks in mood disorders. *J Biol Rhythms* **27**: 339–52.
- McClung CA (2011). Circadian rhythms and mood regulation: insights from pre-clinical models. *Eur Neuropsychopharmacol* **21 Suppl 4**: S683–93.
- McClung CA (2007). Circadian genes, rhythms and the biology of mood disorders. *Pharmacol Ther* **114**: 222–32.

- McClung CA (2013). How might circadian rhythms control mood? Let me count the ways... *Biol Psychiatry* **74**: 242–9.
- McClung CA, Sidiropoulou K, Vitaterna M, Takahashi JS, White FJ, Cooper DC, *et al* (2005). Regulation of dopaminergic transmission and cocaine reward by the Clock gene. *Proc Natl Acad Sci USA* **102**: 9377–81.
- McCutcheon JE, *et al.* (2014). Optical suppression of drug-evoked phasic dopamine release. *Frontiers in neural circuits*. **8**: 114.
- McDearmon EL, Patel KN, Ko CH, Walisser JA, Schook AC, Chong JL, *et al* (2006). Dissecting the functions of the mammalian clock protein BMAL1 by tissue-specific rescue in mice. *Science* **314**: 1304–8.
- Meador-Woodruff JH, Hogg AJ, Smith RE (2001): Striatal ionotropic glutamate receptor expression in schizophrenia, bipolar disorder, and major depressive disorder. *Brain Res Bull* **55**: 631–40.
- Meijer JH, Schwartz WJ (2003). In search of the pathways for light-induced pacemaker resetting in the suprachiasmatic nucleus. *J Biol Rhythms* **18**: 235–49.
- Melo MC, Garcia RF, Linhares Neto VB, Sá MB, Mesquita LM de, Araújo CF de, *et al* (2016). Sleep and circadian alterations in people at risk for bipolar disorder: A systematic review. *J Psychiatr Res* **83**: 211–219.
- Mendlewicz J (2009). Disruption of the circadian timing systems: molecular mechanisms in mood disorders. *CNS Drugs* **23 Suppl 2**: 15–26.
- Mendoza J, Challet E (2014). Circadian insights into dopamine mechanisms. *Neuroscience* **282**: 230–42.
- Meredith GE, Baldo BA, Andrezjewski ME, Kelley AE (2008): The structural basis for mapping behavior onto the ventral striatum and its subdivisions. *Brain Struct Funct* **213**: 17–27.
- Miklowitz DJ, Johnson SL (2006): The psychopathology and treatment of bipolar disorder. *Annu Rev Clin Psychol* **2**: 199–235.
- Milhiet V, Boudebessé C, Bellivier F, Drouot X, Henry C, Leboyer M, *et al* (2014). Circadian abnormalities as markers of susceptibility in bipolar disorders. *Front Biosci (Schol Ed)* **6**: 120–37.
- Mohawk JA, Takahashi JS (2011) Cell autonomy and synchrony of suprachiasmatic nucleus circadian oscillators. *Trends Neurosci* **34**(7): 349-58.
- Moine C Le, Bloch B (1995). D1 and D2 dopamine receptor gene expression in the rat striatum: sensitive cRNA probes demonstrate prominent segregation of D1 and D2 mRNAs in distinct neuronal populations of the dorsal and ventral striatum. *J Comp Neurol* **355**: 418–26.

- Moraga-Amaro R, *et al.* (2014). Dopamine receptor D3 deficiency results in chronic]] and anxiety. *Behav Brain Res* **274**:186-93.
- Morin LP (2013). Neuroanatomy of the extended circadian rhythm system. *Exp Neurol* **243**: 4–20.
- Moriya S, Tahara Y, Sasaki H, Ishigooka J, Shibata S (2015). Phase-delay in the light-dark cycle impairs clock gene expression and levels of serotonin, norepinephrine, and their metabolites in the mouse hippocampus and amygdala. *Sleep Med* **16**: 1352–9.
- Moyer JT, Wolf JA, Finkel LH (2007): Effects of dopaminergic modulation on the integrative properties of the ventral striatal medium spiny neuron. *J Neurophysiol* **98**: 3731–48.
- Mu P, Moyer JT, Ishikawa M, Zhang Y, Panksepp J, Sorg BA, *et al.* (2010): Exposure to cocaine dynamically regulates the intrinsic membrane excitability of nucleus accumbens neurons. *J Neurosci* **30**: 3689–99.
- Mukherjee S, Coque L, Cao J-L, Kumar J, Chakravarty S, Asaithamby A, *et al* (2010). Knockdown of Clock in the Ventral Tegmental Area Through RNA Interference Results in a Mixed State of Mania and Depression-Like Behavior. *Biological Psychiatry* **68**(6):503-511.
- Mundo E, Tharmalingham S, Neves-Pereira M, Dalton EJ, Macciardi F, Parikh SV *et al.* (2003). Evidence that the N-methyl-D-aspartate subunit 1 receptor gene (GRIN1) confers susceptibility to bipolar disorder. *Mol Psychiatry* **8**: 241–245.
- Naylor E, Bergmann BM, Krauski K, Zee PC, Takahashi JS, Vitaterna MH, *et al* (2000). The circadian clock mutation alters sleep homeostasis in the mouse. *J Neurosci* **20**(21): 8138-8143.
- Nestler EJ (2005). Is there a common molecular pathway for addiction? *Nat Neurosci* **8**: 1445–9.
- Nicola SM, Surmeier J, Malenka RC (2000): Dopaminergic modulation of neuronal excitability in the striatum and nucleus accumbens. *Annu Rev Neurosci* **23**: 185–215.
- Nievergelt CM, *et al.* (2006). Suggestive evidence for association of the circadian genes PERIOD3 and ARNTL with bipolar disorder. *Am J Med Genet B Neuropsychiatr Genet*, **141B**(3): 234-41.
- Ozburn AR, Falcon E, Mukherjee S, Gillman A, Arey R, Spencer S, McClung CA (2013): The role of clock in ethanol-related behaviors. *Neuropsychopharmacology* **38**: 2393–400.
- Ozburn A, Falcon E, Twaddle A, Nugent A, Gillman A, Spencer S, *et al* Direct Regulation of Diurnal Drd3 Expression and Cocaine Reward by NPAS2. *Biological Psychiatry* doi:10.1016/j.biopsych.2014.07.030.
- Ozburn AR, Larson EB, Self DW, McClung CA (2012): Cocaine self-administration behaviors in ClockΔ19 mice. *Psychopharmacology (Berl)* **223**: 169–77.

- Ozburn AR, Purohit K, Parekh PK, Kaplan GN, Falcon E, Mukherjee S, *et al* (2016). Functional Implications of the CLOCK 3111T/C Single-Nucleotide Polymorphism. *Front Psychiatry* **7**: 67.
- Panda S, Provencio I, Tu DC, Pires SS, Rollag MD, Castrucci AM, *et al* (2003). Melanopsin is required for non-image-forming photic responses in blind mice. *Science* **301**: 525–7.
- Parekh PK, McClung CA (2015). Circadian Mechanisms Underlying Reward-Related Neurophysiology and Synaptic Plasticity. *Front Psychiatry* **6**: 187.
- Parekh PK, Ozburn AR, McClung CA (2015). Circadian clock genes: effects on dopamine, reward and addiction. *Alcohol* **49**: 341–9.
- Partonen T, *et al.* (2007). Three circadian clock genes Per2, Arntl, and Npas2 contribute to winter depression. *Ann Med* **39**(3): 229-38.
- Perez-Cruz C, Simon M, Flügge G, Fuchs E, Czéh B (2010). Diurnal rhythm and stress regulate dendritic architecture and spine density of pyramidal neurons in the rat infralimbic cortex. *Behavioural brain research* **205**: 406–413.
- Phillips ML, Swartz HA (2014). A Critical Appraisal of Neuroimaging Studies of Bipolar Disorder: Toward a New Conceptualization of Underlying Neural Circuitry and a Road Map for Future Research. *Am J Psychiatry*.
- Pinsonneault JK, Han DD, Burdick KE, Kataki M, Bertolino A, Malhotra AK, *et al* (2011). Dopamine transporter gene variant affecting expression in human brain is associated with bipolar disorder. *Neuropsychopharmacology* **36**: 1644–55.
- Preitner N, Damiola F, Lopez-Molina L, Zakany J, Duboule D, Albrecht U, *et al* (2002). The orphan nuclear receptor REV-ERB α controls circadian transcription within the positive limb of the mammalian circadian oscillator. *Cell* **110**: 251–60.
- Prus AJ, *et al.* (2009). Conditioned Place Preference. in *Methods of Behavior Analysis in Neuroscience*. (ed. J.J. Buccafusco) (Boca Raton, FL).
- Quintero JE, Kuhlman SJ, McMahon DG (2003). The biological clock nucleus: a multiphasic oscillator network regulated by light. *J Neurosci* **23**: 8070–6.
- Rao JS, Kellom M, Reese EA, Rapoport SI, Kim H-WW (2012). Dysregulated glutamate and dopamine transporters in postmortem frontal cortex from bipolar and schizophrenic patients. *Journal of affective disorders* **136**: 63–71.
- Reick M, Garcia JA, Dudley C, McKnight SL (2001). NPAS2: an analog of clock operative in the mammalian forebrain. *Science* **293**: 506–9.
- Reppert SM, Weaver DR (2002). Coordination of circadian timing in mammals. *Nature* **418**: 935–41.

- Richard JM, Castro DC, Difeliceantonio AG, Robinson MJ, Berridge KC (2013). Mapping brain circuits of reward and motivation: in the footsteps of Ann Kelley. *Neurosci Biobehav Rev* **37**: 1919–31.
- Ripperger JAA, Albrecht U (2012). REV-ERB-erating nuclear receptor functions in circadian metabolism and physiology. *Cell Res* **22**: 1319–21.
- Robinson TE, Kolb B (2004). Structural plasticity associated with exposure to drugs of abuse. *Neuropharmacology* **47 Suppl 1**: 33–46.
- Rock P, Goodwin G, Harmer C, Wulff K (2014). Daily rest-activity patterns in the bipolar phenotype: A controlled actigraphy study. *Chronobiol Int* **31**: 290–6.
- Roybal K, Theobald D, Graham A, DiNieri JA, Russo SJ, Krishnan V, *et al.* (2007): Mania-like behavior induced by disruption of CLOCK. *Proc Natl Acad Sci USA* **104**: 6406–11.
- Russo SJ, *et al.* (2009) Nuclear factor kappa B signaling regulates neuronal morphology and cocaine reward. *J Neurosci.* **29**(11): 3529-37.
- Russo SJ, Dietz DM, Dumitriu D, Morrison JH, Malenka RC, Nestler EJ (2010). The addicted synapse: mechanisms of synaptic and structural plasticity in nucleus accumbens. *Trends Neurosci* **33**: 267–76.
- Russo SJ, Nestler EJ (2013). The brain reward circuitry in mood disorders. *Nat Rev Neurosci* **14**: 609–25.
- Sakhi K, Belle MD, Gossan N, Delagrangé P, Piggins HD (2014). Daily variation in the electrophysiological activity of mouse medial habenula neurones. *J Physiol (Lond)* **592**: 587–603.
- Salgado-Delgado R, *et al.* (2011). Disruption of circadian rhythms: a crucial factor in the etiology of depression. *Depress Res Treat* **2011**: 839743.
- Salvadore G, Quiroz JA, Machado-Vieira R, Henter ID, Manji HK, Zarate CA, Jr. (2010). The neurobiology of the switch process in bipolar disorder: a review. *J Clin Psychiatry* **71**(11): 1488-1501.
- Sans N, Prybylowski K, Petralia RS, Chang K, Wang Y-XX, Racca C *et al.* (2003). NMDA receptor trafficking through an interaction between PDZ proteins and the exocyst complex. *Nat Cell Biol* **5**: 520–530.
- Schmidt TM, Chen S-KK, Hattar S (2011). Intrinsically photosensitive retinal ganglion cells: many subtypes, diverse functions. *Trends Neurosci* **34**: 572–80.
- Schultz W (2006). Behavioral theories and the neurophysiology of reward. *Annu Rev Psychol* **57**: 87–115.

- Schultz W, Dayan P, Montague PR (1997). A neural substrate of prediction and reward. *Science* **275**: 1593–9.
- Scott AJ, Monk TH, Brink LL (1997). Shiftwork as a Risk Factor for Depression: A Pilot Study. *Int J Occup Environ Health* **3**: S2–S9.
- Serretti A, Benedetti F, Mandelli L, Lorenzi C, Pirovano A, Colombo C, *et al* (2003). Genetic dissection of psychopathological symptoms: insomnia in mood disorders and CLOCK gene polymorphism. *Am J Med Genet B Neuropsychiatr Genet* **121B**: 35–8.
- Sesack SR, Grace AA (2010). Cortico-Basal Ganglia reward network: microcircuitry. *Neuropsychopharmacology* **35**(1): 27–47.
- Shaltiel G, Maeng S, Malkesman O, Pearson B, Schloesser RJ, Tragon T, *et al.* (2008): Evidence for the involvement of the kainate receptor subunit GluR6 (GRIK2) in mediating behavioral displays related to behavioral symptoms of mania. *Mol Psychiatry* **13**: 858–72.
- Shen W, Hernandez-Lopez S, Tkatch T, Held JE, Surmeier DJ (2004): Kv1.2-containing K⁺ channels regulate subthreshold excitability of striatal medium spiny neurons. *J Neurophysiol* **91**: 1337–49.
- Shuen JA, Chen M, Gloss B, Calakos N (2008). Drd1a-tdTomato BAC transgenic mice for simultaneous visualization of medium spiny neurons in the direct and indirect pathways of the basal ganglia. *J Neurosci* **28**: 2681–5.
- Sidor MM, Spencer SM, Dzirasa K, Parekh PK, Tye KM, Warden MR, *et al.* (2015): Daytime spikes in dopaminergic activity drive rapid mood-cycling in mice. *Mol Psychiatry* **20**: 1406–19.
- Sleipness EP, Jansen HT, Schenk JO, Sorg BA (2008). Time-of-day differences in dopamine clearance in the rat medial prefrontal cortex and nucleus accumbens. *Synapse* **62**: 877–85.
- Sleipness EP, Sorg BA, Jansen HT (2007). Diurnal differences in dopamine transporter and tyrosine hydroxylase levels in rat brain: dependence on the suprachiasmatic nucleus. *Brain Res* **1129**: 34–42.
- Smith RJ, Lobo MK, Spencer S, Kalivas PW (2013). Cocaine-induced adaptations in D1 and D2 accumbens projection neurons (a dichotomy not necessarily synonymous with direct and indirect pathways). *Curr Opin Neurobiol* **23**: 546–52.
- Sohal VS, Zhang F, Yizhar O, Deisseroth K (2009). Parvalbumin neurons and gamma rhythms enhance cortical circuit performance. *Nature* **459**(7247): 698–702.
- Sokoloff P, Foll B Le, Perachon S, Bordet R, Ridray S, Schwartz JC (2001). The dopamine D3 receptor and drug addiction. *Neurotox Res* **3**: 433–41.

- Soria V, Martínez-Amorós E, Escaramís G, Valero J, Pérez-Egea R, García C, *et al* (2010). Differential association of circadian genes with mood disorders: CRY1 and NPAS2 are associated with unipolar major depression and CLOCK and VIP with bipolar disorder. *Neuropsychopharmacology* **35**: 1279–89.
- Spencer S *et al.* (2013). Circadian genes Period 1 and Period 2 in the nucleus accumbens regulate anxiety-related behavior. *Eur J Neurosci* **37**(2): 242-50.
- Spencer S, Torres-Altoro MI, Falcon E, Arey R, Marvin M, Goldberg M, *et al.* (2012): A mutation in CLOCK leads to altered dopamine receptor function. *J Neurochem* **123**: 124–34.
- Spengler ML *et al.* (2012). Core circadian protein CLOCK is a positive regulator of NF-kappaB-mediated transcription. *Proc Natl Acad Sci U S A.* **109**(37): 2457-65.
- Steiner H, Fuchs S, Accili D (1997). D3 dopamine receptor-deficient mouse: evidence for reduced anxiety. *Physiol Behav* **63**(1):137-41.
- Strakowski SM, *et al.* (2005). The functional neuroanatomy of bipolar disorder: a review of neuroimaging findings. *Mol Psychiatry.* **10**: 105-116.
- Tapia-Osorio A, Salgado-Delgado R, Angeles-Castellanos M, Escobar C (2013). Disruption of circadian rhythms due to chronic constant light leads to depressive and anxiety-like behaviors in the rat. *Behav Brain Res* **252**: 1–9.
- Tataroglu O, *et al.* (2004). Effect of lesioning the suprachiasmatic nuclei on behavioral despair in rats. *Brain Res.* **1001**: 118.
- Tohen M, Vieta E (2009). Antipsychotic agents in the treatment of bipolar mania. *Bipolar Disord* **11 Suppl 2**: 45-54.
- Tye KM (2012). Glutamate inputs to the nucleus accumbens: does source matter? *Neuron* **76**: 671–3.
- Uhlhaas PJ, Pipa G, Neuenschwander S, Wibral M, Singer W (2011). A new look at gamma? High- (>60 Hz) gamma-band activity in cortical networks: function, mechanisms and impairment. *Prog Biophys Mol Biol* **105**(1-2): 14-28.
- Vilchis C, Bargas J, Ayala GX, Galván E, Galarraga E (2000): Ca²⁺ channels that activate Ca²⁺-dependent K⁺ currents in neostriatal neurons. *Neuroscience* **95**:745–52.
- Vitaterna MH, Ko CH, Chang A-MM, Buhr ED, Fruechte EM, Schook A, *et al* (2006). The mouse Clock mutation reduces circadian pacemaker amplitude and enhances efficacy of resetting stimuli and phase-response curve amplitude. *Proc Natl Acad Sci USA* **103**:9327–32.
- Wang H, *et al.* (2007). Casein kinase I epsilon gene transfer into the suprachiasmatic nucleus via electroporation lengthens circadian periods of tau mutant hamsters. *Eur J Neurosci* **25**(11): 3359-66.

- Wardlaw SM, Phan TX, Saraf A, Chen X, Storm DR (2014). Genetic disruption of the core circadian clock impairs hippocampus-dependent memory. *Learning & memory (Cold Spring Harbor, NY)* **21**: 417–423.
- Webb IC, Baltazar RM, Wang X, Pitchers KK, Coolen LM, Lehman MN (2010). Diurnal variations in natural and drug reward, mesolimbic tyrosine hydroxylase, and clock gene expression in the male rat. *Journal of biological rhythms* **24**: 465–76.
- Weber M, Lauterburg T, Tobler I, Burgunder J-MM (2004). Circadian patterns of neurotransmitter related gene expression in motor regions of the rat brain. *Neurosci Lett* **358**: 17–20.
- White W, Feldon J, Heidbreder CA, White IM (2000). Effects of administering cocaine at the same versus varying times of day on circadian activity patterns and sensitization in rats. *Behav Neurosci* **114**: 972–82.
- Wickens JR, Wilson CJ (1998): Regulation of action-potential firing in spiny neurons of the rat neostriatum in vivo. *J Neurophysiol* **79**: 2358–64.
- Wiedholz LM, Owens WA, Horton RE, Feyder M, Karlsson R-MM, Hefner K, *et al.* (2008): Mice lacking the AMPA GluR1 receptor exhibit striatal hyperdopaminergia and “schizophrenia-related” behaviors. *Mol Psychiatry* **13**: 631–40.
- Wirz-Justice A, *et al.* (2005). Chronotherapeutics (light and wake therapy) in affective disorders. *Psychol. Med* **35**:939.
- Wittmann M, Dinich J, Merrow M, Roenneberg T (2006). Social jetlag: misalignment of biological and social time. *Chronobiol Int* **23**: 497–509.
- Wolf JA, Moyer JT, Lazarewicz MT, Contreras D, Benoit-Marand M, O'Donnell P, Finkel LH (2005): NMDA/AMPA ratio impacts state transitions and entrainment to oscillations in a computational model of the nucleus accumbens medium spiny projection neuron. *J Neurosci* **25**: 9080–95.
- Wu X, Wiater MF, Ritter S (2010). NPAS2 deletion impairs responses to restricted feeding but not to metabolic challenges. *Physiol Behav* **99**: 466–71.
- Xing B, *et al.* (2013). Effects of immobilization stress on emotional behaviors in dopamine D3 receptor knockout mice. *Behav Brain Res* **243**: 261-6.
- Yanagi M, Joho RH, Southcott SA, Shukla AA, Ghose S, Tamminga CA (2014). Kv3.1-containing K(+) channels are reduced in untreated schizophrenia and normalized with antipsychotic drugs. *Mol Psychiatry* **19**(5): 573-579.
- Young JW, Enkhuizen J van, Winstanley CA, Geyer MA (2011a). Increased risk-taking behavior in dopamine transporter knockdown mice: further support for a mouse model of mania. *J Psychopharmacol (Oxford)* **25**: 934–43.

- Young JW, Henry BL, Geyer MA (2011b). Predictive animal models of mania: hits, misses and future directions. *Br J Pharmacol* **164**: 1263–84
- Zhang L, Evans DS, Raheja UK, Stephens SH, Stiller JW, Reeves GM, *et al* (2015). Chronotype and seasonality: morningness is associated with lower seasonal mood and behavior changes in the Old Order Amish. *J Affect Disord* **174**: 209–14.
- Zhang R, Lahens NF, Ballance HI, Hughes ME, Hogenesch JB (2014). A circadian gene expression atlas in mammals: implications for biology and medicine. *Proc Natl Acad Sci USA* **111**: 16219–24.
- Zhao H, Rusak B (2005). Circadian firing-rate rhythms and light responses of rat habenular nucleus neurons in vivo and in vitro. *Neuroscience* **132**: 519–28.
- Zhou YD, Barnard M, Tian H, Li X, Ring HZ, Francke U, *et al* (1997). Molecular characterization of two mammalian bHLH-PAS domain proteins selectively expressed in the central nervous system. *Proc Natl Acad Sci USA* **94**: 713–8.